

Denitrification of Anthropogenic Nitrogen in Groundwater: Measurement and Modeling Using Stable Isotopic and Mass Balance Approaches

by

Wendy Jeanne Pabich

B.A., Geography (1988)
Dartmouth College

M.S., Geology (1995)
Duke University

M.S., Urban Studies and Planning (1995)
Massachusetts Institute of Technology

Submitted to the Department of Civil and Environmental Engineering
in Partial Fulfillment of the Requirements for the Degree of
Doctor of Philosophy in Environmental Engineering

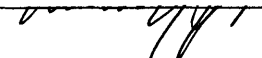
at the

Massachusetts Institute of Technology

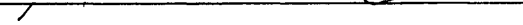
February 2001

© 2001 Massachusetts Institute of Technology

Signature of
Author

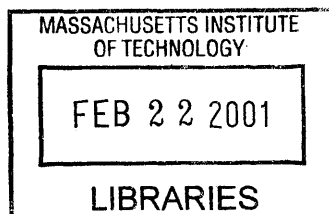

Department of Civil and Environmental Engineering
October 31, 2000

Certified by


Harold F. Hemond
Professor of Civil and Environmental Engineering
Thesis Supervisor

Accepted by


Oral Buyukozturk
Chairman, Department Committee on Graduate Students



ENG

Denitrification of Anthropogenic Nitrogen in Groundwater: Measurement and Modeling Using Stable Isotopic and Mass Balance Approaches

by Wendy Jeanne Pabich

Submitted to the Department of Civil and Environmental Engineering
on October 31, 2000, in Partial Fulfillment of the Requirements for the Degree of
Doctor of Philosophy in Environmental Engineering

ABSTRACT

Denitrification is a microaerophilic, microbially-mediated process, by which nitrate is reduced to biologically-unavailable N_2 gas; the reaction is generally coupled to the oxidation of organic carbon. We hypothesized that denitrification rates in groundwater in the Waquoit Bay watershed on Cape Cod, USA, were controlled by both nitrate and dissolved organic carbon (DOC) concentrations, and that groundwater DOC concentrations were inversely related to the thickness of the vadose (unsaturated) zone through which recharge occurred. We found that the deeper the vadose zone, the lower the concentration of DOC in groundwater near the water table; similarly, DOC concentrations decreased with increasing depth below the water table, suggesting quite active biogeochemical processing in these boundary environments.

We used stable isotope and mass balance approaches to estimate denitrification rates in groundwater at two forested field sites and in a septic system plume. These sites provided a large range of groundwater nitrate and dissolved organic carbon (DOC) concentrations. At all sites, denitrification rates increased with increasing nitrate concentration. First order denitrification rate constants with respect to nitrate were highest where groundwater DOC concentrations were highest: $k = 2.8 \text{ y}^{-1}$ in the septic plume ($\sim 26 \text{ mg C l}^{-1}$), $k = 1.6 \text{ y}^{-1}$ at South Cape Beach (DOC = 0.8 to 23.4 mg C l^{-1}), and $k = 0.25 \text{ y}^{-1}$ at Crane Wildlife (0.1 to 1.9 mg C l^{-1}), suggesting that, independent of nitrate, DOC concentrations exert significant control on denitrification rates. A simulation of N losses along groundwater flowpaths suggests that a saturating kinetics expression with respect to both nitrate and DOC best predicts nitrate concentrations measured at downgradient well ports ($R^2 = 0.96$ for $[\text{NO}_3^-]_{\text{model}}$ vs. $[\text{NO}_3^-]_{\text{meas}}$). In contrast, a saturating kinetics expression with respect to nitrate only, often overpredicts nitrate losses along groundwater flowpaths, particularly where DOC concentration are low, further confirming that DOC concentrations are an important control on groundwater denitrification rates. The magnitude of a nitrate source, its travel distance to shore, and the DOC concentration in groundwater are useful predictors of N downgradient. These relationships can help in designing strategies to control anthropogenic nitrogen loading.

Thesis Supervisor: Harold F. Hemond
Title: Professor of Civil and Environmental Engineering

ACKNOWLEDGMENTS

I am thankful for the many people who provided support, encouragement, and advice during the course of this project. I appreciate the time and efforts of my committee: Harry Hemond, Ivan Valiela, and Penny Chisholm. Many thanks go to my advisor, Harry Hemond, who not only supported my predilection for understanding environmental problems in a holistic manner, but also pushed me to develop rigorous analytical skills and to get my hands dirty in the lab. I am certain these skills will serve me well in the future. I thank him immensely.

Ivan Valiela, at the Boston University Marine Lab opened his laboratory to me and introduced me to the world of “nitrogen loading”. He became a second advisor, working closely with me to formulate a dissertation topic, implement a field program, and produce this document. He taught me much about statistics and presented the viewpoint of an ecologist. I can’t thank him enough for all his support.

Penny Chisholm provided helpful comments on my thesis, and also stands as an inspiring role model as a successful woman in science.

I am indebted to all the people who provided me with technical assistance. John McFarland helped with DOC analysis. Three MIT UROPs, Vanessa Bhark, Alyssa Thorvaldsen, and Amy Watson helped me perform lab work. In Woods Hole, Gabby Tomasky and Erica Stieve helped me in the field, and Jim McClelland taught me how to process samples for stable isotope analysis; Dave Senn helped me install wells; Kevin Kroeger and Liz Westgate collected and analyzed samples from my septic system site; and Kathy Regan and Anne Giblin, of MBL, enabled me to analyze nitrate samples. Denis Leblanc at USGS assisted me tremendously in allowing me access to the Crane Wildlife Reserve Site, showing me how to construct multi-level samplers, installing wells for me, and inviting me to research meetings. Thanks go to Sheila Frankel for a boot camp experience teaching environmental chemistry lab skills to undergraduates, as well as for her general support and friendship.

I am grateful for the community offered by MIT. The companionship, support, entertainment, and discussions, both scientific and irrelevant, provided by all my friends in the Hemond research group, at the Parsons Lab, and in Woods Hole, have made this a very special experience.

Lastly, I thank my great friends, especially the North Shore contingent, for providing endless entertainment, outrageous athletic and other endeavors, trips to the mountains, heart-to-heart discussion, and for keeping me sane during this process. I especially thank Tim and Abby for opening their home and their hearts to me, and most of all, my parents, Diane and Dick, who instilled in me a love of learning, and my family, David, Heather, Jill, Eric, Jeanne, Lenore, Lisa, Irene and Mort for their love and support during a seemingly never-ending career as a graduate student.

Table of Contents

LIST OF TABLES	9
LIST OF FIGURES	10
CHAPTER 1. Introduction	13
1. Anthropogenic nitrogen and eutrophication	14
2. Transformations of nitrogen within aquifers	15
3. Denitrification	16
4. Study goals	18
5. References	23
CHAPTER 2. The effect of vadose zone thickness and depth below the water table on DOC concentration in groundwater on Cape Cod, U.S.A.	29
Abstract	31
1. Introduction	32
2. Materials and methods	34
2.1. Study site	34
2.2. Groundwater sample collection and analysis	35
3. Results and discussion	36
4. Acknowledgments	47
5. References	48
CHAPTER 3. Denitrification rates in groundwater, Cape Cod, U.S.A.: Control by nitrate and dissolved organic carbon concentrations.	52
Abstract	54
1. Introduction	55
2. Approach	57
3. Nitrogen isotope geochemistry	58
4. Study sites	59
5. Methods	63
5.1. Groundwater sample collection	63
5.2. Chemical analysis	63
6. Modeling framework and assumptions	65
6.1. Steady state conditions	68
6.2. Estimating groundwater age (t)	68
6.3. Rayleigh parameters and assumptions	76
6.3.1. Soil-derived $\delta^{15}N$ source signatures at Crane Wildlife Management Area	80

Table of Contents (cont.)

6.3.2. Fertilizer-derived $\delta^{15}N$ -Ammonium source signature at Crane Wildlife Management Area	83
6.3.3. Fertilizer-derived $\delta^{15}N$ -Nitrate source signature at Crane Wildlife Management Area	84
6.3.4. Soil-derived $\delta^{15}N$ source signatures at South Cape Beach	85
6.3.5. Isotopic enrichment factor for nitrification (ϵ_{nit})	88
6.3.6. Isotopic enrichment factor for denitrification (ϵ_{denit})	88
7. Results and discussion	88
7.1. Crane Wildlife Management Area	88
7.1.1. Geochemistry	88
7.1.2. Nitrification	97
7.1.3. 'Apparent $\delta^{15}NO_3^-$ ' model	99
7.1.4. Denitrification	100
7.2. South Cape Beach	110
7.2.1. Geochemistry	110
7.2.2. Nitrification	114
7.2.3. Denitrification	114
7.3. Sensitivity analysis	118
8. Conclusions	124
9. Acknowledgements	127
10. References	128
CHAPTER 4. Fate of nitrogen from a septic system in a nearshore Cape Cod aquifer	135
1. Introduction	136
2. Fate of anthropogenic nitrogen in a nearshore Cape Cod aquifer	138
3. Denitrification rates in groundwater containing septic effluent	145
4. Conclusions	149
5. References	150

Table of Contents (cont.)

CHAPTER 5: An empirical model to predict groundwater denitrification rates, Cape Cod, USA: Substrate limitation by DOC and NO_3^-	151
Abstract	153
1. Introduction	154
2. Saturating Kinetics	156
2.1. Assumption of steady state	158
3. Model parameterization	159
3.1. Half-saturation constants for nitrate (K_{NO_3}) and DOC (K_{DOC})	159
3.2. Denitrifying bacterial population	162
3.3. Maximum bacterial growth rate (μ_{max})	166
3.4. Bacterial yield constant (Y)	166
4. Results and discussion	168
5. Acknowledgements	175
6. References	176
CHAPTER 6: Conclusions	182
1. Conclusions	183
2. Controls on groundwater DOC concentrations	184
3. Groundwater denitrification rates	185
4. Modeling of denitrification using a saturating kinetics expression	186
5. References	188

List of Tables

Table 2.1.	Analysis of variance for multiple regression of effect of depth below table (D_{wt}) and vadose thickness (T_{vad}) on DOC concentration.	39
Table 3.1.	Vogel groundwater age model.	69
Table 3.2.	Nitrification model.	70
Table 3.3.	Rayleigh product formation model.	71
Table 3.4.	'Apparent $\delta^{15}NO_3^-$ ' model.	72
Table 3.5.	Denitrification model.	73
Table 3.6.	Comparison of spatial and temporal variability in groundwater chemistry at South Cape Beach.	75
Table 3.7.	Groundwater age and horizontal distance to upgradient recharge point for Crane Wildlife Management Area wells.	93
Table 3.8.	First order rate constants for denitrification in groundwater at three field sites increase with increasing DOC concentration.	117
Table 5.1.	Parameters and values used in saturating kinetics model for denitrification.	165
Table 5.2.	Estimated values for maximum growth rate (μ_{max}) and yield constant (Y) from the literature, and from our thermodynamic calculations for Y .	167

List of Figures

2.1.	Mean DOC concentration measured at 12 sampling stations at South Cape Beach on 5 sampling dates between March and August 1998.	38
2.2.	DOC concentration as a function of depth below water table for each of three vadose thickness (T_{vad}) strata.	40
2.3.	DOC concentration plotted as a function of depth below water table for each of three vadose thickness (T_{vad}) strata.	42
2.4.	Instantaneous DOC loss rate as a function of depth below water table for each of three vadose thickness (T_{vad}) strata.	44
2.5.	DOC concentrations in groundwater as a function of depth.	45
3.1.	Location of Crane Wildlife Management Area, South Cape Beach, and septic system study sites in and near the Waquoit Bay watershed, Cape Cod, MA.	60
3.2.	Schematic of multi-level sampling wells arranged in a transect Parallel to groundwater flow lines at Crane Wildlife Management Area.	64
3.3.	Stable isotope method for calculating average denitrification rates between recharge and point of sampling for each water sample collected at Crane Wildlife Management Area.	67
3.4.	Temporal variability in groundwater chemistry at Crane Wildlife Management Area.	74
3.5.	Pathways by which fertilizer-derived nitrate and ammonium at Crane Wildlife Management Area are delivered to the water table.	77
3.6.	Pathways by which soil-derived nitrate and ammonium at Crane Wildlife Management Area are delivered to the water table.	78
3.7.	Pathways by which soil-derived nitrate and ammonium at South Cape Beach are delivered to the water table.	79
3.8.	Estimation of $\delta^{15}NO_3^-$ _{source} and $\delta^{15}NH_4^+$ _{source} values for soil-derived N at Crane Wildlife Management Area.	81
3.9.	Frequency plots of measured $\delta^{15}NO_3^-$ at Crane Wildlife Management Area and South Cape Beach.	86
3.10.	Profiles of dissolved oxygen, DOC, and ammonium with depth below water table (D_{wt}) at Crane Wildlife Management Area.	89
3.11.	Profiles of nitrate and $\delta^{15}N$ with depth below water table (D_{wt}) at Crane Wildlife Management Area.	90
3.12.	Recharge zones for 3 wells at Crane Wildlife Management Area.	94
3.13.	Schematic of multi-level sampling (MLS) well transect parallel to groundwater flow lines at Crane Wildlife Management Area.	95
3.14.	$\delta^{15}N$ of nitrate measured at Crane Wildlife Management Area for fertilizer-derived and soil-derived nitrate.	101

List of Figures (cont.)

3.15.	Average denitrification rate versus initial nitrate concentration for two forested sites (South Cape Beach and Crane Wildlife), and for a septic plume.	104
3.16.	Denitrification rates decrease with increasing depth below the water table (D_{wt}) for soil-derived nitrate samples at Crane Wildlife Management Area.	107
3.17.	Lineweaver-Burke plot using fertilizer-derived nitrate samples at Crane Wildlife to derive saturating kinetics parameters.	109
3.18.	Results of simulation predicting nitrate concentration at downgradient well port ($[NO_3^-]_{model}$) using a first order rate expression vs. nitrate concentration measured at that well port ($[NO_3^-]_{meas}$).	111
3.19.	Results of simulation predicting nitrate concentrations at downgradient well ports ($[NO_3^-]_{model}$) using average denitrification rates over the flowpaths (calculated from both initial and final nitrate concentrations) vs. nitrate concentrations measured at those well ports ($[NO_3^-]_{meas}$).	112
3.20.	Results of simulation predicting nitrate concentrations at downgradient well ports ($[NO_3^-]_{model}$) using saturating kinetics expression with respect to nitrate versus nitrate concentrations measured at those well ports ($[NO_3^-]_{meas}$).	113
3.21.	Results of sensitivity analysis of denitrification model for soil-derived nitrate.	119
3.22.	Results of sensitivity analysis of denitrification model for fertilizer-derived nitrate.	120
4.1.	Vertical cross section from the soil surface, water table, and aquifer through our field of multiple sampling wells (elevation relative to mean low water (MLW)).	143
4.2.	NO ₃ ⁻ concentration versus B concentration for samples collected from upper, middle, and lower plumes; NO ₃ ⁻ concentration versus K concentration for all three plumes; NO ₃ ⁻ concentration versus age for upper and middle plumes; B concentration versus age for upper and middle plumes; NO ₃ ⁻ to B ratio versus age for upper and middle plumes; and % Loss of NO ₃ ⁻ versus age for upper and middle plumes.	144
4.3.	Denitrification rates in groundwater containing septic effluent as a function of calculated initial nitrate concentration corrected for dilution.	146
4.4.	Dissolved organic carbon concentrations (DOC) in groundwater as a function of septic system plume age.	147

List of Figures (cont.)

5.1.	Lineweaver-Burke plot for forested sites used to estimate the half-saturation constant for denitrification with respect to nitrate (K_{NO_3}) and the maximum denitrification rate (V_{max}).	160
5.2.	Lineweaver-Burke plot for septic system site used to estimate the half-saturation constant for denitrification with respect to nitrate (K_{NO_3}) and the maximum denitrification rate (V_{max}).	161
5.3.	Denitrifying bacteria as a percentage of total bacterial population versus groundwater nitrate concentration measured in 3 Swedish aquifers.	164
5.4.	Nitrate losses by denitrification simulated over groundwater flowpaths using a saturating kinetics expression with respect to nitrate and dissolved organic carbon (DOC).	171
5.5.	Nitrate losses by denitrification simulated over groundwater flowpaths using a saturating kinetics expression with respect to nitrate.	173

CHAPTER 1:
INTRODUCTION

1. Anthropogenic Nitrogen and Eutrophication

A principal alteration of estuarine and coastal ecosystems worldwide is eutrophication brought about by increasing loads of anthropogenically-derived nitrogen (GESAMP 1990, NRC 1994, Nixon 1986) transported by freshwater to receiving coastal waters (Cole et al. 1993). In the U.S., regional resources such as Long Island Sound and Chesapeake Bay and local sites such as Waquoit Bay and Wellfleet Harbor are experiencing cultural eutrophication. Nitrogen transport rates are of critical importance because rates of coastal production, as well as many other key processes coupled to production, are set by nitrogen supply (Nixon 1986, Nixon et al. 1996, Howarth et al. 1996). The effects of eutrophication on coastal ecosystems are far-ranging, and can include red tides, fish kills, anoxia and hypoxia as currently observed over wide areas of the Gulf of Mexico, contamination of shellfish beds (NRC 2000), and alteration of valuable habitat including loss of eelgrass beds, such as that documented in Waquoit Bay, MA (Costa 1988).

In coastal areas underlain by unconsolidated sands, such as Cape Cod, the majority of land-derived N delivered to the coastal zone is transported by groundwater (Valiela et al. 1992, Cambareri and Eichner 1998). Nitrate contamination of freshwater aquifers is a significant concern since nitrate is toxic to human infants and livestock at high concentrations (Trudell et al. 1986).

Anthropogenic sources of nitrate to groundwater aquifers and coastal systems have increased dramatically, particularly over the last 40 years, with the greatest fluxes of N associated with areas of highest population density. Human activity has increased the flux of nitrogen in the Mississippi River approximately 4-fold, in the rivers of the northeastern United States 8-fold, and in the rivers draining the North Sea more than 10-fold (NRC 2000). The dominant sources of anthropogenic nitrogen are fertilizers, accounting for more than half of the human alteration of the nitrogen cycle (Vitousek et al. 1997); atmospheric deposition of NO_x from fossil fuel combustion, animal feed lots and other agricultural sources, which have increased more than 8-fold over pre-industrial levels (Holland et al. 1999); wastewater, which contributes 12% of the flux of nitrogen from the North Atlantic landscape to the North Atlantic Ocean (Howarth et al. 1996); and non-point sources (NRC 1993).

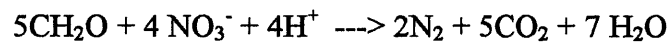
2. Transformations of Nitrogen within Aquifers

Understanding how N is transformed and transported within aquifers is necessary to calculating watershed N budgets, understanding basic nitrogen biogeochemistry, and estimating total N delivery to coastal waters. Previous mass balance data suggests that significant losses of N can occur within watersheds and aquifers (Lee and Olson 1985, Valiela et al. 1992, Valiela and Costa 1988, Weiskel and Howes 1992). Processes capable of attenuating mobile N include dilution, adsorption and incorporation in soils and forest biomass, assimilatory reduction into microbial biomass, dissimilatory nitrate reduction to (sorvable) ammonium (DNRA), and denitrification (Korom 1992). Of these

processes, only denitrification is effectively a permanent sink for biologically available nitrogen, and is hypothesized to be the most significant sink for N in aquifers (Peterjohn and Correll 1984, Valiela et al. 2000).

3. Denitrification

Denitrification, which converts biologically available nitrate to essentially inert N₂ (and small amounts of N₂O) is a microbially-mediated process that uses NO₃⁻ as an electron acceptor:



where organic carbon is represented as a simplified carbohydrate, CH₂O. Several conditions must be met for denitrification to occur, including a viable population of denitrifying bacteria, sufficient concentration of N oxides (NO₃⁻, NO₂⁻, NO and N₂O) as terminal e⁻ receptors, available and suitable e⁻ donors (e.g. primarily dissolved organic matter, but also compounds such as reduced manganese (Mn²⁺), ferrous iron (Fe²⁺) or sulfides, and anaerobic conditions or restricted O₂ availability (Firestone 1982). Rates of denitrification are thought to be governed by the supply of nitrate and carbon compounds, while suppressed by dissolved oxygen (Tiedje et al. 1982, Keeney 1986).

Some authors have argued that due to the aerobic nature of aquifers and the lack of suitable concentrations of labile organic substrates (Fisher 1977, Mulholland 1981), denitrification is unlikely. However, numerous studies suggest that denitrification occurs

in soils (Parkin 1987, Parkin and Robinson 1989, Christensen et al. 1990a, Christensen et al. 1990b, van Kessel et al. 1993, Groffman 1991, Groffman et al. 1996, Groffman and Tiedje 1989) and shallow groundwater (Jacinthe et al. 1998) in anaerobic “hotspots” within otherwise oxygenated waters. The existence of heterotrophic bacteria (*T. pantotropha*, Robertson et al. 1988, Dalsgaard et al. 1995; *Alcaligenes* sp., Krul 1976), and activated sewage sludge (Muller et al. 1995) capable of simultaneous heterotrophic nitrification and aerobic denitrification suggests another means by which denitrification in aerobic aquifers is plausible. In addition, denitrification ($-28.4 \text{ kcal equiv}^{-1}$) is almost as energetically favorable as aerobic respiration ($-29.9 \text{ kcal equiv}^{-1}$); therefore, it seems likely that organisms capable of exploiting this niche exist in groundwater. Finally, recent work suggests that there may be more organic matter in groundwater ($0.7\text{-}27 \text{ mg DOC l}^{-1}$, Ford and Naiman 1989, Fiebig et al. 1990, Fiebig 1995) than was previously thought to occur, providing a source of electron donors for denitrification in groundwater.

Many papers use mass balance methods to argue that significant losses of nitrogen by microbially-mediated denitrification occur in aquifers (Bengtsson and Annadotter 1989, Bottcher et al. 1990, Bragan et al. 1997a, Bragan et al. 1997b, Clay et al. 1996, Gillham 1991, Gold et al. 1998, Groffman et al. 1996, Jacinthe et al. 1998, Korom 1992, Peterjohn and Correll 1984, Valiela et al. 1992, Valiela et al. 2000, Verchot et al. 1997). Convincing evidence for denitrification in groundwater includes experimental injections in which NO_3^- disappears downgradient faster than conservative tracers, and in which the loss of NO_3^- is accompanied by increases in bicarbonate believed to be derived from

carbon mineralization associated with microbial denitrification (Korom 1991, Trudell et al. 1986). Other evidence suggests that changes in the ratio of N isotopes ($^{15}\text{N}/^{14}\text{N}$) in ambient NO_3^- or in injections of isotopically-enriched tracers, and/or changes in the concentration of N_2 , derive from denitrification in groundwater (Fustec et al. 1991, Mariotti et al. 1988, Smith et al. 1991, Vogel et al. 1981).

Rates of denitrification reported in the literature vary over several orders of magnitude (.004 to 1.05 mg N kg⁻¹ dry sediment per day in laboratory core incubations; 0.04 to 2.17 $\mu\text{M h}^{-1}$ in aquifers containing N derived from agriculture, Korom 1992), and likely reflect both the variability in biogeochemical conditions across aquifer settings and differing experimental approaches. Denitrification rates measured in controlled laboratory experiments have been modeled using the Michaelis-Menten enzyme kinetic equation with respect to nitrate concentration (Engberg and Schroeder 1975), and as a first-order function of organic carbon substrate (Brenner and Argamann 1990). It is our hypothesis that denitrification rates vary systematically with nitrate and DOC concentrations in groundwater.

4. Study Goals

The goal of this study was to estimate groundwater denitrification rates in the Waquoit Bay aquifer on Cape Cod, to examine how they vary as a function of nitrate and DOC concentrations, and to construct a predictive model that might be used to assess groundwater denitrification rates across the range of geochemical conditions present in

this aquifer. Waquoit Bay, a shallow estuary located on the southwest coast of Cape Cod, Massachusetts, is experiencing increasing eutrophication from anthropogenic nitrogen. Nitrogen loads to this system have been measured and modeled as function of land use patterns in the watershed (Nitrogen Loading Model, NLM, Valiela et al. 1997, Valiela et al. 2000), and consist primarily of wastewater (50%), fertilizer (17%), and atmospheric deposition. In NLM, a constant fraction of N reaching the water table (35%) is assumed to be lost by denitrification during transport through the underlying aquifer en route to Waquoit Bay.

Nitrate reduction rates, however, are likely to vary as a function of both electron donor and nitrate concentrations; N loss rates in groundwater, therefore, should be modeled to reflect variable chemical conditions. On Cape Cod, measured groundwater nitrate concentrations vary by several orders of magnitude. Concentrations in groundwater range from 0 to 2.7 μM beneath forested areas (Seely 1997), from < 1 to ~ 1,000 μM in the suburban subwatersheds of Waquoit Bay (Valiela et al. 2000) and around a pond in a residential area (Kroeger et al 1999), up to 1,800 μM within the Massachusetts Military Reservation wastewater plume (Savoie and LeBlanc 1998), and as high as 4,300 μM in close proximity to a septic tank (our unpublished data). Denitrification rates within this Cape Cod aquifer are likely to be similarly variable.

In this thesis, we investigated the controls on DOC fluxes to groundwater (Ch. 2). We hypothesized that 1) groundwater DOC concentrations decrease as the thickness of

the vadose zone (T_{vad}) through which recharge occurs increases, and 2) DOC concentrations in the saturated zone decrease with increasing depth below the water table (D_{wt}). We tested these hypotheses by measuring DOC concentrations in groundwaters beneath a range of vadose thicknesses and at a range of depths below the water table. We found that the deeper the vadose zone, the lower the concentration of DOC in groundwater near the water table; similarly, DOC concentrations decreased rapidly with increasing depth below the water table, suggesting quite active biogeochemical processing in these boundary environments.

In Chapter 3, we used a stable isotopic approach to estimate average denitrification rates occurring along groundwater flowpaths at two forested sites (Crane Wildlife Management Area and South Cape Beach) in and near the Waquoit Bay watershed. These sites provided a large range of groundwater nitrate (<1 to 91 μM) and DOC (0.04 to 23 mg C l^{-1}) concentrations. Denitrification rates increased with both increasing initial nitrate and DOC concentrations, ranging from 0 to $2.1 \times 10^{-3} \mu\text{M N h}^{-1}$. We compared these rates to those that we measured using mass balance of N in a septic plume (Ch. 4). First order denitrification rate constants with respect to nitrate were highest where groundwater DOC concentrations were highest: $k = 2.8 \text{ y}^{-1}$ in the septic plume ($\sim 26 \text{ mg C l}^{-1}$), $k = 1.6 \text{ y}^{-1}$ at South Cape Beach (DOC = 0.8 to 23.4 mg C l^{-1}), and $k = .25 \text{ y}^{-1}$ at Crane Wildlife (0.1 to 1.9 mg C l^{-1}), suggesting that denitrification rates were controlled by both nitrate and DOC concentration. We simulated N losses along groundwater flowpaths for the Crane Wildlife site; the results of this analysis suggested

that for the low DOC conditions at this site, a saturating kinetics expression with respect to nitrate best predicts nitrate concentrations measured at the downgradient well ports ($R^2 = 0.96$ for $[\text{NO}_3^-]_{\text{model}}$ vs. $[\text{NO}_3^-]_{\text{meas}}$).

In Chapter 5, we present an empirically-based saturating kinetics model describing groundwater denitrification under carbon and nitrate-limited conditions. Denitrification rates were described using a kinetic expression with double substrate limitation (with nitrate as the terminal electron acceptor and dissolved organic carbon (DOC) as the electron donor). The kinetic parameters were estimated from our field data (half saturation constant for NO_3^- (K_{NO_3})) and USGS field data (bacterial population ($[B]$), and from data available in the literature (maximum bacterial growth rate (μ_{max}), half saturation constant for DOC (K_{DOC}), and bacterial yield constant (Y)). The proposed model is able to reasonably predict N losses along groundwater flow paths, measured at the two forested sites, where DOC ranged from 0.04 to 23 mg C l^{-1} and nitrate ranged from <1 to 91 μM . Using higher values for the bacterial population ($[B]$) and the half-saturation constant (K_{NO_3}), we were also able to predict N losses due to denitrification within the very different biogeochemical conditions of the septic system plume ($[\text{NO}_3^-]_{\text{max}} \sim 4,400 \mu\text{M}$, $[\text{DOC}] \sim 26 \text{ mg C}^{-1}$, and presumably a larger and more active bacterial population). The model performs well over the wide range of geochemical conditions found at the three sites within this watershed ($R^2 = 0.92$, $m = 1.0$ for measured vs. modeled).

We conclude that the magnitude of the nitrate source, its travel distance to shore, and the DOC concentration in groundwater are useful predictors of N downgradient. The saturating kinetics model, with double substrate limitation by nitrate and DOC, developed here, provides a valuable tool for planners and managers interested in designing management strategies to control nitrogen loading to coastal waters. Such a model might be used in the design of setback limits for septic systems, in assessing the value of open spaces for N load reduction, in regulating wastewater disposal, and in watershed-wide land use planning.

5. References

- Bengtsson G., & Annadotter H (1989) Nitrate reduction in a groundwater microcosm determined by ^{15}N gas chromatography-mass spectrometry. *Appl. Env. Microbiol.* 55: 2861-2870.
- Bottcher J., Strebel O, Voerkelius S, & Schmidt H-L (1990) Using isotope fractionation of nitrate-nitrogen and nitrate-oxygen for evaluation of microbial denitrification in a sandy aquifer. *J. Hydrol.* 114: 413-424.
- Bragan RJ, Starr JL, & Parkin T (1997a) Acetylene transport in shallow groundwater for denitrification rate measurement. *J. Envir. Qual.* 26: 1524-1530.
- Bragan RJ, Starr JL, & Parkin TB (1997b) Shallow groundwater denitrification rates measured by acetylene block. *J. Envir. Qual.* 26: 1531-1538.
- Brenner A, & Argamann Y (1990) Effect of feed composition, aerobic volume fraction and recycle rate on nitrogen in the single-sludge system. *Wat. Res.* 24: 1041-1049.
- Cambareri TC, & Eichner EM (1998) Watershed delineation and ground water discharge to a coastal embayment. *Ground Wat.* 36(4): 626-634.
- Christensen S, Simkins S, & Tiedje JM (1990a) Spatial variation in denitrification: Dependency of activity centers on the soil environment. *Soil Sci. Soc. Am. J.* 54: 1608-1613.
- Christensen S, Simkins S, Tiedje JM (1990b) Temporal patterns of soil denitrification: Their stability and causes. *Soil Sci. Soc. Am. J.* 54: 1614-1618.
- Clay DE, Clay SA, Moorman TB, Brix-Davis K, Scholes KA, & Bender AR (1996) Temporal variability of organic C and nitrate in a shallow aquifer. *Wat. Res.* 30: 559-568.
- Cole JJ, Peierls BL, Caraco NF & Pace ML (1993) Nitrogen loading of rivers as a human-driven process *in* McDonnell MJ & Pickett STA (eds.) *Humans as Components of Ecosystems: The Ecology of Subtle Human Effects and Populated Areas* (pp 138-154). Springer-Verlag, New York, New York, U.S.A.
- Costa JE (1988) Distribution, production, and historical changes in abundance of eelgrass (*Zostera marina*) in southeastern Massachusetts. Ph.D. Thesis. Boston University, 352 p.

Dalsgaard T, de Zwart J, Robertson LA, Kuenen JG, & Revsbech NP (1995) Nitrification, denitrification and growth in artificial *Thiosphaera pantotropha* biofilms as measured with a combined microsensors for oxygen and nitrous oxide. *FEMS Microb. Ecol.* 17: 137-148.

Engberg DJ, & Schroeder ED (1975) Kinetics and stoichiometry of bacterial denitrification as a function of cell residence time. *Wat. Res.* 9: 1051-1054.

Fiebig DM, Lock MA, & Neal C (1990) Soil water in the riparian zone as a source of carbon for a headwater stream. *J. Hydrol.* 116:217-237.

Fiebig DM (1995) Groundwater discharge and its contribution of dissolved organic carbon to an upland stream. *Arch. Hydrobiol.* 134:129-155.

Firestone MK (1982) Biological denitrification *in* Nitrogen in Agricultural Soils, Stevenson, F.J., Ed. *Agron. Monogr.* 22, American Society of Agronomy, Madison, WI, 8

Fisher SG, & Likens GE (1973) Energy flow in Bear Brook, New Hampshire: An integrative approach to stream ecosystem metabolism. *Ecol. Monogr.* 48:421-439.

Ford TE, & Naiman RJ (1989) Groundwater-surface water relationships in boreal forest watersheds: Dissolved organic and inorganic nutrient dynamics. *Can. J. Fish. Aquat. Sci.* 46:41-49.

Fustec E, Mariotti A, Grillo X, & Sajus J (1991) Nitrate removal by denitrification in alluvial groundwater: Role of a former channel. *J. of Hydrol.* 123: 337-354.

GESAMP (1990) State of the Marine Environment. Rep. Stud. No. 39, Joint Group of Experts on the Scientific Aspects of Marine Pollution. United Nations Environment Programme. 111 p.

Gillham RW (1991) Nitrate contamination of ground water in southern Ontario and the evidence for denitrification. pp. 181-198 *in* Bogardi, I. and R.D. Kuzelka, editors. Nitrate Contamination. NATO ASI Series G, Vol. 30.

Gold AJ, Jacinthe PA, Groffman PM, Wright WR, & Puffer PH (1998) Patchiness in groundwater nitrate removal in a riparian forest. *J. Envir. Qual.* 27: 146-155.

Groffman PM (1991) Ecology of nitrification and denitrification in soil evaluated at scales relevant to atmospheric chemistry. p. 201-217, *in* JE Rogers and WB Whitman (ed.) Microbial production and consumption of greenhouse gases: Methane, nitrogen oxides, and halomethanes. Am. Soc. Microbiol., Washington, D.C.

Groffman PM, Howard G, Gold AJ, & Nelson WM (1996) Microbial nitrate processing in shallow groundwater in a riparian forest. *J. Environ. Qual.* 25: 1309-1316.

Groffman PM, & Tiedje (1989) Denitrification in north temperate forest soils: Spatial and temporal patterns at the landscape and seasonal scales. *Soil Biol. Biochem.* 21:613-620.

Holland EA, Dentener BH, Braswell BH, & Sulzman JM (1999) Contemporary and pre-industrial global reactive nitrogen budgets. *Biogeochemistry* 46:7-43.

Howarth RW, Billen G, Swaney D, Townsend A, Jaworski N, Lajtha K, Downing JA, Elmgren R, Caraco N, Jordan T, Berendse F, Freney J, Kudeyarov V, Murdoch P, & Zhao-Liang Z (1996) Regional nitrogen budgets and riverine nitrogen and phosphorus fluxes for the drainages to the North Atlantic Ocean: natural and human influences. *Biogeochemistry* 35:75-79.

Jacinte PA, Groffman PM, Gold AJ, & Mosier A (1998) Patchiness in microbial nitrogen transformations in groundwater in a riparian forest. *J. Environ. Qual.* 27: 156-164.

Keeney D (1986) Sources of nitrate to groundwater. *Crit. Rev. Environ. Contam.* 6:257-304.

Korom SF (1992) Natural denitrification in the saturated zone: A review. *Wat. Resources Res.* 28: 1657-1668.

Korom SF (1991) Denitrification in the unconsolidated deposits of the Heber Valley aquifer, Ph. D. thesis, 176 pp., Utah State Univ. Logan, Utah.

Krul JM (1976) Dissimilatory nitrate and nitrite reduction under aerobic conditions by an aerobically and anaerobically grown *Alcalgenes* sp. and by activated sludge. *J. Appl. Bacteriol.* 40:245-260.

Lee V, & Olson S (1985) Eutrophication and management initiatives for the control of nutrient inputs to Rhode Island coastal lagoons. *Estuaries* 8: 191-202.

Leenheer J, Malcolm RL, McKinley PW, & Eccles LA (1974) Occurrence of dissolved organic carbon in selected ground-water samples in the United States. *J. Res. U.S. Geol. Surv.* 2(3): 361-369.

Mariotti A, Landreau A, & Simon B (1988) ^{15}N isotope biogeochemistry and natural denitrification process in groundwater: Application to the chalk aquifer of northern France. *Geochim. Cosmochim. Acta* 52: 1869-1878.

Muller EB, Stouthamer AH, & van Verseveld HW (1995) Simultaneous NH₃ oxidation and N₂ production at reduced O₂ tensions by sewage sludge subcultured with chemolithotrophic medium. *Biodegrad.* 6: 339-349.

Mulholland PJ (1981) Organic carbon flow in a swamp-stream ecosystem. *Ecol. Monogr.* 51:307-322.

National Research Council (NRC) (2000) *Clean Coastal Waters: Understanding and Reducing the Effects of Nutrient Pollution.* National Academy Press, Washington, D.C. 405 p.

National Research Council (NRC) (1994) *Priorities for Coastal Science,* National Academy Press, Washington D.C. 88 p.

National Research Council (NRC) (1993) *Managing Wastewater in Coastal Urban Areas.* National Academy Press, Washington, D.C.

Nixon S, Oviatt CA, Frithsen J, and Sullivan B (1986) Nutrients and the productivity of estuarine and coastal marine ecosystems. *J. Limnol. Soc. S. Africa,* 12: 43-71.

Nixon SW, Ammerman JW, Atkinson LP, Berounsky VM, Billen G, Boicourt WC, Boyton WR, Church TM, DiToro DM, Elmgren R, Garber JH, Giblin AE, Jahnke RA, Owens NJP, Pilson MEQ, & Seitzinger SP (1996) The fate of nitrogen and phosphorus at the land-sea margin of the North Atlantic Ocean. *Biogeochemistry* 35: 141-180.

Parkin TB, & Robinson JA (1989) Stochastic models of soil denitrification. *Soil Sci. Soc. Am. J.* 49:651-957.

Parkin TB (1987) Soil microsites as a source of denitrification variability. *Soil Sci. Soc. Am. J.* 51: 1194-1199.

Parkin TB, Starr JL, & Meisinger JJ (1987) Influence of sample size on measurement of soil denitrification. *Soil Sci. Soc. Am. J., Div. S-3 - Soil Microbiology and Biochemistry,* 51: 1492-1501.

Peterjohn WT, & DL Correll (1984) Nutrient dynamics in an agricultural watershed: Observations on the role of riparian forest. *Ecol.* 65: 256-268.

Robertson LA, van Niel EWJ, Torremans RAM, & Kuenen JG (1988) Simultaneous nitrification and denitrification in aerobic chemostat cultures of *Thiosphaera pantotropa*. *Appl. Env. Microbiol.* 1988, 54: 2812-2818.

Savoie J, & LeBlanc DR (1998) *Water-Quality Data and Methods of Analysis for Samples Collected Near a Plume of Sewage-Contaminated Ground Water,* Ashumet

Valley, Cape Cod, Massachusetts, 1993-94. 97-4269, U.S. Department of the Interior, U.S. Geological Survey, Marlborough, Massachusetts.

Seely BA (1997) Atmospheric deposition and flux dynamics of nitrogen in the coastal forests of the Waquoit Bay Watershed, Cape Cod, MA. Ph.D. Thesis, Boston University, Boston, MA, 153 pp.

Smith RL, Howes BL, & Duff JH (1991) Denitrification in nitrate-contaminated groundwater: Occurrence in steep vertical geochemical gradients. *Geochim. Cosmochim. Acta* 55: 1815-1825.

Tiedje JM, Sextone AJ, Myrold DD, & Robinson A (1982) Denitrification: Ecological niches, competition and survival. *Antonie van Leeuwenhoek* 48:569-583.

Trudell MR, Gillham RW, & Cherry JA. (1986) An in-situ study of the occurrence and rate of denitrification in a shallow unconfined sand aquifer. *J. Hydrol.* 83: 251-268.

Valiela I, Collins G, Kremer J, Lajtha K, Geist M, Seely B, Brawley J, & Sham C.H. (1997) Nitrogen loading from coastal watersheds to receiving estuaries: new method and application. *Ecol. Appl.* 7(2): 358-380.

Valiela I & Costa J (1988) Eutrophication of Buttermilk Bay, a Cape Cod coastal embayment: Concentrations of nutrients and watershed nutrient budgets. *Environ. Manag.* 12: 539-553.

Valiela I, Foreman K, LaMontagne M, Hersh D, Costa J, Peckol P, DeMeo-Anderson B, D'Avanzo C, Babione M, Sham CH, Brawley J, & Lajtha K (1992) Couplings of watersheds and coastal waters: Sources and consequences of nutrient enrichment in Waquoit Bay, Massachusetts. *Estuaries* 15: 443-457.

Valiela I, Geist, M, McClelland J, & Tomasky G (2000) Nitrogen loading from watersheds to estuaries: Verification of the Waquoit Bay Nitrogen Loading Model. *Biogeochemistry* 49: 277-293.

van Kessel C, Pennock DJ, & Farrell RE (1993) Seasonal variations in denitrification and nitrous oxide evolution at the landscape scale. *Soil Sci. Soc. Amer. J.* 57: 988-995.

Vitousek PM, Aber J, Howarth RW, Likens GE, Matson PA, Schindler DW, Schlesinger WH, & Tilman GD (1997) Human alteration of the global nitrogen cycle: causes and consequences. 1, Ecological Society of America, Washington, D.C.

Vogel JC, Talma AS, & Heaton THE (1981) Gaseous nitrogen as evidence for denitrification in groundwater. *J. Hydrol.* 50: 191-200.

Weiskel PK, & Howes BL (1992) Differential transport of sewage-derived nitrogen and phosphorus through a coastal watershed. *Environ. Sci. Tech.* 26: 352-360.

CHAPTER 2:

**THE EFFECT OF VADOSE ZONE THICKNESS AND DEPTH
BELOW THE WATER TABLE ON DOC CONCENTRATION
IN GROUNDWATER ON CAPE COD, U.S.A**

Accepted by Biogeochemistry

Running head: DOC in groundwater

Article type: General research

Title: The effect of vadose zone thickness and depth below the water table on DOC concentration in groundwater on Cape Cod, U.S.A.

Authors: Wendy J. Pabich^{1*}, Ivan Valiela², and Harold F. Hemond¹.

Affiliations: 1) Massachusetts Institute of Technology, Department of Civil and Environmental Engineering, Ralph M. Parsons Laboratory, Cambridge, MA 02138, U.S.A.

2) Boston University Marine Program, Marine Biological Laboratory, Woods Hole, MA 02543, U.S.A.

Corresponding author: Wendy J. Pabich
c/o Boston University Marine Program
Marine Biological Laboratory
Woods Hole, MA 02543
USA
Telephone: (508) 289-7615
Fax: (508) 289-7949
Email: wjpabich@mit.edu

Key words: Cape Cod, DOC, groundwater, saturated zone, vadose

Abstract. Changes in concentration of dissolved organic carbon (DOC) reflect biogeochemical processes that determine chemical composition of groundwater and other natural waters. We found that the deeper the vadose zone, the lower the concentration of DOC in groundwater near the water table, indicating that considerable attenuation of surface-derived DOC occurred in the vadose zone. Under vadose zones <1.25 m, DOC concentrations at the surface of the water table ranged to >20 mg l⁻¹ C, while for vadose zones >5.0 m, DOC never exceeded 2.0 mg l⁻¹ C. DOC concentrations also decreased exponentially with increasing depth below the water table, most notably in the upper two meters, implying continued attenuation in the upper layer of the saturated zone. Ninety-nine percent of the DOC was attenuated by the time the water reached a depth of 19 m below the water table. DOC concentrations in shallow groundwater show considerable spatial variability, but the concentration of DOC at any one site is surprisingly stable over time. The largest source of variation in DOC concentration in groundwater therefore is spatial rather than temporal, suggesting that local heterogeneities play an important role in DOC delivery to shallow groundwater. Our results highlight both the importance of shallow vadose areas in DOC delivery to groundwater and the need to distinguish where samples are collected in relation to flow paths before conclusions are made about mean groundwater DOC concentrations. The substantial losses of DOC in the vadose zone and in shallow depths within the aquifer suggest quite active biogeochemical processes in these boundary environments.

1. Introduction

DOC alters chemical composition of surface and ground waters by acting as a substrate for microbial catabolism, an electron acceptor for anaerobic respiration, and a ligand for metal complexation, and by providing protons for acid/base chemistry, and nutrients that stimulate biological productivity. DOC is generated in soil organic horizons by microbial metabolism, root exudates, and leaching of organic matter (Schiff et al. 1996) and transported by recharge water to the saturated zone (Cronan and Aiken 1985; Thurman 1985; Clay et al. 1996) or by surface runoff (Jordan et al. 1997) to surface water bodies. Export of DOC from forested catchments depends on a complex, seasonally and spatially varying interplay of production, decomposition, sorption, precipitation, and hydrology (Cronan and Aiken 1985; Schiff et al. 1996).

DOC concentrations change as the organic matter is transported from the surface of a watershed to receiving waters. Cronan and Aiken (1985), McDowell and Likens (1988), Schiff et al. (1990), Easthouse et al. (1992), and Kookana and Naidu (1998) demonstrated that DOC in soil solutions decreased as recharge water percolates through soil horizons, from $> 70 \text{ mg l}^{-1} \text{ C}$ in upper soil horizons to $1\text{-}2 \text{ mg l}^{-1} \text{ C}$ in lower soil horizons. Mechanisms that may attenuate organic carbon as it percolates through soils include sorption and complexation with mineral surfaces (e.g. Fe and Al oxides and hydroxides) and clay minerals (Thurman 1985), microbial oxidation to CO_2 (Chapelle 1992), precipitation, flocculation and formation of insoluble complexes (Kookana and Naidu 1998), and filtering of organic colloids (Wan and Tokunaga 1997).

Several authors have pointed to the importance of the length or duration of hydrologic flow paths in controlling DOC delivery (Cronan and Aiken 1985). Easthouse et al. (1992) contend that work on inorganic constituents (Sullivan et al. 1986, Lawrence et al. 1988, Neal et al. 1989, Mulder et al. 1990) has demonstrated the importance of hydrologic flow paths in explaining variations in stream water chemistry. Similarly, Schiff et al. (1996) highlighted the importance of flow paths when they concluded that recently-fixed labile DOC leached from the A horizon or litter layer can only reach the stream via short flow paths that bypass locations where significant soil sorption occurs. Recharge is often spotty, and preferential flow paths, or fingers are likely to develop even in relatively homogeneous sandy soils (Parlange et al. 1999), potentially resulting in variable transport of DOC to groundwater.

Little information is available about the fate and transport of DOC either in the vadose zone or after it has reached the saturated zone. It seems likely that transport through the vadose zone and through groundwater aquifers provides additional opportunity for DOC to be attenuated by mechanisms similar to those thought to attenuate DOC in the unsaturated zone (e.g., sorption, complexation, microbial oxidation, precipitation, flocculation, formation of insoluble complexes, and filtering of organic colloids). Thus we hypothesize that: 1) groundwater DOC concentrations decrease as the thickness of the vadose zone (T_{vad}) through which recharge occurs increases, and 2) DOC concentrations in the saturated zone decrease with increasing depth below the water table (D_{wt}). We tested these hypotheses by measuring DOC concentrations in

groundwaters beneath a range of vadose thicknesses and at a range of depths below the water table.

2. Materials and methods

2.1 Study site

This work was carried out in the watershed of Waquoit Bay, a shallow estuary on the southwestern shore of Cape Cod, Massachusetts, subject to increasing eutrophication from groundwater-transported nitrogen. The watershed is underlain by an unconsolidated sole-source sand and gravel aquifer (Barlow and Hess 1993, Leblanc et al. 1986). The aquifer matrix is comprised of primarily quartz and feldspar sand (95%) with some ferromagnesian aluminosilicates and oxides (5%); sand grains are coated with hydrous oxides of aluminum and iron (Stollenwerk 1996). Average groundwater velocity is approximately 0.4 m per day (LeBlanc 1991), and annual recharge is 53 cm yr⁻¹ (Barlow and Hess 1993, LeBlanc 1984). Groundwater discharge to Waquoit Bay and its tributaries accounts for 89% of the total freshwater input to Waquoit Bay (Cambareri 1998), and is the primary avenue by which land-derived nitrogen is delivered to the estuary (Valiela et al. 1997).

We sampled groundwater near South Cape Beach and Sage Lot Pond in the southern part of the watershed (SCB), and in the Crane Wildlife Management Area to the north (CWMA). Both areas have mixed pitch pine and scrub oak forest cover and are typical of forested areas throughout Cape Cod. Other data are from USGS wells located in and near the watershed (Savoie and LeBlanc 1998).

2.2 Groundwater sample collection and analysis

At SCB, we collected groundwater using a drive-point piezometer and hand pump. Samples were taken in duplicate after multiple well volumes had been pumped and the water ran clear (generally after pumping 1-2 liters). We sampled from 12 stations on each of five sampling dates; we reached the water table in 56 of the 60 sampling attempts.

At CWMA, we installed and sampled from 3 multi-level sampling devices (MLS) (LeBlanc 1991). Each MLS had between 9 and 15 ports spanning from just below the water table to a maximum depth of 9.3 m below the water table. At each port a 0.64 cm diameter polyethylene tube protruded through a central 3.2 cm PVC pipe and was covered with a nylon screen (Smith et al. 1991). We collected groundwater samples in duplicate using a peristaltic pump (Geopump 2, Geotech Environmental Equipment, Inc.) after purging a minimum of 3 well volumes (13.8 ml per m tube length) from each port.

All samples were collected in 15 ml amber glass vials (Supelco #27088-U) previously soaked in a 5% Extran bath to remove any traces of organic carbon. Samples from the MLSs were filtered in-line during pumping using 0.7 μm Whatman GF/F filters. Samples obtained using the piezometer were vacuum filtered through the same GF/F filters upon return to the lab. All samples were acidified to $\text{pH} \approx 2$ with 5N HCl and stored in a cold room ($T = 4\text{ }^{\circ}\text{C}$) until analysis.

At SCB, we located the surface of the water table by first driving the piezometer below the water table (verified by drawing water), and then pulling it out of the ground in 0.1 m increments and attempting to pump at each position. We recorded the water table position as that depth where we could no longer draw water through the piezometer. At CWMA, we measured the thickness of the vadose zone by lowering a Fisher m-SCOPE Water Level Indicator into a nearby monitoring well (< 20 m) and measured the distance of the water table from land surface. Depth to the water table was tabulated for USGS wells in Savoie and LeBlanc (1998).

We measured DOC concentrations in triplicate Ar-purged samples using high temperature catalytic oxidation (HTCO) with infrared detection of CO₂ (Shimadzu TOC 5000). DOC data for USGS wells were taken from Savoie and LeBlanc (1998). Many of the USGS wells were drilled to investigate groundwater pollution emanating from the Massachusetts Military Reservation. We collected data only from wells located in areas of clean groundwater, either outside the boundaries of mapped wastewater plumes or having methyl blue active substances (MBAS) below 0.02 mg l⁻¹.

3. Results and Discussion

Groundwater DOC concentrations varied from 0.04 to 23.38 mg C l⁻¹ and averaged 2.31 ± 0.30 mg C l⁻¹. The wells provided a range of vadose thicknesses (T_{vad}) from 0.5 m to 17.5 m and water table depths (D_{wt}) from 0.01 to 51.8 m. We found, as did Cronan and Aiken (1985) and Easthouse et al. (1992), that DOC concentrations were

quite variable spatially, but more consistent temporally. For example, at the 12 SCB stations, where the vadose zone was routinely less than 1.5 m, DOC ranged from < 1 to 23 mg C l⁻¹, with a coefficient of variation of 77% (Fig. 2.1). Despite this spatial variability, when we sampled on 5 sampling dates at each of the 12 stations at SCB, we found that DOC was consistently high at some sampling points and consistently low at others. The average of the coefficients of variation of the time series data for each of the 12 stations was 37%. These observations suggests that local-scale heterogeneities in properties such as soil composition and thickness, the position of the water table relative to the soil organic layer, hydrologic flow paths, and recharge rates may provide more variation than temporal changes.

Concentrations of DOC were inversely related to both T_{vad} and D_{wt} (multiple regression of log transformed values, $R^2 = 0.68$, $p < 0.001$, Table 2.1). The two variables, T_{vad} and D_{wt} , were relatively independent: the highest variance inflation factor (VIF) (Sokal and Rohlf 1995) was 1.3, which suggests only minimal correlation between independent variables. To evaluate the relative influence of T_{vad} and D_{wt} on DOC concentration, we calculated Kruskal's index of importance (average of squared partial correlation coefficients) (Sokal and Rohlf 1995); the index was 0.58 for D_{wt} , and 0.23 for T_{vad} . This indicates that depth below the water table was relatively more important than vadose thickness in predicting DOC concentration. These analyses suggest that T_{vad} and

Figure 2.1. Mean DOC concentrations measured at 12 sampling stations at South Cape Beach on 5 sampling dates in 1998. Coefficient of variation between sampling stations is 77%; mean of coefficients of variation calculated for each sampling station is 37%. Standard error bars are shown.

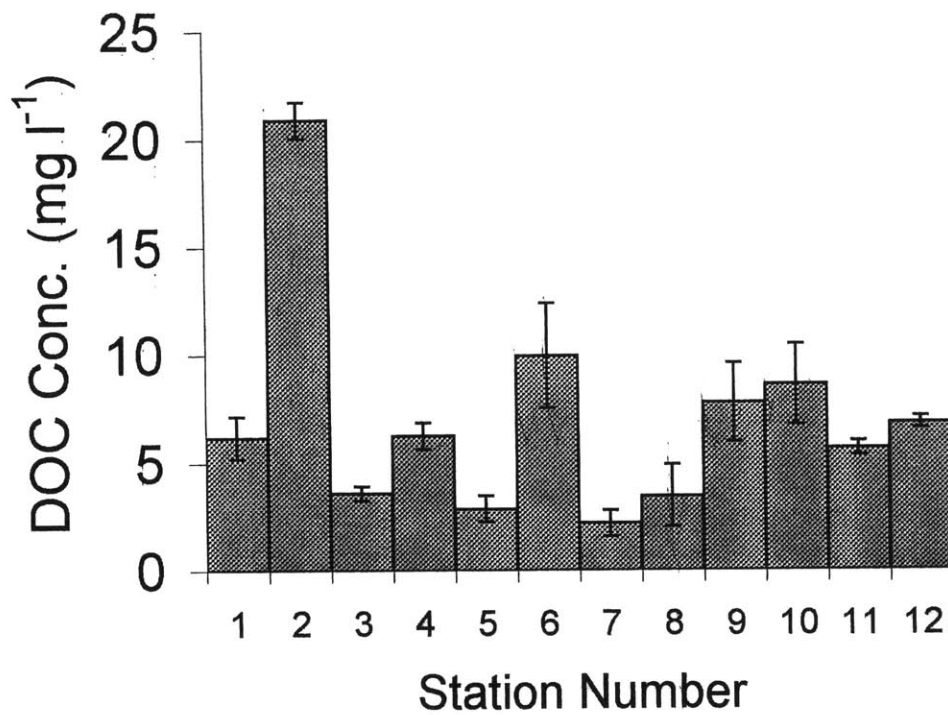


Table 2.1. Analysis of variance for multiple regression of effect of depth below the water table (D_{wt}) and vadose thickness (T_{vad}) on DOC concentration. Data were log-transformed. Regression equation: $\log \text{DOC} = -0.52D_{wt} - 0.39T_{vad} + 0.19$; $R^2 = 0.68$; df = degrees of freedom, SS = sum of squares, MS = mean squares, and F = sample variance. For probability < 0.001 , $df = 2$ and 189 , critical F value (F_{crit}) < 7.32 .

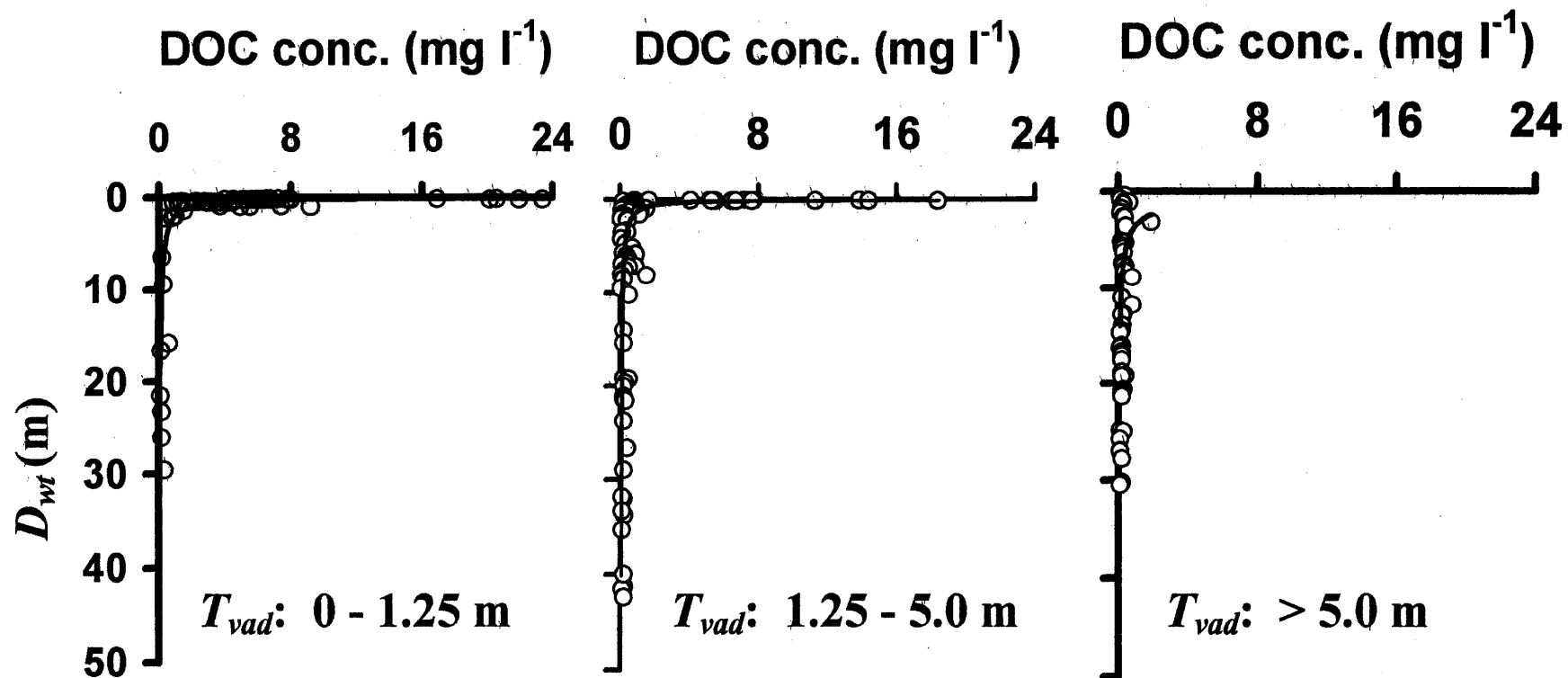
	df	SS	MS	F
Regression	2	58.58	29.29	204.90***
T_{vad}	1	4.58	4.58	32.02***
D_{wt}	1	30.86	30.86	215.89***
Residual	189	27.02	0.14	
Total	191	85.59	0.45	

D_{wt} were relatively independent, and both contributed significantly to DOC concentrations in the aquifer.

To examine in more detail the effect of varying vadose thickness on losses of DOC within the aquifer, we stratified the data into three categories of T_{vad} (0-1.25, 1.25-5.00, and >5.00 m), and plotted DOC as a function of depth below the water table (Fig. 2.2). DOC concentrations at the water table were highest in groundwater under areas with the shallowest vadose zones, and decreased with increasing vadose thickness. This supports the hypothesis that DOC concentrations decrease as T_{vad} increases.

DOC concentrations also decreased with increasing depth below the water table. Reductions occurred particularly within the upper few meters of the water table, and resulted in DOC losses totaling two orders of magnitude. To better examine the

Figure 2.2. DOC concentration as a function of depth below water table for each of three vadose thickness (T_{vad}) strata: 0 - 1.25m, 1.25 - 5.0 m, and > 5.0 m.

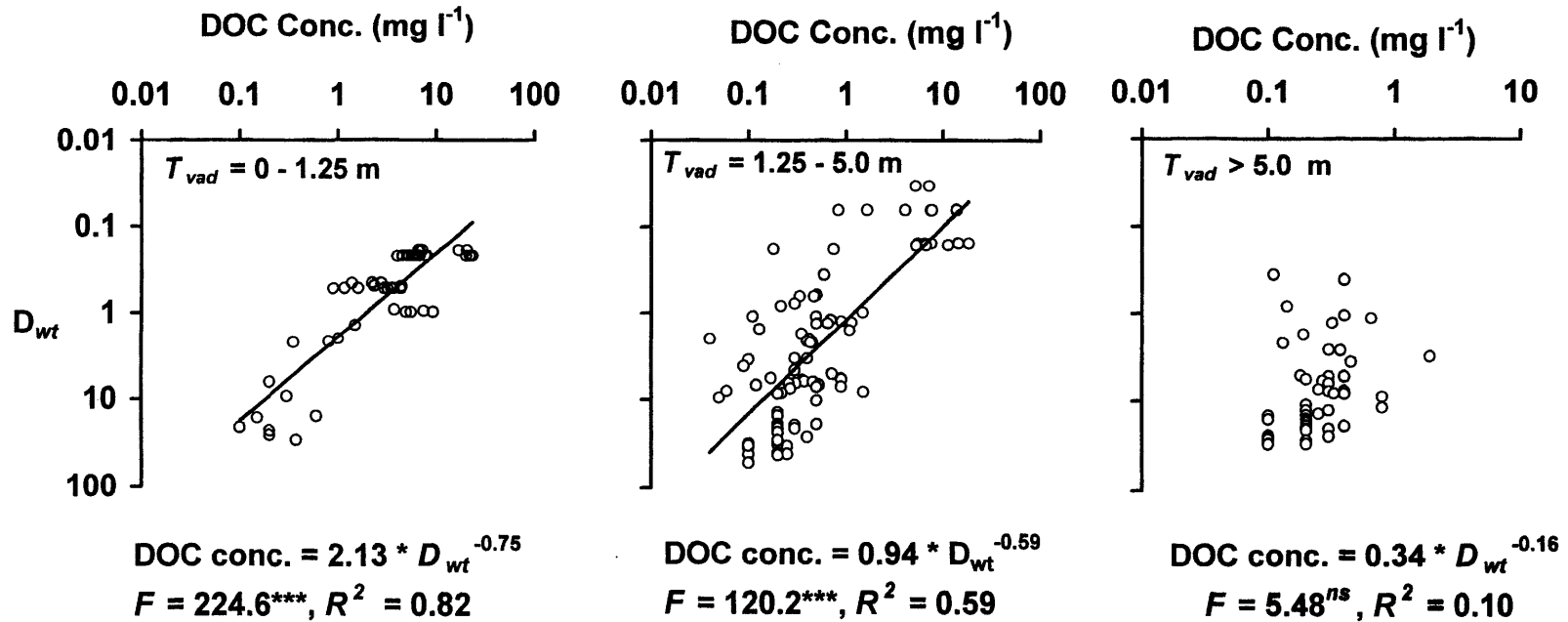


reduction of DOC concentration with D_w , we log-transformed the data (Fig. 2.3). The data could be reasonably well fit with an exponential curve ($R^2 = 0.82$ for $T_{vad} = 0-1.25$; $R^2 = 0.59$ for $T_{vad} = 1.25 - 5.0$ m; $R^2 = 0.10$ for $T_{vad} > 5.0$ m). These losses imply that DOC reaching groundwater was biologically labile. For $T_{vad} = 0 - 1.25$ m, 99% of the DOC was lost by the time a depth of 19 m was reached. A surprising result is that regardless of vadose thickness, and thus of the concentration of DOC at the surface of the water table, the DOC concentration at the deepest wells was similarly low (about 0.1 mg C l^{-1}) (Fig. 2.3). It is as if the labile portion of the DOC was intercepted in the vadose zone *or* in the aquifer, and that in either case, DOC concentrations at depth converged.

In this aquifer, depth is a remarkably close proxy for time (Solomon et al. 1995, Portniaguine and Solomon 1998). Using data on age of the groundwater in this aquifer, we can calculate that at a depth of 19 m, groundwater has traveled approximately 15.8 years since recharge (Vogel 1967). Therefore, for $T_{vad} = 0 - 1.25$ m, the mean DOC loss rate between the surface and 19 m was approximately $1.5 \text{ mg C l}^{-1} \text{ yr}^{-1}$. In contrast, for $T_{vad} > 5$ m, the loss rate over this same distance was about $0.12 \text{ mg C l}^{-1} \text{ yr}^{-1}$. The difference in attenuation rates supports the conclusion that T_{vad} strongly controls the transport and concentration of DOC reaching the surface of the aquifer.

We further investigated the depth dependence of the DOC loss rate by taking the first derivative (dy/dz) of the fitted curve (a power function curve fit) for each T_{vad}

Figure 2.3. DOC concentration plotted as a function of depth below water table (D_{wt}) for each of three vadose thickness (T_{vad}) strata: 0 - 1.25 m, 1.25 - 5.0 m, and > 5.0 m. Axes are logarithmic; *** denotes probability < 0.001, *ns* = not significant.



category (Fig. 2.4). The DOC loss rate quickly diminished with depth for all T_{vad} categories. At depth (~30 m), where DOC losses were small, the rate of attenuation was lowest for groundwater beneath the thickest vadose zones. This supports the notion that processes in the vadose zone affect the quality of the DOC in the saturated zone (and thus the rate at which it is metabolized). It seems that the more labile forms of DOC are selectively removed during transport through the unsaturated zone, so that only more refractory DOC may reach the aquifer in those areas with thick vadose zones.

Our interest in understanding how DOC is distributed in groundwater stems from the larger question of how nitrogen is transported to receiving waters and to what degree denitrification in groundwater is limited by the supply of DOC. Research suggests that many aquifers do not contain sufficient organic matter to produce the anaerobic conditions required for denitrification (Bryan, 1981; Parkin and Meisinger, 1989; Thurman, 1985; Barcelona, 1984; Lind and Eiland, 1989; McCarty and Bremner, 1982; Obenhuber and Lawrence, 1991). Groundwater DOC values reported in the literature from a wide range of aquifer settings and depths (Fig. 2.5) suggest, first, that there are many places where groundwater contains significant concentrations of DOC. These concentrations may be sufficiently high to support denitrification. Our measurements of DOC concentrations fall within the wide range reported in the literature. The data in Figure 2.5 can also be used to make a second point: sampling groundwater at depth may provide underestimates of DOC dynamics in aquifers. The rather steep gradient in DOC

Figure 2.4. Instantaneous DOC loss rate as a function of depth below water table for each of three vadose thickness strata (T_{vad}): 0 - 1.25m, 1.25 - 5.0 m, and >5.0 m. Loss rate was calculated as the first derivative (dy/dz) of the fitted power curve for DOC versus D_{wt} for each of the 3 T_{vad} classes, and solved for at each measured depth.

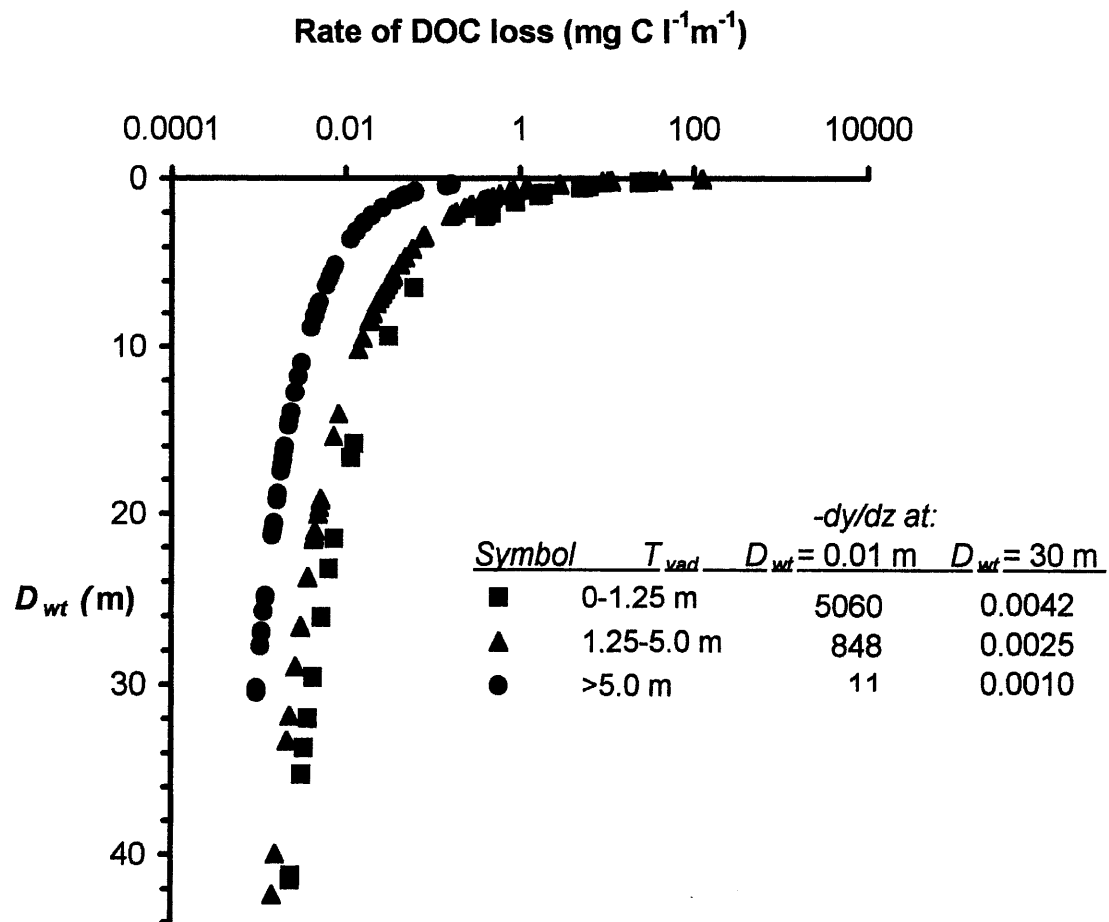
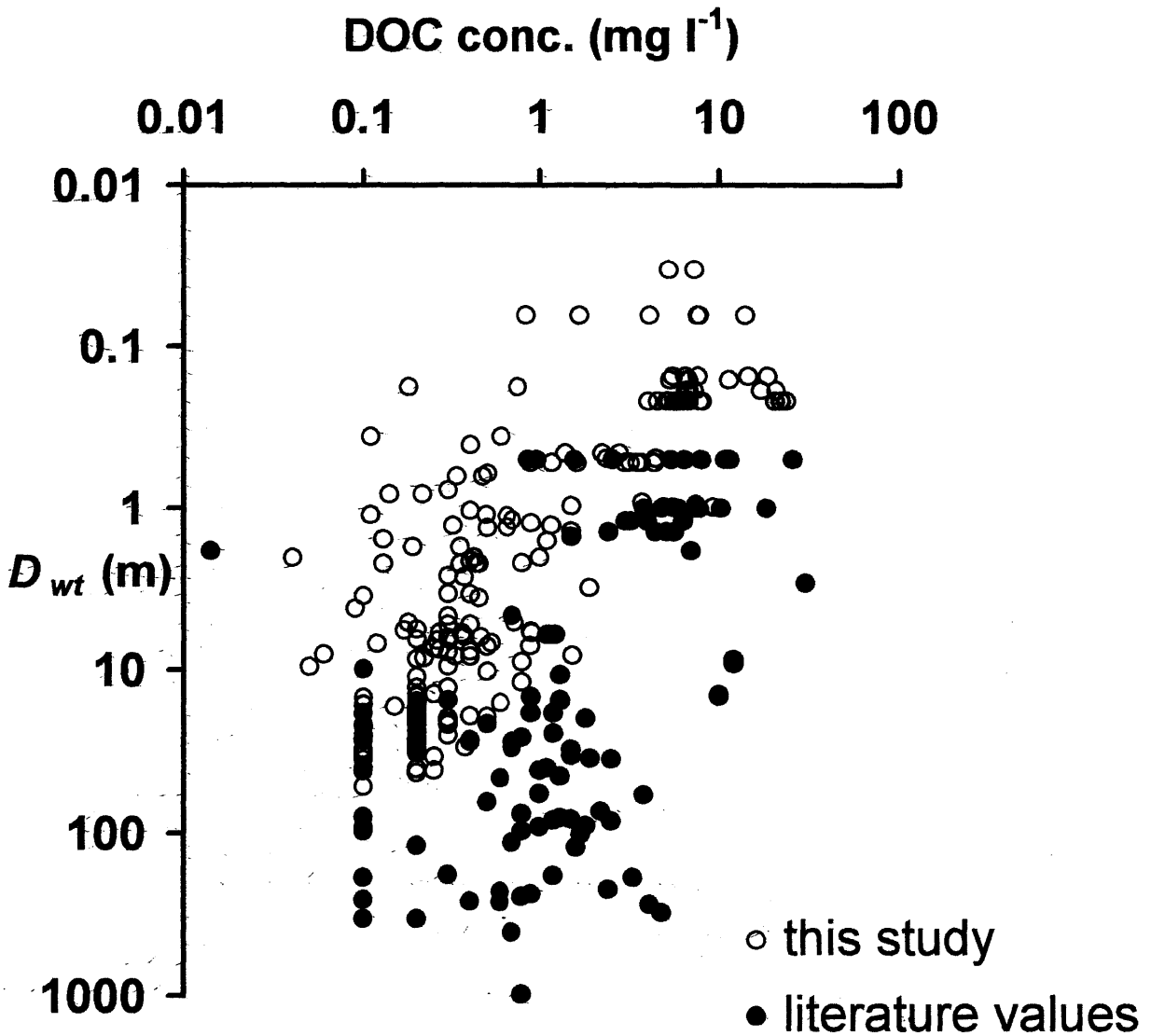


Figure 2.5. DOC concentrations in groundwater as a function of depth. White circles represent the data from this study. Black circles represent data from the literature (Leenheer et al. 1974; Aelion et al. 1997; Ellis et al. 1998; Ford & Naiman 1989; Hakenkamp et al. 1994; Hendricks & White 1995; Keller 1991; Rutherford & Hynes 1987; Schindler & Krabbenhoft 1998).



concentration that we found near the water table suggests that measurements of DOC in samples from deep groundwater wells may not only fail to describe the dynamics of DOC, but may underestimate mean groundwater DOC concentrations. The strong attenuation of DOC concentration within the vadose zone and the upper portion of the water table suggests that these sites are potentially those where biogeochemical transformations, including denitrification, should be active, and should be measured.

The comparison of published DOC concentrations (black circles, Fig. 2.5) relative to the values we report here (white circles, Fig. 2.5) also makes a third point: in general, despite the scatter in the data, it appears that DOC concentrations do decrease with increasing depth below the water table. Of course, the scatter of points from the diverse sites makes the pattern less obvious, but it is nonetheless true that the larger concentrations of DOC tend to lie in the shallower layers, as we demonstrate in our own data in some detail.

The results we include here demonstrate that there are tight biogeochemical couplings among components of the below-ground ecosystems. Labile DOC is intercepted near or in boundaries layers, either in the vadose zone or in the shallow aquifer, leaving only a small concentration of DOC for transport to open receiving waters. Such large decreases in DOC must follow significant stoichiometric relationships linking carbon dynamics to other elements. Investigation of the stoichiometry is the next step suggested by the large transformations documented in this paper.

4. Acknowledgements

MIT Sea Grant (# 65591) and a National Estuarine Research Reserve (NERRS) Graduate Fellowship from the National Oceanic and Atmospheric Association (NA77OR024) supported this work. We thank Denis LeBlanc of the US Geological Survey, Marlborough, MA for well construction and installation, site access, and worthy advice; John MacFarland at MIT for assistance with the Shimadzu TOC analyzer; Vanessa Bhark also at MIT, who helped analyze our DOC samples as part of her summer internship; and Gabrielle Tomasky, at the Boston University Marine Program, for field and lab assistance.

5. References

- Aelion CM, Shaw JN & Wahl M (1997) Impact of suburbanization on ground water quality and denitrification in coastal aquifer sediments. *J. of Exper. Mar. Biol. Ecol.* 213: 31-51
- Barcelona MJ (1984) TOC determination in groundwater. *Ground Water* 22: 18-24
- Barlow PM & Hess KM (1993) Simulated Hydrologic Responses of the Quashnet River Stream-Aquifer System to Proposed Ground-Water Withdrawals, Cape Cod, Massachusetts. U.S. Geological Survey, Water-Resources Investigations Report 93-4-64, Marlborough
- Bryan BA (1981) Physiology and biochemistry of denitrification. In: Delwiche CC (Ed) *Denitrification, Nitrification, and Atmospheric Nitrous Oxide* (pp 67-84). Wiley, New York
- Cambareri TC & Eichner EM (1998) Watershed delineation and ground water discharge to a coastal embayment. *Ground Water* 36: 626-634
- Chapelle FH (1992) *Ground-Water Microbiology & Geochemistry*. John Wiley & Sons, Inc., New York
- Clay DE, Clay SA, Moorman TB, Brix-Davis K, Scholes KA & Bender AR (1996) Temporal variability of organic C and nitrate in a shallow aquifer. *Water Res.* 30: 559-568
- Cronan CS & Aiken GR (1985) Chemistry and transport of soluble humic substances in forested watersheds of the Adirondack Park, New York. *Geochim. Cosmochim. Acta* 49: 1697-1705
- Ellis B, Stanford JA & Ward JV (1998) Microbial assemblages and production in alluvial aquifers of the Flathead River, Montana, USA. *J. N. Am. Benthol. Soc.* 17: 382-402
- Easthouse KB, Mulder J, Christophersen N & Seip HM (1992) Dissolved organic carbon fractions in soil and stream water during variable hydrological conditions at Birkenes, Southern Norway. *Water Resources Res.* 28: 1585-1596
- Ford T & Naiman RJ (1989) Groundwater-surface water relationships in boreal forest watersheds: dissolved organic carbon and inorganic nutrient dynamics. *Can. J. Fish. Aquat. Sci.* 46: 41-49
- Hakenkamp C, Palmer MA & James BR (1994) Metazoans from a sandy aquifer: dynamics across a physically and chemically heterogeneous groundwater system. *Hydrobiologia* 287: 195-206

- Hendricks S & White DS (1995) Seasonal biogeochemical patterns in surface water, subsurface hyporheic, and riparian ground water in a temperate stream ecosystem. *Arch. Hydrobiol.* 134: 459-490
- Jordan TE, Correll DL & Weller DE (1997) Relating nutrient discharges from watersheds to land use and streamflow variability. *Water Resources Res.* 33: 2579-2590
- Keller C (1991) Hydrogeochemistry of a clayey till 2. Sources of CO₂. *Water Resources Res.* 27: 2555-2564
- Kookana, RS & Naidu R (1998) Vertical heterogeneity in soil properties and contaminant transport through soil profiles. In: P Dillon & Simmers I (Eds) *International Contributions to Hydrology 18: Shallow Groundwater Systems* (pp 15-28). A.A. Balkema, Rotterdam
- Lawrence GB, Driscoll CT & Fuller RD (1988) Hydrologic control of aluminum chemistry in an acidic headwater stream. *Water Resources Res.* 24: 659-669
- LeBlanc DR (1984) Sewage plume in a sand and gravel aquifer, Cape Cod, Massachusetts. U.S. Geological Survey, Water-supply paper 2218, Washington
- LeBlanc DR, Guswa JH, Frimpter MH & Londquist CJ (1986) Ground-water resources of Cape Cod, Massachusetts: U.S. Geological Survey Hydrologic Atlas 692
- LeBlanc DR, Garabedian SP, Hess KM, Gelhar LW, Quadri RD, Stollenwerk KG & Wood WW (1991) Large-scale natural gradient tracer test in sand and gravel, Cape Cod, Massachusetts 1. Experimental design and observed tracer movement. *Water Resources Res.* 27: 895-910
- Leenheer J, Malcolm RL, McKinley PW & Eccles LA (1974) Occurrence of dissolved organic carbon in selected ground-water samples in the United States. *J. Res. U.S. Geol. Survey* 2: 361-369
- Lind A & Eiland F (1989) Microbial characterization and nitrate reduction in subsurface soils. *Biol. Fert. Soils* 8: 197-203
- McCarty GW & Bremner JM (1992) Availability of organic carbon for denitrification of nitrate in subsoils. *Biol. Fert. Soils* 14: 219-222
- McDowell WH & Likens GE (1988) Origin, composition, and flux of dissolved organic carbon in the Hubbard Brook Valley. *Ecol. Monogr.* 58: 177-195
- Mulder J, Pijpers M & Christophersen N (1991) Water flow paths and the spatial distribution of soils and exchangeable cations in an acid rain impacted and a pristine catchment (Norway). *Water Resources Res.* 27: 2919-2928

Neal C, Reynolds B, Stevens P & Hornung M (1989) Hydrogeochemical controls for inorganic aluminium in acid stream and soil waters at two upland catchments in Wales. *J. Hydrol.* 106:155-175

Obenhuber D & Lowrance R (1991) Reduction of nitrate in aquifer microcosms by carbon additions. *J. Environ. Qual.* 20: 255-258

Parkin TB & Meisinger JJ (1989) Denitrification below the crop rooting zone as influenced by surface tillage. *J. Environ. Qual.* 18: 12-16

Parlange, J.-Y., Steenhuis TS, Haverkamp R, Barry DA, Culligan PJ, Hogarth WL, Parlange MB, Ross P & Stagnitti F (1999) Soil properties and water movement. In: Parlange MB & JW Hopmans (Eds) *Vadose Zone Hydrology*. Oxford University Press, New York

Portniaguine O & Solomon DK (1998) Parameter estimation using groundwater age and head data, Cape Cod, Massachusetts. *Water Resources Res.* 34: 637-645

Rutherford J & Hynes HBN (1987) Dissolved organic carbon in streams and groundwater. *Hydrobiologia* 154: 33-48

Savoie J & LeBlanc DR (1998) Water-Quality Data and Methods of Analysis for Samples Collected Near a Plume of Sewage-Contaminated Ground Water, Ashumet Valley, Cape Cod, Massachusetts, 1993-94. U.S. Geological Survey, Marlborough

Schiff SL, Aravena R, Trumbore SE, Hinton MJ, Elgood R & Dillon PJ (1997) Export of DOC from forested catchments on the Precambrian Shield of Central Ontario: clues from ^{13}C and ^{14}C . *Biogeochemistry* 36:43-65

Schindler J & Krabbenhoft DP (1998) The hyporheic zone as a source of dissolved organic carbon and carbon gases to a temperate forested stream. *Biogeochemistry* 43: 157-174

Smith RL, Howes BL & Duff JH (1991) Denitrification in nitrate-contaminated groundwater: occurrence in steep vertical geochemical gradients. *Geochim. Cosmochim. Acta* 55: 1815-1825

Sokal RR & Rohlf FJ (1995) *Biometry: The Principles and Practice of Statistics in Biological Research*. W.H. Freeman and Company, New York

Solomon DK, Poreda RJ, Cook PG & Hunt A (1995) Site characterization using $^3\text{H}/^3\text{He}$ ground-water ages, Cape Cod, MA. *Ground Water* 33: 988-996

Stollenwerk KG (1996) Simulation of phosphate transport in sewage-contaminated groundwater, Cape Cod, Massachusetts. *Appl. Geochem.* 11: 317-324

Thurman EM (1985) *Organic Geochemistry of Natural Waters*. Martinus Nijhoff/DR W. Junk Publishers, Dordrecht

Sullivan TJ, Christopherson N, Muniz IP, Seip HM & Sullivan PD (1986) Aqueous aluminium chemistry response to episodic increases in discharge. *Nature* 323: 324-327

Valiela I, Collins G, Kremer J, Lajtha K, Geist M, Seely B, Brawley J, and Sham CH (1997) Nitrogen loading from coastal watersheds to receiving estuaries: new method and application. *Ecol. Appl.* 7: 358-380

Vogel JC (1967) Investigation of groundwater flow with radiocarbon. In: *Isotopes in Hydrology* (pp. 355-369). IAEA-SM-83/24, Vienna

Wan J & Tokunaga TK (1997) Film straining of colloids in unsaturated porous media: conceptual model and experimental testing. *Environ. Sci. Technol.* 31: 2413-2420

CHAPTER 3:

DENITRIFICATION RATES IN GROUNDWATER, CAPE COD, U.S.A.: CONTROL BY NITRATE AND DISSOLVED ORGANIC CARBON CONCENTRATIONS

Running head: Denitrification in groundwater

Article type: General research

Title: Denitrification rates in groundwater, Cape Cod, USA:
Control by NO_3^- and DOC concentrations

Authors: Wendy J. Pabich^{1*}, Harold F. Hemond¹, and Ivan Valiela².

Affiliations: 1) Massachusetts Institute of Technology, Department of
Civil and Environmental Engineering, Ralph M. Parsons
Laboratory, Cambridge, MA 02138, U.S.A.

2) Boston University Marine Program, Marine Biological
Laboratory, Woods Hole, MA 02543, U.S.A.

Corresponding author: Wendy J. Pabich
c/o Boston University Marine Program
Marine Biological Laboratory
Woods Hole, MA 02543
USA
Telephone: (508) 289-7615
Fax: (508) 289-7949
Email: wjpabich@mit.edu

Key words: Cape Cod, denitrification, groundwater, nitrogen
attenuation, saturated zone

Abstract. Eutrophication by land-derived anthropogenic nitrogen (N) is a major cause of alterations to coastal systems worldwide. Modeling N delivery to coastal waters is therefore critical to designing appropriate land use and management strategies to control N loading. Key to calculating watershed N budgets is understanding N losses by denitrification as groundwater is transported through aquifers en route to receiving estuaries. We used a stable isotope approach to estimate denitrification rates in groundwater in and near the Waquoit Bay watershed on Cape Cod, USA. Two field sites provided a large range of groundwater nitrate and dissolved organic carbon (DOC) concentrations. Nitrification, although understandably important in the soils layer and vadose zone, produced only minimal amounts of nitrate in the saturated zone, evidently due to a limited supply of ammonium in the groundwater. Denitrification rates increased with both increasing initial nitrate and DOC concentrations, and ranged from 0 to $2.1 \times 10^{-3} \mu\text{M N h}^{-1}$. We compared these rates to those measured in a septic plume (Ch. 4). First order denitrification rate constants with respect to nitrate were highest where groundwater DOC concentrations were highest, suggesting that, independent of nitrate concentration, DOC concentration exerts a significant control on denitrification rates. In previous work (Ch. 2) we showed that groundwater DOC concentrations decreased as the thickness of the vadose (unsaturated) zone through which recharge occurred increased. As a result, higher denitrification rates are likely to be found in those areas where the vadose zone is thinnest. A simulation of N losses along groundwater flowpaths at Crane Wildlife suggests that a saturating kinetics expression with respect to nitrate best predicts nitrate concentrations measured at the downgradient well ports. We conclude that it is critical to consider the magnitude of individual NO_3^- sources, travel distances to shore, and DOC concentrations in groundwater in assessing the downgradient impact of various N sources, and in designing strategies to control anthropogenic nitrogen loading.

1. Introduction

Eutrophication by land-derived anthropogenic nitrogen (N) is a major cause of alterations to coastal ecosystems worldwide (GESAMP 1990, NRC 1994, Nixon 1986). In the US, Long Island Sound, NY, and Chesapeake Bay, MD, and sites such as Waquoit Bay and Wellfleet Harbor on Cape Cod, MA, are experiencing cultural eutrophication. In these and many other estuaries, excess nutrients, largely N, are inducing loss of commercially important fish species, contamination of shellfish beds, and alteration of valuable habitat including eelgrass beds (Costa 1988, GESAMP 1990, NRC 1994, NRC 2000, Nixon et al. 1986, Howarth et al. 1996).

In coastal areas underlain by unconsolidated sands, such as Cape Cod, the majority of land-derived N delivered to the coastal zone is transported by groundwater (Valiela et al. 1992). Understanding how N is transformed and transported within aquifers is therefore necessary to calculating watershed N budgets, understanding basic nitrogen biogeochemistry, and estimating total N delivery to coastal waters. Previous mass balance data suggests that significant losses of N can occur within watersheds and aquifers (Lee and Olson 1985, Valiela et al. 1992, Valiela and Costa 1988). Processes capable of attenuating mobile N include dilution, adsorption and incorporation in soils and forest biomass, assimilatory reduction into microbial biomass, dissimilatory nitrate reduction to (sorvable) ammonium (DNRA), and denitrification (Korom 1992).

Denitrification is a significant sink for N in aquifers, as argued in many papers using mass balance methods (Bengtsson and Annadotter 1989, Bottcher et al. 1990,

Bragan et al. 1997, Bragan et al. 1997a, Clay et al. 1996, Gillham 1991, Gold et al. 1998, Groffman et al. 1996, Jacinthe et al. 1998, Korom 1992, Peterjohn and Correll 1984, Valiela et al. 1992, Valiela et al. 2000, Verchot et al. 1997). Convincing evidence for denitrification in groundwater includes experimental injections in which NO_3^- disappears downgradient faster than conservative tracers, and in which the loss of NO_3^- is accompanied by increases in bicarbonate believed to be derived from carbon mineralization associated with microbial denitrification (Korom 1991, Trudell et al. 1986). Other evidence suggests that changes in the ratio of N isotopes ($^{15}\text{N}/^{14}\text{N}$) in ambient NO_3^- or in injections of isotopically-enriched tracers, and/or changes in the concentration of N_2 , derive from denitrification in groundwater (Fustec et al. 1991, Mariotti et al. 1988, Smith et al. 1991, Vogel et al. 1981). Rates of denitrification reported in the literature span several orders of magnitude (0.004 to $1.05 \text{ mg N kg}^{-1}$ dry sediment per day in laboratory core incubations; 0.04 to $2.17 \mu\text{M h}^{-1}$ in aquifers containing N derived from agriculture, Korom 1992), and likely reflect both the variability in biogeochemical conditions across aquifer settings and differing experimental approaches.

Denitrification rates measured in controlled laboratory experiments have been modeled using the Michaelis-Menten enzyme kinetic equation with respect to nitrate concentration (Engberg and Schroeder 1975), and as a first-order function of organic carbon substrate (Brenner and Argamann 1990). Because, in general, reduction rates are likely to vary as a function of both electron donor and nitrate concentrations, N loss rates in groundwater should be modeled to reflect variable chemical conditions.

Concentrations of organic matter and nitrate in groundwater are patchy and may result in spatially variable denitrification rates. DOC concentrations in groundwater range from 0.1-27 mg DOC l⁻¹ (Pabich et al. submitted, Ford and Naiman 1989, Fiebig et al. 1990, Fiebig 1995), and mean concentrations may be higher than previous studies suggest (e.g. Leenheer et al. 1974). On Cape Cod, measured groundwater nitrate concentrations vary by several orders of magnitude. Concentrations in groundwater range from 0 to 2.7 μM beneath forested areas (Seely 1997), from < 1 to ~ 1,000 μM in the suburban subwatersheds of Waquoit Bay (Valiela et al. 2000) and around a pond in a residential area (Kroeger et al 1999), up to 1,800 μM within the Massachusetts Military Reservation wastewater plume (Savoie and LeBlanc 1998), and as high as 4,300 μM in close proximity to a septic tank (our unpublished data). Denitrification rates within this Cape Cod aquifer are likely to be similarly variable. The goal of this study was to estimate groundwater denitrification rates and to examine how they vary as a function of nitrate and DOC concentrations.

2. Approach

Stable isotopes of N have been used effectively to study denitrification (Mariotti et al. 1988, Bottcher et al. 1990, Smith et al. 1991). We used such an approach to estimate both nitrification and denitrification rates occurring in groundwater after the time of recharge to the water table. We measured ¹⁵N natural abundance variations (Mariotti et al. 1988) in ammonium and nitrate in groundwater samples obtained from wells installed in locations within the aquifer where NO₃⁻ and DOC concentrations differed significantly. Using the Rayleigh equation, which expresses the evolution of the

isotopic composition of residual nitrate (or ammonium) during denitrification (or nitrification), we estimated initial ammonium and nitrate concentrations at the water table, from which losses due to nitrification and denitrification were assessed. Such mass balance data were coupled with a groundwater age model (Vogel 1967) to estimate nitrification and denitrification rates, respectively.

3. Nitrogen isotope geochemistry

Because denitrifying organisms preferentially utilize the lighter isotope of nitrogen (^{14}N), fractionation of the nitrogen isotopes in the reactants and the products occurs. The result is a predictable enrichment of ^{15}N in residual substrate NO_3^- and depletion in the N_2 and N_2O products of denitrification. This process has been described as a single-step, unidirectional reaction (Mariotti et al. 1981, 1988), in which the ^{15}N content of the NO_3^- is a simple function of the progress of the reaction.

Isotopic fractionation occurs as a result of many biological (and abiotic) reactions, including both nitrification and denitrification. The Rayleigh equation expresses the evolution of the isotopic composition of the residual (reactant) material, and can be used to model both nitrification and denitrification. The relationship is expressed as:

$$(1) \quad \delta_s = \delta_{s0} + \epsilon \ln (C/C_0),$$

where δ_s represents the isotopic ratio ($\delta^{15}\text{N}$ or $^{15}\text{N}/^{14}\text{N}$) of the reactant at time t , δ_{s0} is the $\delta^{15}\text{N}$ of the reactant at time = 0, ϵ is the isotope enrichment factor (‰) of the reaction, C

is the reactant content at time t , and C_0 is the initial reactant content. Stable isotopic ratios are expressed as δ values in per mil (‰) deviations from standard atmospheric nitrogen where:

$$(2) \quad \delta^{15}N = [(R_{sample}/R_{standard}) - 1] \times 1000, \text{ and } R = {}^{15}N/{}^{14}N.$$

The isotopic composition of the reaction product (NO_3^- for nitrification, N_2 for denitrification) becomes progressively heavier as the reaction proceeds, and can be calculated for any given amount of substrate consumed, using a modified version of the Rayleigh expression:

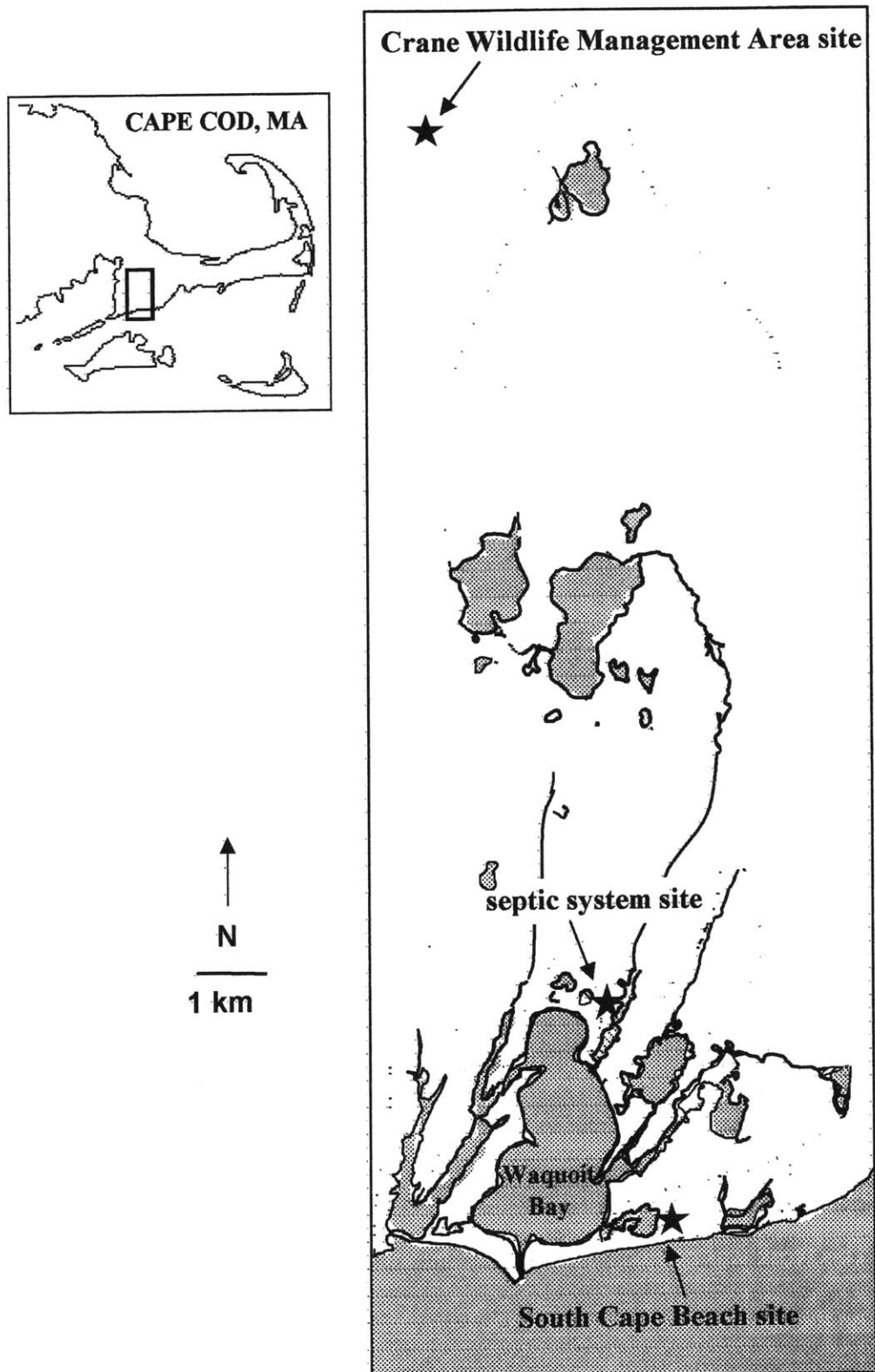
$$(3) \quad \delta^{15}N_{product} = \delta^{15}N_{reactant} - \epsilon [f \ln f / (1 - f)]$$

where $\delta^{15}N_{product}$ is the $\delta^{15}N$ of the product of the reaction (e.g., NO_3^- or N_2), $\delta^{15}N_{reactant}$ is the $\delta^{15}N$ of the reactant (e.g., NH_4 or NO_3^-), ϵ is the isotopic enrichment factor for the reaction, and f is the unreacted fraction of the substrate (Mariotti et al. 1981). We used the Rayleigh equation (Eq. 1) to assess the rates of both nitrification and denitrification in our groundwater samples, and the product formation expression (Eq. 3) to calculate the $\delta^{15}N$ value of NO_3^- produced via nitrification beneath the water table.

4. Study Sites

This work was carried out in or near the watershed of Waquoit Bay, a shallow estuary on the southwestern shore of Cape Cod, Massachusetts (Fig. 3.1), subject to

Figure 3.1. Location of Crane Wildlife Management Area, South Cape Beach, and septic system study sites in and near the Waquoit Bay watershed, Cape Cod, MA.



increasing eutrophication from groundwater-transported nitrogen. The watershed is underlain by an unconsolidated sole-source sand and gravel aquifer (Barlow and Hess 1993, Leblanc et al. 1986). The aquifer matrix is comprised primarily of quartz and feldspar sand (95%) with some ferromagnesian aluminosilicates and oxides (5%); sand grains are coated with hydrous oxides of aluminum and iron (Stollenwerk 1996). Average groundwater velocity is approximately 0.4 m per day (LeBlanc 1991), and mean annual recharge is 53 cm yr⁻¹ (Barlow and Hess 1993, LeBlanc 1984). Groundwater discharge to Waquoit Bay and its tributaries accounts for 89% of the total freshwater input to Waquoit Bay (Cambareri 1998), and is the primary avenue by which land-derived nitrogen is delivered to the estuary (Valiela et al. 1997).

We sampled groundwater at two sites that differed in DOC and NO₃⁻ concentrations: the Crane Wildlife Management Area to the north of the Waquoit Bay watershed, and South Cape Beach near the Bay (Fig. 3.1). DOC concentrations in the underlying groundwater at these two field sites differed because of differences in the thickness of their vadose zones. We have shown (Pabich et al. submitted) that groundwater DOC concentrations at these sites are inversely related to the thickness of the vadose zone through which recharge occurs, presumably because DOC is attenuated during transport through the unsaturated zone by sorption to mineral surfaces (e.g. Fe and Al oxides and hydroxides) and clay minerals (Thurman 1985), microbial oxidation to CO₂ (Chapelle 1992), precipitation, flocculation and formation of insoluble complexes (Kookana and Naidu 1998), and filtering of organic colloids (Wan and Tokunaga 1997). DOC concentrations beneath shallow vadose zones also appear to be more spatially

variable than beneath thick vadose zones. The vadose zone thickness is generally less than a meter at South Cape Beach, and, correspondingly, groundwater DOC concentrations were relatively high and variable (range = 0.8 to 23.4 mg C l⁻¹, mean = 7.0 mg C l⁻¹). In contrast, at Crane Wildlife, depth to groundwater ranged from 4 to 5.5 m, and groundwater DOC concentrations were consistently low (range = 0.04 to 1.9 mg C l⁻¹, mean = 0.4 mg C l⁻¹).

Groundwater nitrate concentrations differed at the two sites as well. The land cover at South Cape Beach consists of mixed pitch pine and scrub oak forest typical of forested areas throughout Cape Cod. At this site, the only sources of nitrate are presumably soil organic matter and precipitation. Measured groundwater nitrate concentrations at this site ranged from 0 to 4.0 μM, consistent with nitrate concentrations found beneath other forested areas in the Waquoit Bay watershed (Seely 1997).

Land cover at Crane Wildlife is similar to that at South Cape Beach, except that the site also contains several abandoned fields, and is downgradient from a golf course on the Massachusetts Military Reservation; additional sources of nitrate to groundwater include fertilizers applied regularly to the golf course (John Callahan, manager, Falcon Golf Course, personal communication) and periodically to the abandoned fields (Richard Turner, MA Division of Fish & Wildlife, personal communication). The inter- and intra-site differences in groundwater DOC and nitrate concentrations provided the opportunity to evaluate the role of both DOC and NO₃⁻ as controls on denitrification rate.

5. Methods

5.1. Groundwater sample collection

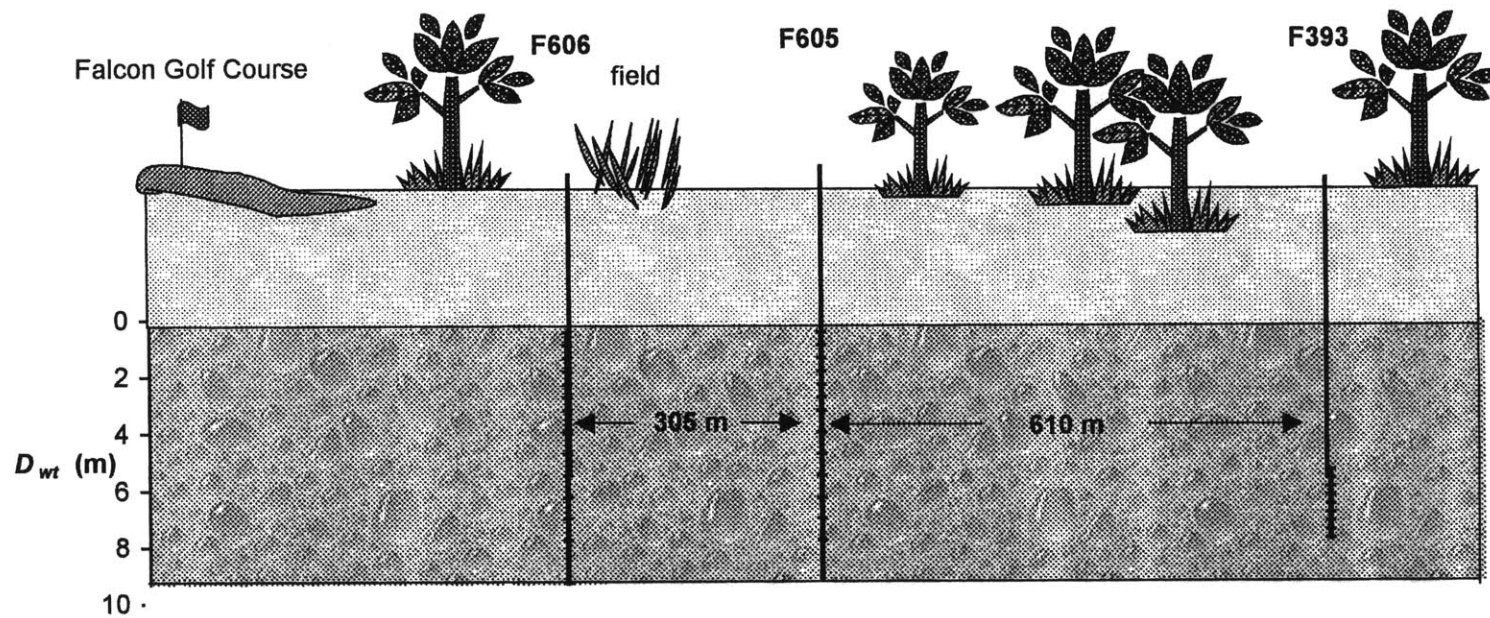
At Crane Wildlife, we installed and sampled groundwater from three multi-level sampling wells (MLSs; LeBlanc 1991) arranged in a transect parallel to groundwater flow (Fig. 3.2). Groundwater flow direction was determined using a MODFLOW model (Masterson et al. 1997). Each MLS had between 9 and 15 ports spanning from just below the water table to a maximum depth of 9.3 m below the water table. At each port a 0.64 cm diameter polyethylene tube protruded through a central 3.2 cm PVC pipe and was covered with a nylon screen (Smith et al. 1991). Samples were taken in duplicate during June 1998 using a peristaltic pump (Geopump 2, Geotech Environmental Equipment, Inc.) after purging a minimum of 3 well volumes (13.8 ml per m tube length) from each port.

At South Cape Beach, we established and sampled from 12 sampling stations around the perimeter of Sage Lot Pond (Fig. 3.1) in March, June and August 1998. Groundwater was sampled using a drive-point piezometer and hand pump. Samples were taken in duplicate after purging groundwater through the piezometer (generally 1-2 liters) until the water was free of visible turbidity.

5.2. Chemical analysis

All samples were collected in acid-washed 250 ml plastic bottles. Samples from the MLSs were filtered in-line during pumping using 0.7 μm Whatman GF/F filters.

Figure 3.2. Schematic of multi-level sampling (MLS) wells (USGS wells F606, F605, and F393) arranged in a transect parallel to groundwater flow lines at Crane Wildlife Management Area. Well and sampling port locations are shown relative to depth below water table (D_{wt}).



Samples obtained using the piezometer were vacuum filtered through the same filters upon return to the lab. All samples were acidified to $\text{pH} \approx 2$ with 5N HCl and stored in a cold room ($T = 4 \text{ }^\circ\text{C}$) until analysis.

We measured NO_3^- concentrations using a Dionex ion chromatograph (DX-120) with a conductivity detector; for samples with concentrations of $\text{NO}_3^- < 3.2 \text{ } \mu\text{M}$ the ion chromatograph was coupled to a Waters 484 Tunable Absorbance detector (UV). The UV detector allowed for measurement of NO_3^- as low as $0.10 \text{ } \mu\text{M}$. Ammonium was measured using the OPA fluorescence method of Holmes et al. (1999). We used both Hydrolab Minisonde and YSI 85 probes to measure dissolved oxygen and specific conductivity in the field. DOC concentrations in triplicate Ar-purged samples were measured using high temperature catalytic oxidation (HTCO) with infrared detection of CO_2 (Shimadzu TOC 5000). Stable isotope analysis of nitrate and ammonium was conducted by David Harris at University of California, Davis, and by Robert Michener at the Boston University Stable Isotope Laboratory using Finnigan Delta S isotope ratio mass spectrometers, and expressed in per mil notation (Eq. 2). Samples were prepared for analysis using an adaptation of the ammonium diffusion method for oceanic nitrate (Sigman et al. 1997).

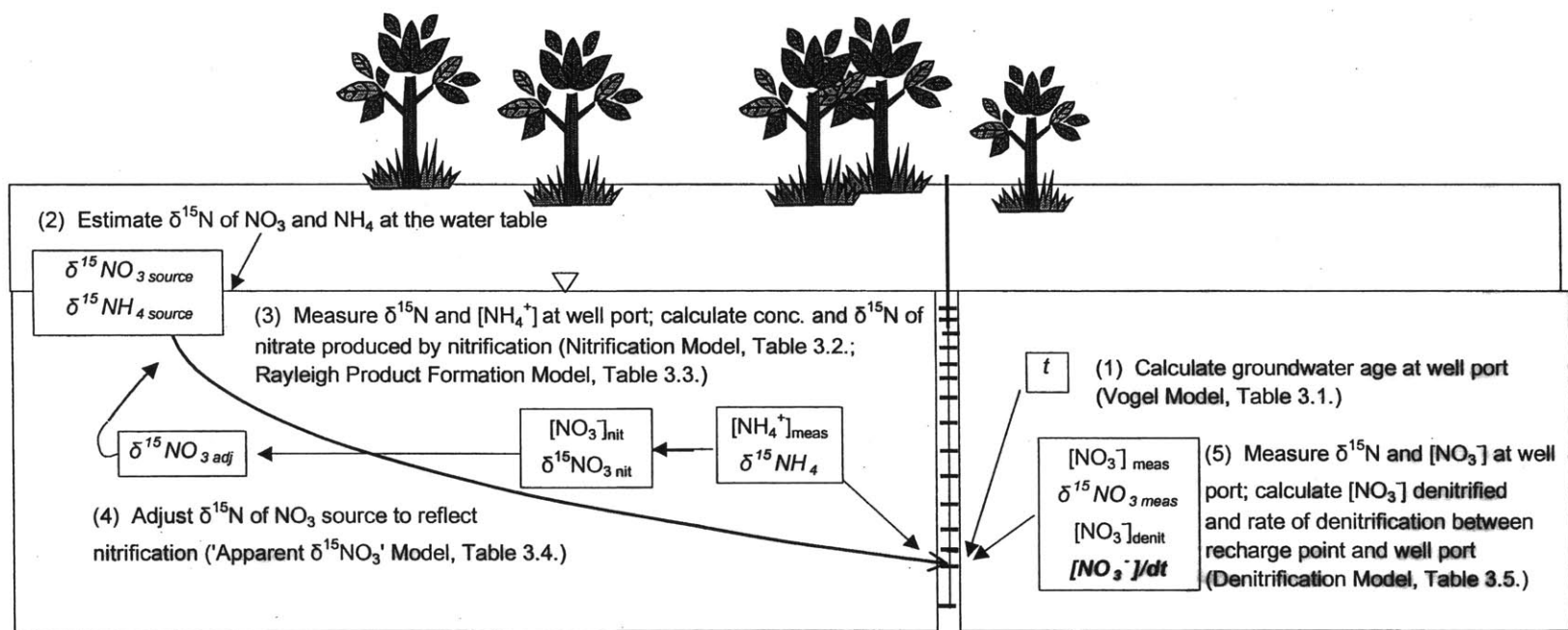
6. Modeling Framework and Assumptions

For each groundwater sample collected at Crane Wildlife, we calculated the average denitrification rate occurring over the groundwater flowpath, between the point

of recharge and the point of sampling. These calculations included five steps (Fig. 3.3), namely:

- (1) Calculation of groundwater age (t) at each well port using the Vogel Groundwater Age Model (Vogel 1967; Table 3.1);
- (2) Estimation of the isotopic signature of nitrogen in nitrate ($\delta^{15}NO_3^-$ source) and ammonium ($\delta^{15}NH_4^+$ source) at the water table;
- (3) Calculation of the concentration ($[NO_3^-]_{nit}$) and isotopic signature of nitrate ($\delta^{15}NO_3^-$ nit) produced via nitrification in the groundwater parcel between recharge and sampling using the Nitrification Model (Table 3.2) and the Rayleigh Product Formation Model (Table 3.3);
- (4) Adjustment of the isotopic signature of the source nitrate to reflect the effects of nitrification ($\delta^{15}NO_3^-$ adj; 'Apparent $\delta^{15}NO_3^-$ ' Model, Table 3.4); and,
- (5) Use of measured isotopic ratios ($\delta^{15}NO_3^-$ meas) and nitrate concentrations ($[NO_3^-]_{meas}$) at each well port, to calculate the concentration of nitrate denitrified ($[NO_3^-]_{denit}$) and the average rate of denitrification over the length of the groundwater flowpath (dNO_3^-/dt ; Denitrification Model, Table 3.5).

Figure 3.3. Stable isotopic method for calculating average denitrification rate between recharge and point of sampling for each water sample collected at Crane Wildlife Management Area.



The assumptions and parameters used in each step are compiled in Tables 3.1 – 3.5, and discussed in more detail below.

6.1. Steady State Conditions

Our calculations assume that the groundwater system is at steady state. At both the Crane Wildlife and South Cape Beach sites, temporal variability in groundwater chemistry (dissolved O₂, DOC, NH₄⁺, and NO₃⁻ concentrations) over 2 to 8 sampling dates between March 1998 and April 1999 was minimal (Fig. 3.4 and Table 3.6), supporting this assumption.

6.2. Estimating Groundwater Age (*t*)

Groundwater age (*t*) at each of the well ports was estimated using a model that describes distribution of travel times in an unconfined aquifer in which recharge is spatially uniform (Vogel 1967, Fig. 3.3 (1)& Table 3.1). In this model,

$$(4) \quad t = (\alpha H/W) * \ln (H /h)$$

where *t* = time since recharge to the water table in years; α = porosity; *H* = total depth of aquifer in meters; *W* = recharge rate in meters per year; and *h* = height over bottom of aquifer in meters. Solomon et al. (1995) used tritium and helium isotope analyses at the nearby Massachusetts Military Reservation (Falmouth, MA) to confirm that in this aquifer, measured vertical groundwater age profiles agree well with ages modeled using the Vogel equation.

Table 3.1. Vogel Groundwater Age Model: Quantities, estimation methods, and values used.

Model equation: $t = (\alpha H/W) * \ln (H / h)$.

Solve for: t .

Quantity	Description	Input vs. Output	Means of Calculating and/or Estimating	Value Used in/Produced by Model
t	Groundwater age (time since recharge, y)	Output		0.1 to 7.0 years
α	Aquifer porosity	Input	Literature (Leblanc 1991)	0.39
H	Total depth of aquifer (m)	Input	Literature (Barlow & Hess 1993)	33 m
W	Groundwater recharge rate (m y ⁻¹)	Input	Literature (Barlow & Hess 1993, LeBlanc 1984)	.53 m y ⁻¹
z	Depth of sampling port below water table (m)	Input	Measured at each well port	0.2 to 9.7 m
h	Height of sampling point over bottom of aquifer ($H - z$)	Input	Calculated ($H - z$)	23.3 to 33.1 m

Table 3.2. Nitrification Model: Quantities, estimation methods, and values used.

Model equations: $\delta^{15}NH_4^+_{meas} = \delta^{15}NH_4^+_{source} + \epsilon * \ln ([NH_4^+]_{meas} / [NH_4^+]_{source})$;

$[NO_3]_{nit} = [NH_4^+]_{source} - [NH_4^+]_{meas}$; and

Nitrification rate = $([NO_3]_{nit}) / t$;

Solve for: $[NH_4^+]_{source}$, $[NO_3]_{nit}$, and Nitrification rate.

Quantity	Description	Input vs. Output	Means of Calculating and/or Estimating	Value Used in/Produced by Model
$\delta^{15}NH_4^+_{source}$	$\delta^{15}N$ of NH_4^+ at the water table	Input	Soil: Measured in upper well ports Fertilizer: Literature (Hübner 1986, Kendall & McDonnell 1998)	Soil: +1.6 ‰ Fertilizer: -1.9 ‰
$[NH_4^+]_{source}$	NH_4^+ concentration at the water table	Output		Soil: .04 to 4.1 μM Fertilizer: .01 to 2.4 μM
$\delta^{15}NH_4^+_{meas}$	$\delta^{15}NH_4^+$ measured at each well port	Input	Measured at each well port	Soil: -11.2 to +10.0 ‰ Fertilizer: + 5.9 to +14.9 ‰
$[NH_4^+]_{meas}$	NH_4^+ concentration at each well port	Input	Measured at each well port	Soil: <.01 to 2.9 μM Fertilizer: <.01 to 1.8 μM
ϵ_{nit}	Enrichment factor for nitrification reaction	Input	Literature (Kendall & McDonnell 1998)	-21 ‰
$[NO_3]_{nit}$	Quantity of nitrate produced via nitrification	Output		Soil: 0 to 1.2 μM Fertilizer: 0 to 0.8 μM
t	Groundwater age (time since recharge)	Input	Vogel model (Table 1)	0.1 to 7.0 years
Nitrification rate	Average rate of nitrification over flow path	Output		Soil: mean = $1.0 \times 10^{-4} \mu M h^{-1}$ Fertilizer: mean = $5.6 \times 10^{-6} \mu M h^{-1}$

Table 3.3. Rayleigh Product Formation Model: Quantities, estimation methods, and values used.

Model equation: $\delta^{15}\text{NO}_3^-_{\text{nit}} = \delta^{15}\text{NH}_4^+_{\text{meas}} - \epsilon_{\text{nit}} * [f * \ln f / (1 - f)];$

$$f = ([\text{NH}_4^+]_{\text{source}} - [\text{NO}_3^-]_{\text{nit}}) / [\text{NH}_4^+]_{\text{source}};$$

Solve for: $\delta^{15}\text{NO}_3^-_{\text{nit}}$.

Quantity	Description	Input vs. Output	Means of Calculating and/or Estimating	Value Used in/Produced by Model
$\delta^{15}\text{NO}_3^-_{\text{nit}}$	$\delta^{15}\text{N}$ of NO_3^- produced via nitrification	Output		Soil: -15.6 to -21.3 ‰ Fertilizer: -15.2 to 21.6 ‰
$\delta^{15}\text{NH}_4^+_{\text{meas}}$	$\delta^{15}\text{NH}_4^+$ measured at each well port	Input	Measured at each well port	Soil: -11.2 to +10.0 ‰ Fertilizer: + 5.9 to +14.9 ‰
ϵ_{nit}	Enrichment factor for nitrification reaction	Input	Literature (Kendall & McDonnell 1998)	-21 ‰
f	Unreacted fraction of substrate	Input	Calculated	Soil: 0.71 to 0.90 Fertilizer: 0.46 to 0.98

Table 3.4. 'Apparent $\delta^{15}\text{NO}_3$ ' Model: Quantities, estimation methods, and values used.

Model equations: $\delta^{15}\text{NO}_3_{\text{adj}} * [\text{NO}_3]_{\text{adj}} = \delta^{15}\text{NO}_3_{\text{source}} * [\text{NO}_3]_{\text{source}} + \delta^{15}\text{NO}_3_{\text{nit}} * [\text{NO}_3]_{\text{nit}}$
 $[\text{NO}_3]_{\text{adj}} = [\text{NO}_3]_{\text{source}} + [\text{NO}_3]_{\text{nit}}$

Solve for: $\delta^{15}\text{NO}_3_{\text{adj}}$.

Quantity	Description	Input vs. Output	Means of Calculating and/or Estimating	Value Used in/Produced by Model
$\delta^{15}\text{NO}_3_{\text{source}}$	$\delta^{15}\text{N}$ of NO_3^- at the water table	Input	Soil: Measured in upper well ports Fertilizer: Literature (Wells & Krothe 1989)	Soil: +3.4 ‰ Fertilizer: -3.2 ‰
$[\text{NO}_3]_{\text{source}}$	NO_3^- concentration at the water table	Input	Soil: Estimated from lysimeter flux measurements (Seely 1997) Fertilizer: Literature (Valiela et al. 2000, Cohen et al. 1990)	Soil: 1.4 μM Fertilizer: 100 μM
$\delta^{15}\text{NO}_3_{\text{nit}}$	$\delta^{15}\text{N}$ of NO_3^- produced via nitrification	Input	Rayleigh Product Model (Table 3)	Soil: -15.6 to -21.3 ‰ Fertilizer: -15.2 to 21.6 ‰
$[\text{NO}_3]_{\text{nit}}$	Quantity of nitrate produced via nitrification	Input	Nitrification Model (Table 2)	Soil: 0 to 1.2 μM Fertilizer: 0 to 0.8 μM
$\delta^{15}\text{NO}_3_{\text{adj}}$	$\delta^{15}\text{N}$ of NO_3^- just below water table, adjusted for Concentration of NO_3^- just below water table, adjusted for nitrification	Output		Soil: -1.8 ‰ Fertilizer: -3.3 to -3.1 ‰
$[\text{NO}_3]_{\text{adj}}$	NO_3^- concentration just below water table, adjusted for nitrification	Input	Assumed $[\text{NO}_3]_{\text{nit}} \ll [\text{NO}_3]_{\text{adj}}$, therefore, $[\text{NO}_3]_{\text{adj}} \sim [\text{NO}_3]_{\text{source}}$	Soil: 1.4 μM Fertilizer: 100 μM

Table 3.5. Denitrification Model: Quantities, estimation methods, and values used.

Model equations: $\delta^{15}NO_3_{meas} = \delta^{15}NO_3_{adj} + \epsilon_{denit} * \ln ([NO_3]_{meas} / [NO_3]_{adj})$;

$[NO_3]_{denit} = [NO_3]_{adj} - [NO_3]_{meas}$; and

Denitrification rate = $[NO_3]_{denit} / t$;

Solve for: $[NO_3]_{adj}$, $[NO_3]_{denit}$, and Denitrification rate.

Quantity	Description	Input vs. Output	Means of Calculating and/or Estimating	Value Used in/Produced by Model
$\delta^{15}NO_3_{adj}$	$\delta^{15}N$ of NO_3^- just below water table, adjusted for nitrification	Input	'Apparent $\delta^{15}NO_3^-$ ' Model (Table 4)	Soil: -1.8 ‰ Fertilizer: -3.3 to -3.1 ‰
$[NO_3]_{adj}$	Concentration of NO_3^- just below water table, adjusted for	Output	Assumed $[NO_3]_{nit} \ll [NO_3]_{adj}$; therefore, $[NO_3]_{adj} \sim [NO_3]_{source}$	Soil: 1.4 μM Fertilizer: 100 μM
$\delta^{15}NO_3_{meas}$	$\delta^{15}NO_3$ measured at each well port	Input	Measured at each well port	Soil: -2.2 to +4.6 ‰ Fertilizer: +0.2 to +6.0 ‰
$[NO_3]_{meas}$	NO_3^- concentration measured at each well port	Input	Measured at each well port	Soil: 0.2 to 1.4 μM Fertilizer: 1.6 to 68.4 μM
ϵ_{denit}	Enrichment factor for denitrification reaction	Input	Literature (Bates & Spalding 1998, Klein & Kaplan 1975, Mariotti et al. 1981 and 1988, Parrott 1994, Smith et al. 1991)	-14 ‰
$[NO_3]_{denit}$	Quantity of nitrate denitrified	Output	Nitrification Model (Table 2)	Soil: 0 to 1.2 μM Fertilizer: 0 to 0.8 μM
t	Groundwater age (time since recharge)	Input (Vogel)	Vogel Model (Table 1)	0.1 to 7.0 years
Denitrification rate	Average rate of denitrification over flow path	Output		Soil: 0 to $1.2 \times 10^{-4} \mu M h^{-1}$ Fertilizer: 2.3×10^{-3} to $2.1 \times 10^{-3} \mu M h^{-1}$

Figure 3.4. Temporal variability in groundwater chemistry at Crane Wildlife Management Area. Mean concentrations of dissolved oxygen, DOC, ammonium, and nitrate, measured on 2 to 8 sampling dates between March 1998 and April 1999, are plotted against depth below the water table (D_{wt}). Standard error bars are shown.

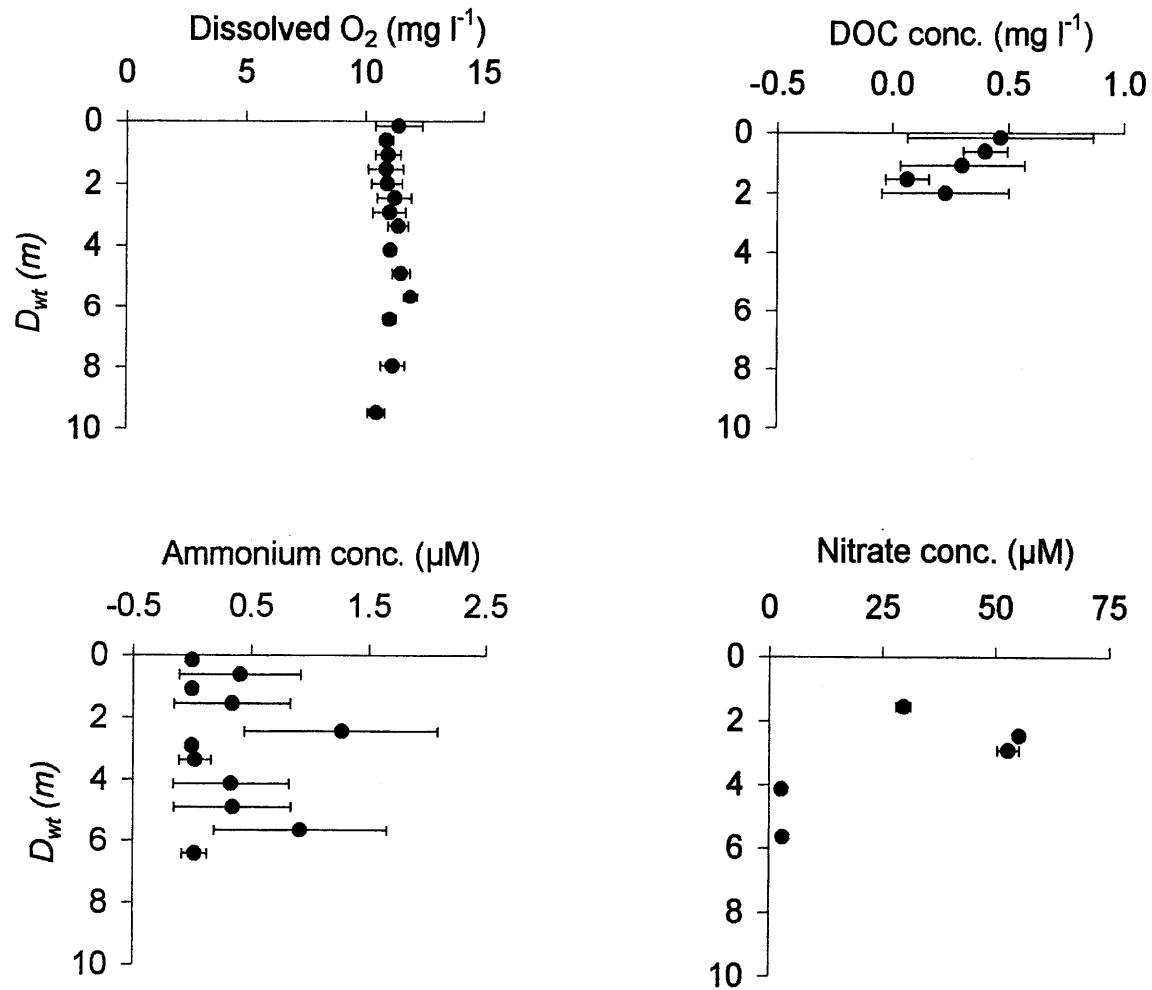


Table 3.6. Comparison of spatial and temporal variability in groundwater chemistry at South Cape Beach. Coefficient of variation is shown for measurements of dissolved oxygen, dissolved organic carbon (DOC), ammonium, nitrate and $\delta^{15}\text{NO}_3^-$ at 10 to 12 sampling stations located around the perimeter of Sage Lot Pond near South Cape Beach both on one sampling date (spatial variability), and for one sampling station over 2 to 8 sampling dates (temporal variability).

Measurement	Spatial Variability			Temporal Variability		
	Mean	Coefficient of Variation	Number of Sampling Locations	Mean	Coefficient of Variation	Number of Sampling Dates
Dissolved O ₂ (mg l ⁻¹)	6.74	46%	11	3.28	53%	8
DOC (mg l ⁻¹)	6.85	76%	12	20.90	9%	5
Ammonium (µM)	1.33	114%	10	5.94	56%	6
Nitrate (µM)	0.51	133%	11	0.33	56%	6
$\delta^{15}\text{NO}_3^-$ (‰)	-1.82	145%	11	-2.61	60%	2

6.3. Rayleigh Parameters and Assumptions

To use the Rayleigh equation to evaluate nitrification and denitrification in the saturated zone, it was necessary to make several simplifying assumptions about nitrogen transformations in the various subsurface compartments (soil, vadose zone, and groundwater). To estimate initial concentrations of ammonium and nitrate (C_0) from measured downgradient concentrations (C) and $\delta^{15}\text{N}$ values (δ_s), we estimated the $\delta^{15}\text{N}$ value of the source ammonium and nitrate (δ_{s0}) at the water table (Fig. 3.3(2)). We recognized that the pathways by which ammonium and nitrate are derived from fertilizer are likely to differ from those by which inorganic N is derived from soil, resulting in different $\delta^{15}\text{N}$ signals at the water table ($\delta^{15}\text{NH}_{4\text{source}}$ and $\delta^{15}\text{NO}_{3\text{source}}$) for the two different sources (fertilizer and soil organic N, Figs. 3.5-3.7, Tables 3.2 & 3.4). It was also necessary to estimate the isotopic enrichment factor for both the nitrification (ϵ_{nit} , Table 3.2) and denitrification reactions (ϵ_{denit} , Table 3.5).

We assumed that nitrate generated in soils or from fertilizer was transported through the vadose zone by recharge with no fractionation in the unsaturated zone. This assumption is consistent with work by Fogg et al. (1998) demonstrating that the $\delta^{15}\text{N}$ “fingerprint” of nitrate did not change significantly during NO_3^- transport to groundwater through thick vadose zones (>12 m). We also neglected fractionation in N isotopes in the saturated zone by mechanisms other than denitrification and nitrification (e.g., mineralization, sorption/desorption, etc.). Mineralization usually causes only a small fractionation (+-1‰) between soil organic matter and soil ammonium (Kendall and

Figure 3.5. Pathways by which fertilizer-derived nitrate and ammonium at Crane Wildlife Management Area are delivered to the water table. Fractionations associated with N transformations, and the values used for $\delta^{15}N$ at the water table ($\delta^{15}NO_3^-$ source and $\delta^{15}NH_4^+$ source) and for $\delta^{15}N$ adjusted for nitrification near the water table ($\delta^{15}NO_3^-$ adj), are shown.

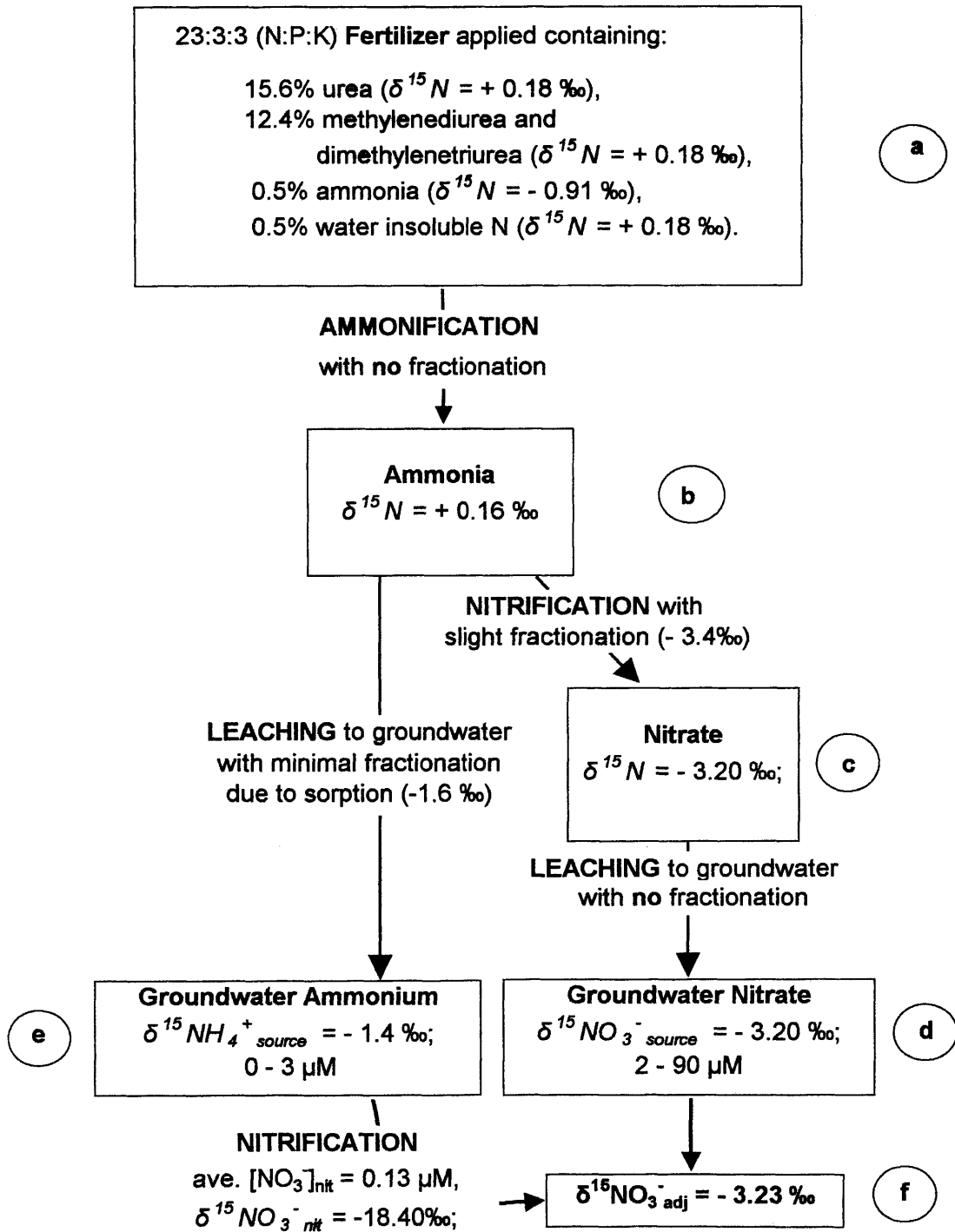


Figure 3.6. Pathways by which soil-derived nitrate and ammonium at Crane Wildlife Management Area are delivered to the water table. Fractionations associated with N transformations, and the values used for $\delta^{15}N$ at the water table ($\delta^{15}NO_3^-$ source and $\delta^{15}NH_4^+$ source) and for $\delta^{15}N$ adjusted for nitrification near the water table ($\delta^{15}NO_3^-$ adj) are shown.

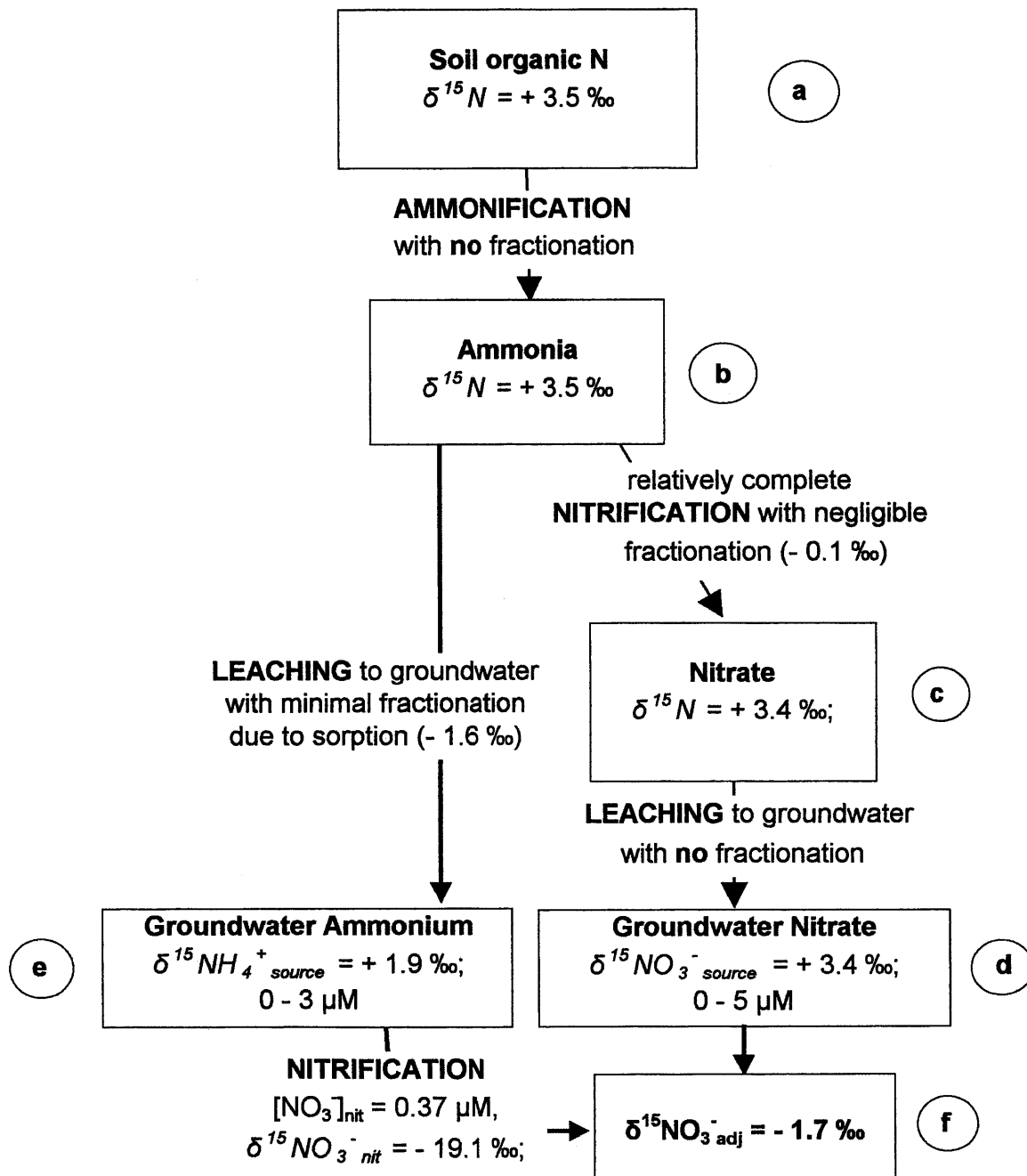
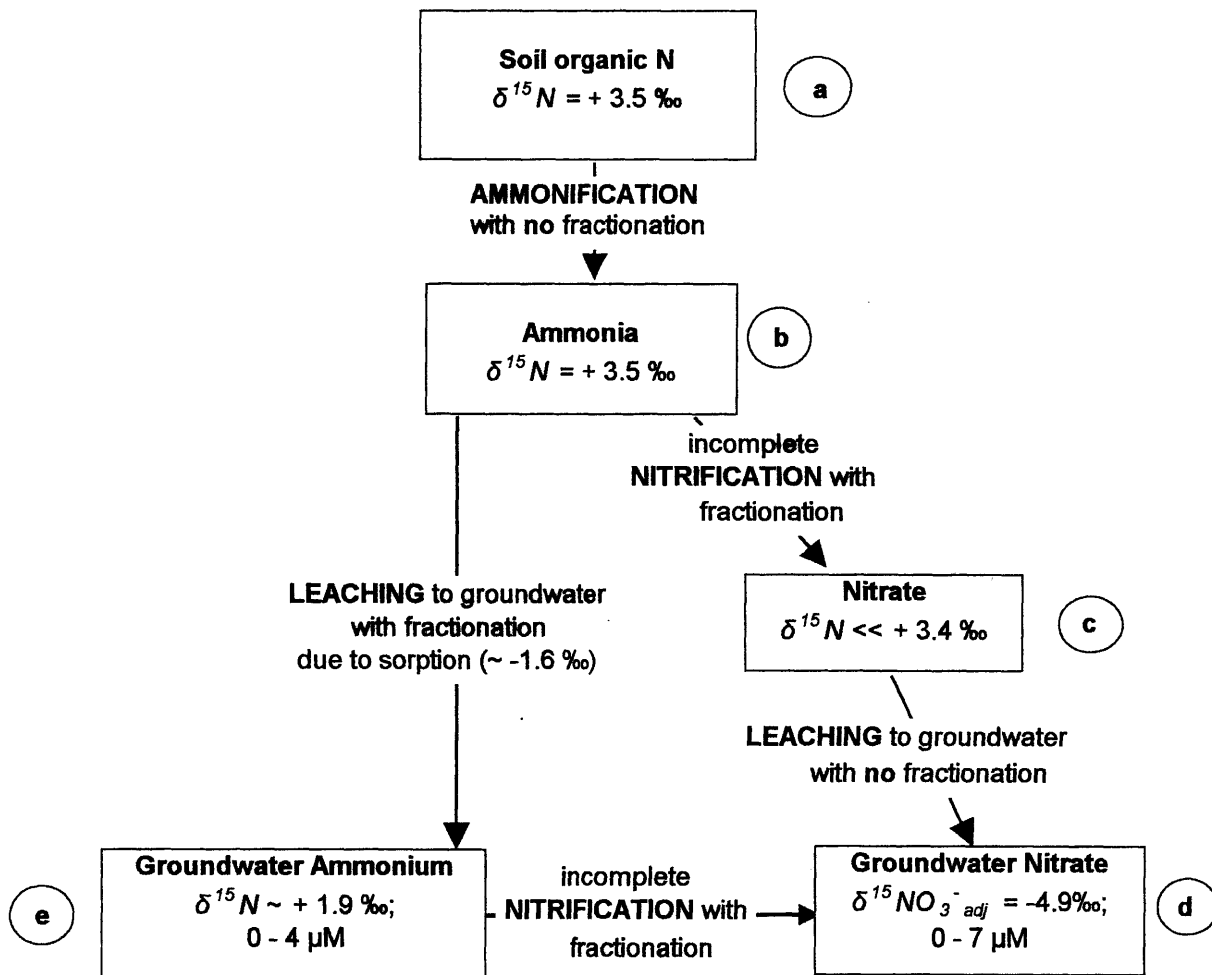


Figure 3.7. Pathways by which soil-derived nitrate and ammonium at South Cape Beach are delivered to the water table. Fractionations associated with N transformations, and the values used for $\delta^{15}N$ at the water table ($\delta^{15}NO_3^-$ *source* and $\delta^{15}NH_4^+$ *source*) and for $\delta^{15}N$ adjusted for nitrification near the water table ($\delta^{15}NO_3^-$ *adj*) are shown.



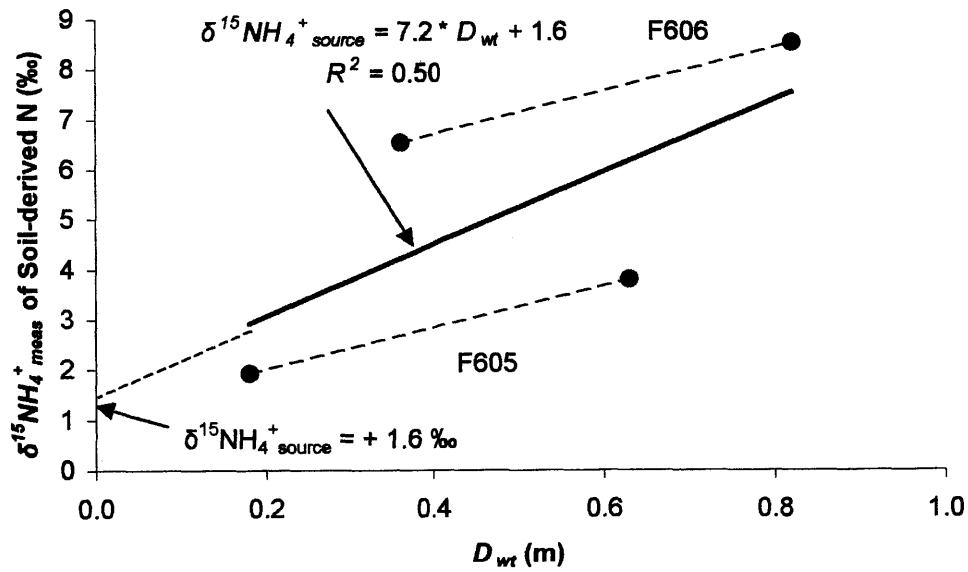
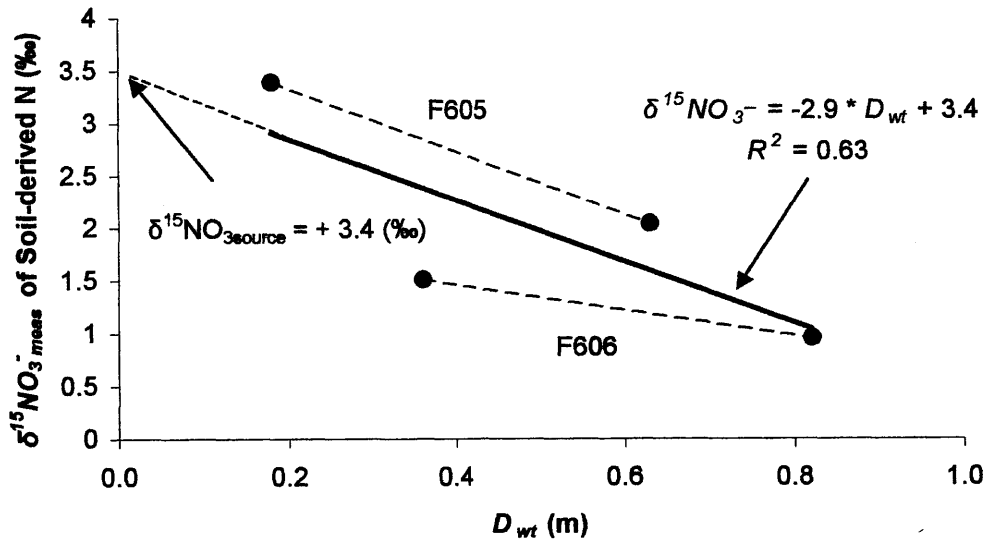
McDonnell 1998). Sorption/desorption can cause +1 to +8 ‰ isotope fractionations as a result of isotope exchange on the charged surfaces of clays and other materials.

However, the majority of ammonium sorption is likely to have occurred above the water table in the soil organic horizons, with little sorption to the quartz sand particles that comprise the bulk of the aquifer matrix. There is little evidence for nitrate sorption in soils (Kendall and McDonnell 1998). Thus, mineralization and sorption/desorption are likely to exert minor influences of isotopic signatures in the saturated zone.

6.3.1. Soil-Derived $\delta^{15}N$ Source Signatures at Crane Wildlife Management Area

To estimate the $\delta^{15}N$ values for nitrate ($\delta^{15}NO_3^-$ source) and ammonium ($\delta^{15}NH_4^+$ source) at the water table, we used a linear regression through a plot of measured $\delta^{15}N$ values versus depth below water table (D_{wt}) for those samples at Crane Wildlife in closest proximity to the water table (4 samples; Fig. 3.8). While it would have been preferable to use more than four data points to estimate the source $\delta^{15}N$ values, we did not have additional data from which to do so. In addition, the apparent inverse relationship in the values of $\delta^{15}NO_3^-$ and $\delta^{15}NH_4^+$ in the groundwater profiles (Fig. 3.11) suggests a coupling of these signals due to fractionating reactions (i.e., nitrification and denitrification) as the water mass ages. Therefore, it seemed most reasonable to use only the youngest samples (those impacted the least by fractionating reactions) in our estimation of $\delta^{15}N$ values at the water table. Using these linear regressions, we extrapolated the $\delta^{15}N$ values for ammonium and nitrate at the water table ($D_{wt} = 0$ m), and used these values to represent the isotopic signature of the source ammonium ($\delta^{15}NH_4^+$ source = + 1.6 ‰) and source nitrate ($\delta^{15}NO_3^-$ source + 3.4 ‰).

Figure 3.8. Estimation of $\delta^{15}\text{NO}_3^-$ (top panel) and $\delta^{15}\text{NH}_4^+$ (bottom panel) values for soil-derived N at Crane Wildlife Management Area. Measured $\delta^{15}\text{N}$ values are plotted against depth below the water table (D_{wt}) for samples from the four shallowest well ports at the site. The y-intercept of a linear regression through the points provides an estimate of the $\delta^{15}\text{N}$ value at the water table ($D_{wt} = 0$; $\delta^{15}\text{NO}_3^-$ source = + 3.4 ‰; $\delta^{15}\text{NH}_4^+$ source = + 1.6 ‰). Dashed lines show linear regressions for individual wells (F605 and F606).



Our $\delta^{15}N_{\text{source}}$ values are consistent with what we might expect to find for ammonium and nitrate derived from soil, which has $\delta^{15}N$ values ranging between -10 and $+15\text{‰}$, with the majority of soils falling between $+2$ and $+5\text{‰}$ (Kendall and McDonnell 1998). Ammonium derives from soil organic N via ammonification with minimal fractionation ($+ \text{ or } - 1 \text{‰}$, Kendall & McDonnell 1998), producing ammonium with $\delta^{15}N$ values similar to that of soil organic nitrogen (Koba et al. 1998; Fig. 3.6 a & b, and 3.7 a & b). Sorption/desorption of ammonium on the charged surfaces of clays and other material, and other retardation processes, can decrease the $\delta^{15}N$ value of the more “mobile” ammonium (Delwiche & Stein 1970, Kendall & McDonnell 1998, Hübner 1986). The $\delta^{15}N$ value we estimated for ammonium at the water table ($\delta^{15}NH_4^+_{\text{source}} = +1.6 \text{‰}$) is consistent with ammonification of soil organic N ($+2$ to $+5 \text{‰}$; mean $\sim 3.5 \text{‰}$) followed by slight fractionation during transport through the soil profile and vadose zone (-1.9‰).

The $\delta^{15}N$ value that we estimated for nitrate at the water table ($\delta^{15}NO_3^-_{\text{source}} = +3.4 \text{‰}$) is consistent with the literature; measurements of $\delta^{15}N$ of soil water nitrate derived from soil organic N range from about -10 to $+12 \text{‰}$, with mean values ranging from -3 to $+5 \text{‰}$ (Fogg et al. 1998). Further, since fractionation during nitrification is minimal in N-limited systems (Kendall and McDonnell 1998), we expect that nitrate produced via nitrification of soil-derived ammonium, with no further fractionation during transport through the vadose zone, would result in $\delta^{15}N$ of nitrate at the water table similar to that of soil organic N ($\sim 3.5 \text{‰}$). In our system, fractionation may have been on the order of -0.1‰ .

6.3.2. Fertilizer-Derived $\delta^{15}N$ -Ammonium Source Signature at Crane Wildlife

Management Area

Fertilizer containing nitrogen (N), phosphorus (P), and potassium (K) at a ratio of 23:3:3 was historically applied to the upgradient golf course (John Callahan, manager, Falcon Golf Course, personal communication). Discussions with the fertilizer manufacturer led us to believe that the N content of this particular fertilizer would have been 0.5% ammonia, 15.6% urea nitrogen, 12.4% water soluble nitrogen (methylenediurea and dimethylenetriurea nitrogen), and 0.5% water insoluble nitrogen.

Hübner (1986) compiled $\delta^{15}N$ values for numerous fertilizers and reported that the mean $\delta^{15}N$ was -0.91 ± 1.88 ‰ for ammonium in 39 fertilizer samples, and $+0.2 \pm 1.27$ ‰ for urea in 8 fertilizer samples. The fertilizer applied to the golf course was comprised primarily of organic forms of nitrogen (~98%). If we assume that ammonification of organic fertilizer N proceeds with essentially zero fractionation (± 1 ‰, Kendall & McDonnell 1998) to produce ammonium with the same $\delta^{15}N$ value as urea ($+0.2$ ‰), the bulk signal of ammonium derived from this fertilizer would be $+0.2$ ‰ (2% from ammonium fertilizer, 98% from urea; Fig. 3.5 b). Assuming that ammonia from fertilizer undergoes fractionation due to sorption to soils and in the vadose zone to the same degree as we hypothesize for soil-derived ammonium (-1.9 ‰), we calculated that the $\delta^{15}N$ value of ammonium at the water table would be -1.7 ‰, which we assigned as the source signature (Fig. 3.5 e).

6.3.3. Fertilizer-Derived $\delta^{15}N$ –Nitrate Source Signature at Crane Wildlife Management Area

We assumed that after application, fertilizer ammonium and urea compounds undergo relatively complete ammonification and nitrification within the soil horizons, with slight fractionation, and that the nitrate produced is largely leached through the vadose zone to the water table during recharge, with no further transformations occurring in the vadose zone. This would result in nitrate at the water table bearing a $\delta^{15}N$ signature only slightly more negative than that of the original fertilizer ammonium (+0.2 ‰, Fig. 3.5 b) and urea. This is an important distinction, since the isotopic enrichment factor (ϵ) for nitrification is quite large (–12 and –29 ‰, Kendall and McDonnell 1998), and incomplete nitrification would result in significant fractionation between the ammonium reactant and the nitrate product.

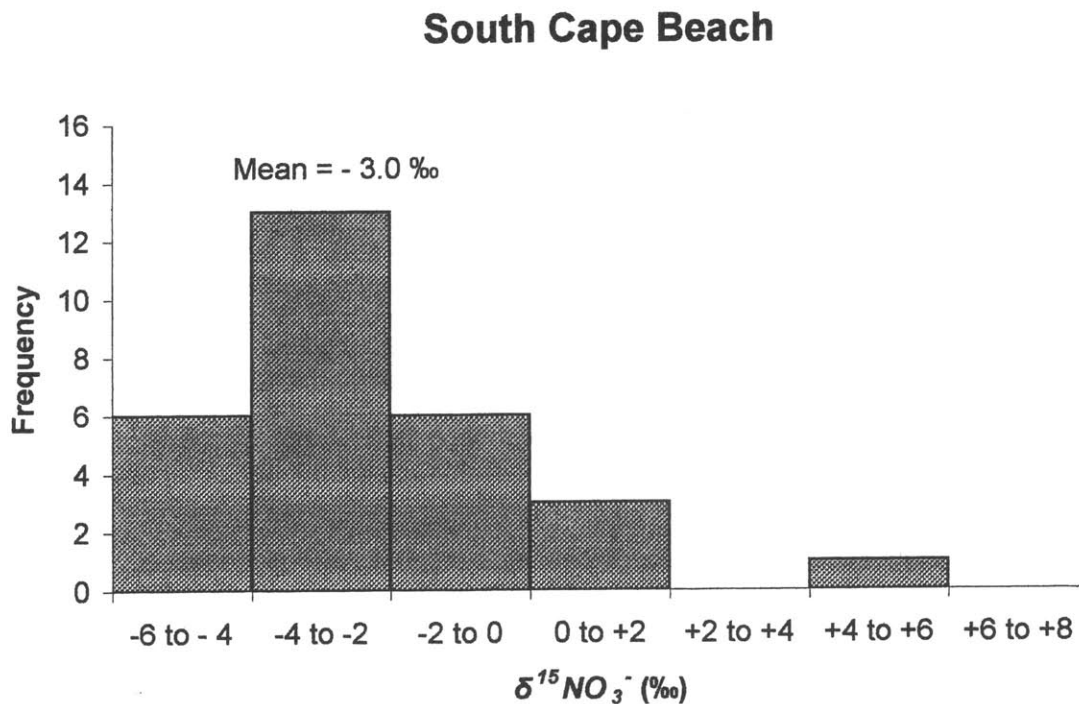
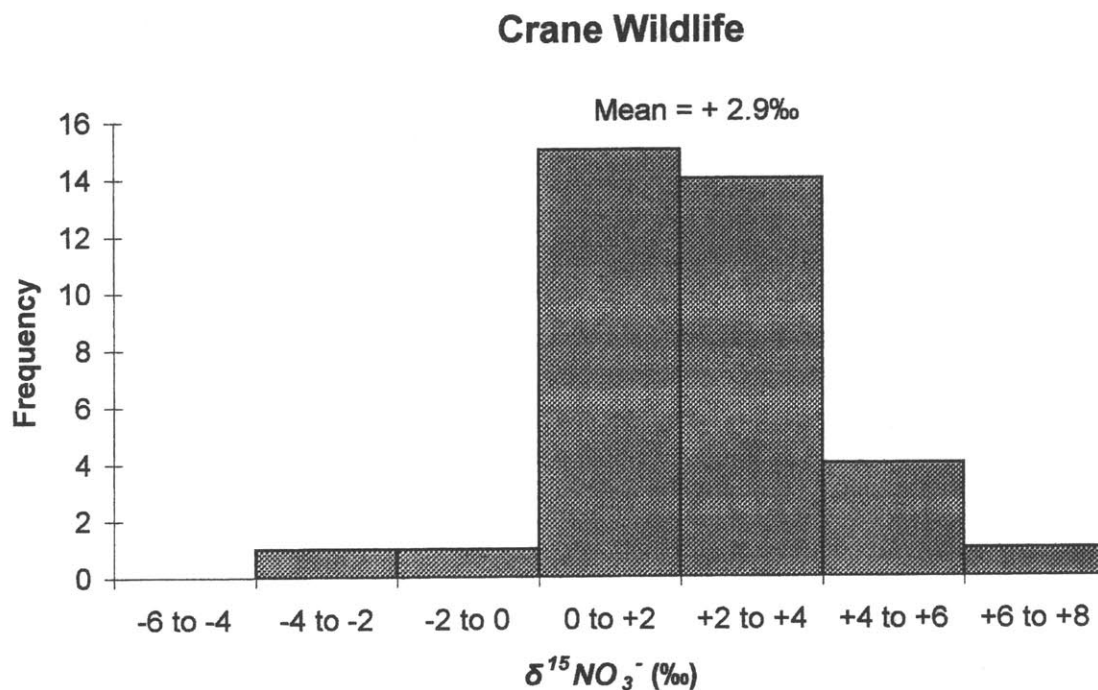
An assumption of fairly complete nitrification is consistent with work by Wells & Krothe (1989) who measured $\delta^{15}N$ values and leachable nitrate and ammonium concentrations in soil samples beneath several fertilized fields. They demonstrated that ammonium concentrations in the soil, in all but one case, were below detection limits, and that nitrate had low $\delta^{15}N$ values (averaging –3.2 ‰) reflective of the original fertilizer. From this evidence, they concluded that complete nitrification of anhydrous ammonium fertilizers had occurred with only minimal fractionation. We assumed that the $\delta^{15}N$ of the fertilizer-derived nitrate at the water table would be similar to that measured by Wells & Krothe (1989), or –3.2 ‰ (Fig. 3.5 c), consistent with the range of $\delta^{15}N$ values reported in the literature for fertilizer (–8 to +6.2 ‰, Freyer and Aly 1974,

Kohl et al. 1971, Kreitler 1977, Mariotti and Letolle 1977), and suggesting limited depletion (-3.4 ‰) relative to the fertilizer ammonium (+0.2 ‰). A greater degree of fractionation during nitrification of fertilizer-derived N (-3.4 ‰) than during nitrification of soil-derived N (-0.1 ‰) is expected due to the higher N concentrations associated with fertilizer, which promote fractionation (Kendall and McDonnell 1998).

6.3.4. Soil-Derived $\delta^{15}N$ Source Signatures at South Cape Beach

A comparison of frequency plots of the $\delta^{15}N$ value of nitrate measured at South Cape Beach and at Crane Wildlife (Fig. 3.9) suggests that there is a significant difference in the distributions of the $\delta^{15}N$ values at the two sites. The central tendency of the $\delta^{15}N$ values at South Cape Beach has been shifted by about -4 ‰ relative to those at Crane Wildlife, such that the modal $\delta^{15}NO_3^-$ category at South Cape Beach (-4 to -2 ‰) is approximately 4 ‰ lighter than the modal category (0 to + 2 ‰) at Crane Wildlife. A similar shift is observed in the means (+2.9 ‰ and -3.0 ‰ at Crane Wildlife and South Cape Beach, respectively). We presume that at South Cape Beach, nitrification in the unsaturated zone was less complete than at Crane Wildlife. At Crane Wildlife, the soil was significantly separated from the groundwater (~ 5 m), resulting in longer travel times for water recharging through the forest soils to the underlying groundwater. In contrast, the vadose zone at South Cape Beach was shallow (< 1 m), providing only minimal separation between the mineral soil, where ammonium is produced, and the groundwater. The shorter hydrologic flowpaths at South Cape Beach may have provided less time for nitrification to occur in the unsaturated zone. Less complete nitrification would result in greater fractionation between the soil-derived ammonium and the nitrate product; thus the

Figure 3.9. Frequency plots of measured $\delta^{15}NO_3^-$ at Crane Wildlife Management Area and South Cape Beach. The modal category at South Cape Beach (-4 to -2 ‰) is about 4 ‰ lower than at Crane Wildlife Management Area (0 to +2 ‰).



groundwater nitrate at South Cape Beach would bear a lower $\delta^{15}\text{NO}_3^-$ value than at Crane Wildlife ($\delta^{15}\text{NO}_3^-_{\text{source}} = + 3.4 \text{ ‰}$), where longer flowpaths through the unsaturated zone may have allowed for more complete nitrification.

This hypothesis is supported by our measurements of inorganic N at both sites. At South Cape Beach, ammonium made up a much larger fraction, on average, of the total inorganic nitrogen ($\text{NH}_4 + \text{NO}_3^-$, 57%), than at Crane Wildlife (13 %). Assuming that nitrate derives primarily from nitrification of ammonium, these data suggest that nitrification at South Cape Beach is less complete than at Crane Wildlife.

Because we did not measure $\delta^{15}\text{NH}_4^+$ at South Cape Beach, we could not directly correct the $\delta^{15}\text{NO}_3^-_{\text{source}}$ value to reflect the effects of nitrification taking place beneath the water table. Instead, we assumed that the lowest $\delta^{15}\text{N}$ value measured in our shallow groundwater samples (- 4.9 ‰) was reflective of the effects on nitrification on the isotopic signature of the source nitrate, and assigned this value to $\delta^{15}\text{NO}_3^-_{\text{adj}}$. This value is 3.2 ‰ lower than the adjusted source value calculated for Crane Wildlife (-1.7 ‰; see Results), consistent with less complete nitrification at South Cape Beach than at Crane Wildlife. Use of our lowest measured $\delta^{15}\text{N}$ value implies that no denitrification has occurred in that particular water parcel (since $\delta^{15}\text{NO}_3^-_{\text{meas}} = \delta^{15}\text{NO}_3^-_{\text{adj}}$). In reality, this may be a conservative estimate of the impacts of nitrification, since denitrification may have increased $\delta^{15}\text{N}$ from some lower value to that which we measured (- 4.9 ‰). If the impacts of nitrification are, in fact, greater than what we estimate, then our calculated

denitrification rates for South Cape Beach represent a conservative estimate of N reduction rates at this site.

6.3.5. Isotopic Enrichment Factor for Nitrification (ϵ_{nit})

Isotopic fractionation during nitrification results in isotopic enrichment (ϵ_{nit}) of residual ammonium between -12 and -29 ‰ (Kendall and McDonnell 1998). We used the mean of this range, or -21 ‰, as ϵ for this analysis (Table 3.2).

6.3.6. Isotopic Enrichment Factor for Denitrification (ϵ_{denit})

In the literature, values of ϵ_{denit} ranged from -4.7 ‰ in the Chalk aquifer in France to -30 ‰ in an aquifer in the Kalahari (Vogel et al., 1981; Heaton, 1986), to as large as -40 ‰ in the marine environment (Cline and Kaplan 1975). Enrichment factors measured in groundwater in the sewage plume at the Massachusetts Military Reservation (MMR) on Cape Cod averaged -14 ‰ (Smith et al. 1991). We chose to use -14 ‰ as ϵ_{denit} for our model, since this value was derived from the same aquifer system (Table 3.5) and falls in the midrange of the literature values.

7. Results and Discussion

7.1. Crane Wildlife Management Area

7.1.1. Geochemistry

Figures 3.10 and 3.11 shows depth profiles of dissolved oxygen (3.10a), dissolved organic carbon (3.10b), ammonium (3.10c), and nitrate (3.11a), as well as $\delta^{15}NO_3^-_{meas}$ and $\delta^{15}NH_4^+_{meas}$ for fertilizer-derived N ($> 1.5 \mu M NO_3^-$; (3.11.b)) and soil-derived N (< 1.5

Figure 3.10. Profiles of dissolved oxygen, DOC, and ammonium with depth below groundwater (D_{wt}) at Crane Wildlife Management Area. Concentrations measured in wells F606 (top row), F605 (middle row), and F393 (bottom row), as sampled in July 1998, are shown.

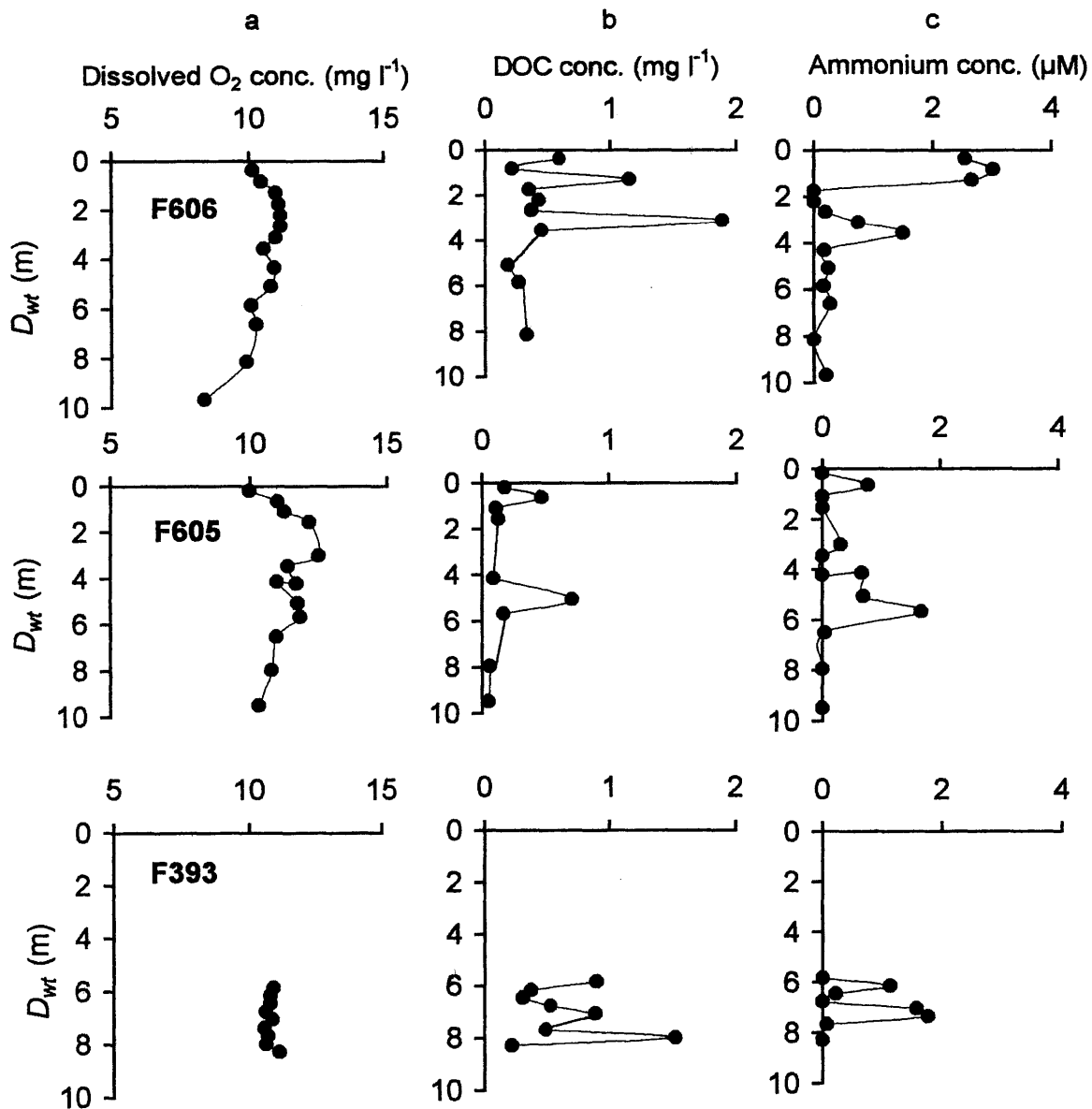
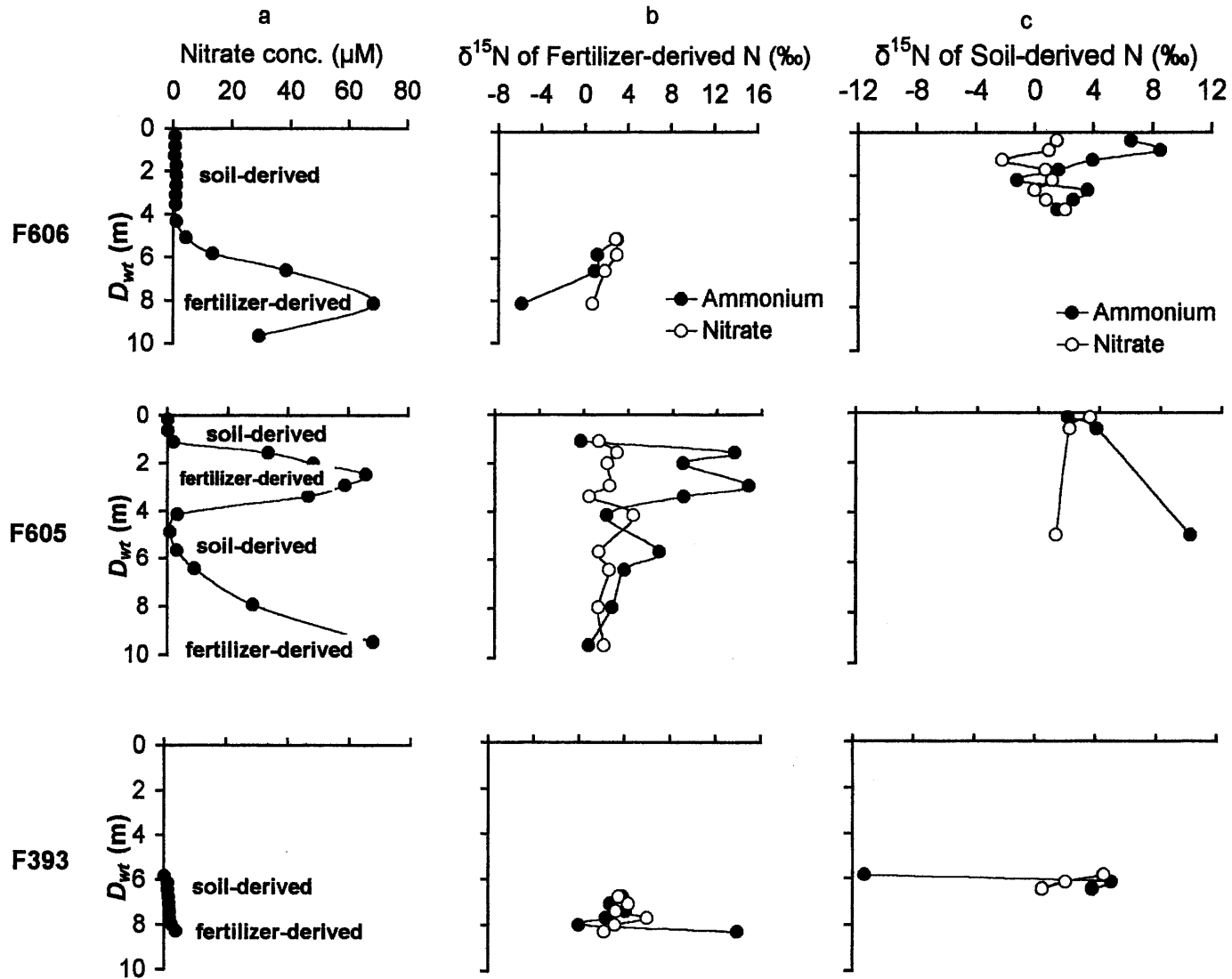


Figure 3.11. Profiles of nitrate and $\delta^{15}N$ with depth below water table (D_{wt}) at Crane Wildlife Management Area. Concentrations measured at wells F606 (top row), F605 (middle row), and F393 (bottom row), as sampled in July 1998, are shown.



$\mu\text{M NO}_3^-$; (3.11.c)) measured for the three Crane Wildlife wells on one sampling date.

These measurements are consistent with measurements made on several other sampling dates (Fig. 3.4).

Groundwater was oxygenated at all depths (8.4 to 12.9 mg O₂ l⁻¹, averaging 10.9 mg O₂ l⁻¹). For the two wells with ports near the surface of the water table (F605 and F606), DO decreased slightly with increasing depth below the water table, though the regression was only significant for F606 (F = 0.009). DOC concentrations at this site ranged from 0.1 to 1.9 mg C l⁻¹ and averaged 0.5 mg C l⁻¹. Ammonium concentrations ranged from 0 to 2.9 μM and averaged 0.6 μM , consistent with calculations we made of groundwater ammonium concentration at the water table (3.2 μM) using estimates of the ammonium flux from soil to groundwater at three similarly forested sites within the Waquoit Bay watershed (Seely 1997).

Nitrate concentrations were low (<1.5 μM) in portions of the profile, suggestive of low-level soil-derived NO₃⁻ emanating from forested cover. This concentration range is consistent with estimates of groundwater nitrate concentrations (0 to 2.7 μM) that we made from nitrate flux measurements by Seely (1997) beneath forested areas in the Waquoit Bay watershed. The nitrate profiles also show several well-defined peaks, with concentrations much greater than would be expected if soil leaching were the only source. We suspected that the peaks of up to 68 $\mu\text{M NO}_3^-$ observed in the profiles for F606 and F605 derive from an additional (presumably fertilizer) nitrate source (> 1.5 μM

NO_3^-). $\delta^{15}\text{N}$ of nitrate ranged from -2.2 to $+6.0$ ‰, and averaged $+2.1$ ‰; $\delta^{15}\text{N}$ of ammonium ranged from -11.2 to $+15$ ‰, and averaged $+3.7$ ‰ (Fig. 3.11 b & c).

We back-calculated the flowpaths between each well port and its upgradient recharge location, and examined the land use at each recharge point. We first estimated groundwater age using the Vogel (1967) model (Eq. 4 & Table 3.1), assuming that the thickness of the aquifer, H , was the distance between the water table and the bottom of the uppermost, highly conductive, medium- to fine-sand strata. Using geologic cross-sections for this area of the Cape (Masterson et al. 1997), we estimated that this layer was approximately 60 m thick in the vicinity of our site. Since groundwater flow is almost entirely in the horizontal direction within this aquifer (LeBlanc et al. 1991), we next estimated the travel distance between the sampling port and the point of recharge for each water mass by multiplying groundwater age at that port by mean groundwater velocity (0.4 m per day, LeBlanc et al. 1991). We then backtracked each water mass the calculated travel distance upgradient (Table 3.7) along south-southwest trending flowpaths modeled by the US Geological Survey using MODFLOW (Masterson et al. 1997) to the appropriate recharge points, and located these points on a USGS topographic map. Figure 3.12 is a planar view of the recharge zones calculated in Table 3.7.

Our backcast calculations suggest that the land use at the recharge points for the three wells is consistent with our hypothesis that the high measured nitrate concentrations derived from fertilizer, and the low concentrations derived from soil. For example, the water mass containing the uppermost nitrate concentration peak in well F605 (1 – 4.2 m

Table 3.7. Groundwater age and horizontal distance to upgradient recharge point for Crane Wildlife Management Area wells. Groundwater age was calculated using the Vogel model (Eq. 4, Vogel 1967); distance to recharge point was calculated assuming that horizontal groundwater flow velocity is 0.39 m day^{-1} (Leblanc 1991).

Well- Port Number	Depth below Water Table (m)	Groundwater Age (yrs)	Distance to Recharge Point (km)
F393-1	5.52	4.03	0.57
F393-2	5.83	4.28	0.61
F393-3	6.13	4.53	0.64
F393-4	6.44	4.78	0.68
F393-5	6.74	5.03	0.72
F393-6	7.05	5.30	0.75
F393-7	7.35	5.55	0.79
F393-8	7.66	5.82	0.83
F393-9	7.96	6.08	0.87
F605-2	0.18	0.12	0.02
F605-3	0.63	0.43	0.06
F605-4	1.09	0.74	0.10
F605-5	1.55	1.05	0.15
F605-6	2.01	1.36	0.19
F605-7	2.46	1.68	0.24
F605-8	2.92	2.00	0.28
F605-9	3.38	2.32	0.33
F605-10	4.14	2.86	0.41
F605-11	4.90	3.41	0.49
F605-12	5.66	3.97	0.57
F605-13	6.43	4.54	0.65
F605-14	7.95	5.69	0.81
F605-15	9.47	6.89	0.98
F606-2	0.36	0.24	0.03
F606-3	0.82	0.55	0.08
F606-4	1.27	0.86	0.12
F606-5	1.73	1.17	0.17
F606-6	2.19	1.49	0.21
F606-7	2.65	1.81	0.26
F606-8	3.10	2.13	0.30
F606-9	3.56	2.45	0.35
F606-10	4.32	3.00	0.43
F606-11	5.08	3.55	0.51
F606-12	5.85	4.11	0.58
F606-13	6.61	4.68	0.67
F606-14	8.13	5.84	0.83
F606-15	9.66	7.03	1.00

Figure 3.12. Recharge zones for 3 wells at Crane Wildlife Management Area. Distance to upgradient recharge point was calculated by determining groundwater age at each well port using the Vogel model (1967), multiplying age by groundwater flow velocity ($\sim 0.4 \text{ m day}^{-1}$; Leblanc 1991), and backtracking the resulting flow distance upgradient in the direction of groundwater flow (MODFLOW (Masterson et al. 1997) to the recharge point.

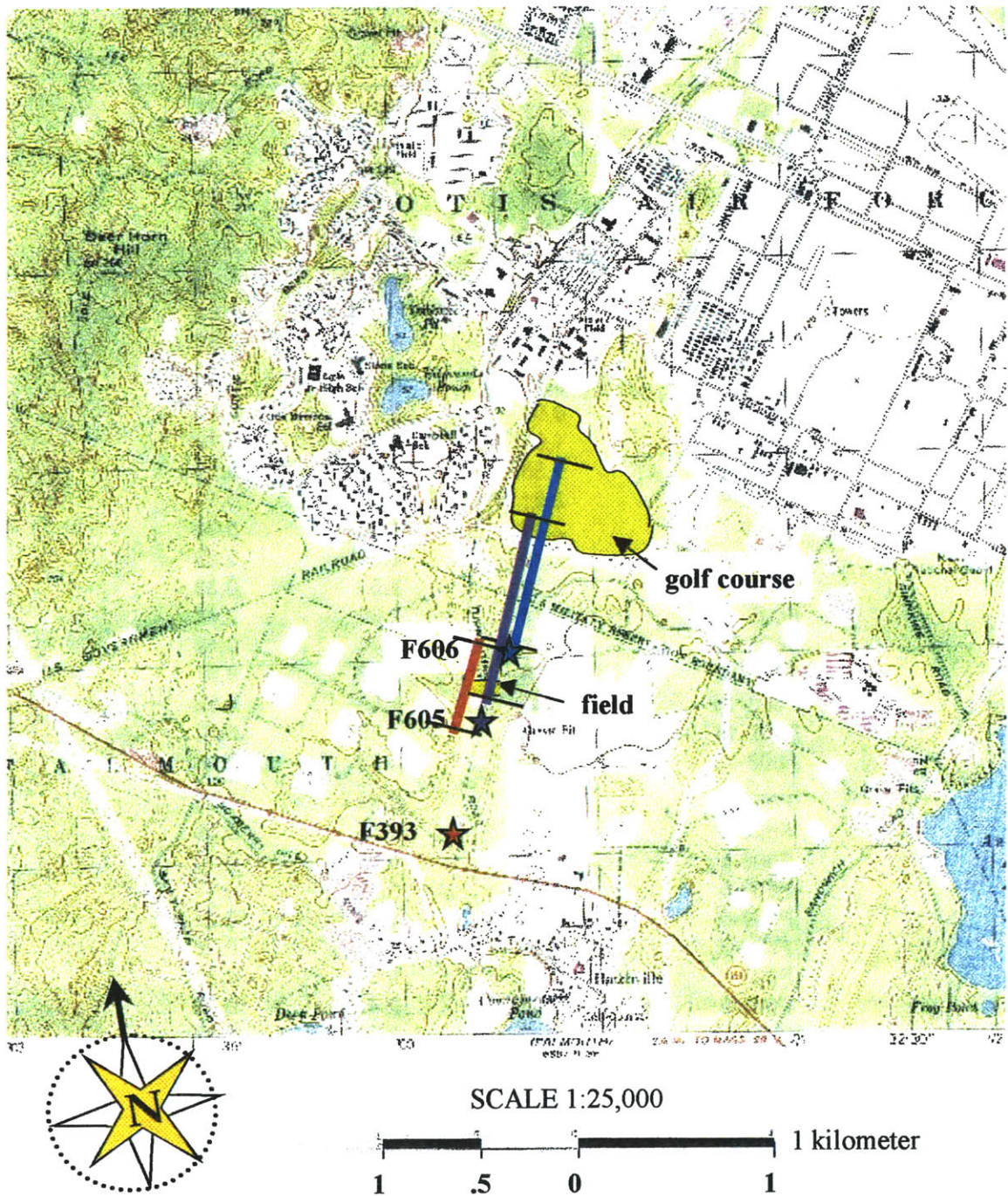
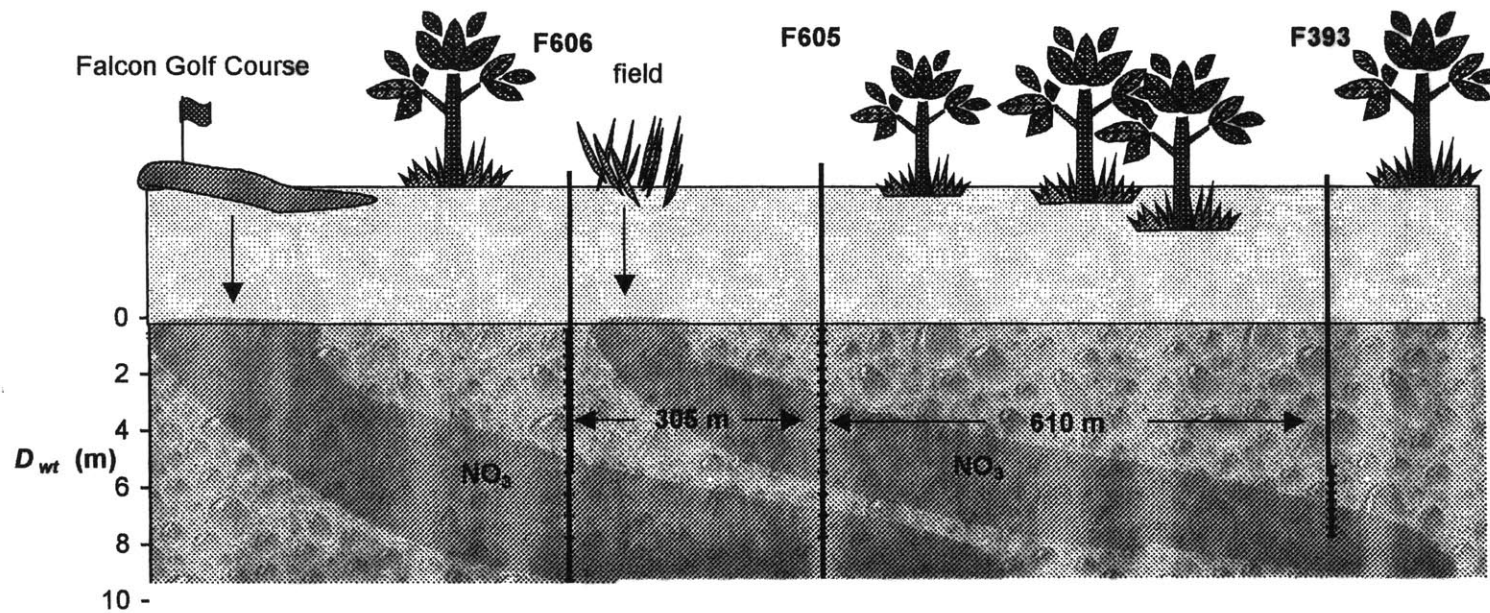


Figure 3.13. Schematic of multi-level sampling (MLS) well transect parallel to groundwater flow lines at Crane Wildlife Management Area. Sources of nitrate and inferred plume configurations are shown relative to depth below water table (D_{wt}), and well and sampling port locations.



below the water table) was 0.7 to 2.9 years old and originated 0.1 to 0.4 km upgradient (Table 3.7). This recharge point coincides with an abandoned field (Figs. 3.12 & 3.13), in the midst of primarily forested cover, which is managed by the Massachusetts Division of Fish and Wildlife to provide habitat for pheasant, bobwhites, and rabbits. Land management practices here have included plowing and occasional top dressing with fertilizer and ground limestone (Richard Turner, Massachusetts Division of Fish & Wildlife, personal communication), which is likely to be the source of the nitrate we measured downgradient.

The water mass containing the one NO_3^- peak in the upgradient well (F606, 5.1 – 9.7 m below the water table) and the lower nitrate concentration peak at well F605 (5.7 – 9.5 m below the water table) was estimated to be 3.6 – 7.0 years old at F606 and 4.0 - 6.9 years old at F605 (Table 3.7). The recharge point for this parcel of water was calculated to be 0.5 to 1.0 km upstream of F606, corresponding to the position of the Falcon Golf Course (Figs. 3.12 & 3.13), where 23:3:3 (N:P:K) had been applied during the time period (1991-2) when recharge of the water we sampled would have occurred. The recharge points for most other well ports mapped to areas with forested cover. The schematic in Figure 3.13 shows inferred fertilizer plume configurations relative to depth below water table (D_{wt}), and well and sampling port locations.

Before estimating denitrification rates for each groundwater sample, we segregated the samples by nitrate concentration into those containing fertilizer-derived nitrate ($>1.5 \mu\text{M}$) and those containing soil-derived nitrate ($<1.5 \mu\text{M}$), consistent with

measurements of nitrate fluxes from forests (Seely 1997) and with our measured groundwater nitrate profiles (Fig. 3.11 a). This was necessary because the $\delta^{15}N$ source values for soil-derived ammonium ($\delta^{15}NH_4^+$ source; Table 3.2) and nitrate ($\delta^{15}NO_3^-$ source; Table 3.4) differ from those of fertilizer-derived ammonium and nitrate. In segregating the data in this manner, we implicitly assumed that the nitrate concentration gradients observed in the groundwater nitrate profiles (from the edges of the fertilizer plumes to the concentration peaks) were due to concentration variations at the source rather than to mixing via diffusion between two nitrate end-members, fertilizer-derived nitrate and soil-derived nitrate. The implications of this assumption for the calculated denitrification rates are discussed further in section 7.1.4. Denitrification.

7.1.2. Nitrification

Our model assumes that nitrification of ammonium supplied to the water table ($[NH_4^+]_{source}$) occurs fairly rapidly, and due to mixing, impacts the $\delta^{15}N$ signal of the pool of nitrate supplied to the water table ($\delta^{15}NO_3^-$ source). We assessed the effect of nitrification (Nitrification Model, Table 3.2 & Fig. 3.3(3)) in the following manner. For each groundwater sample, we measured the isotopic signature ($\delta^{15}NH_4^+$ meas) and concentration ($[NH_4^+]_{meas}$) of ammonium. Using the Rayleigh equation (Eq. 1; Table 3.2), we solved for initial ammonium concentration (C_0 in Eq. 1; $[NH_4^+]_{source}$ in Table 3.2), and the mass balance loss of NH_4^+ between the groundwater recharge and the sampling point ($C_0 - C$ in Eq. 1; $[NH_4^+]_{nit}$ in Table 3.2). This difference represented the total mass of N nitrified in each groundwater sample since recharge. We estimated an average, integrated nitrification rate (dNH_4^+/dt) over the life of each water parcel by dividing the total mass

of N nitrified ($[\text{NO}_3^-]_{\text{nit}} = [\text{NH}_4^+]_{\text{nit}}$) by groundwater age (t), calculated using the Vogel model (Eq. 4; Table 3.1).

Total nitrate produced via nitrification averaged 0.4 μM over 1.8 years for soil-derived N and 0.1 μM over 4.1 years for fertilizer-derived N. These rates are several orders of magnitude less important than denitrification in terms of moles of N transformed (see section on denitrification). Mean groundwater nitrification rate ($2.1 \times 10^{-5} \mu\text{M h}^{-1}$) was several orders of magnitude less than water column nitrification rates measured in eutrophic lakes (D'Angelo and Reddy 1993, Gelda et al. 2000). This is not surprising, given that the flux of ammonium to groundwater beneath forested areas (Seely 1997) results in relatively low concentrations of ammonium at the water table surface ($\sim 3.2 \mu\text{M}$, our calculations), which are likely to limit nitrification. In a soil-stream interface, Hedin et al. (1998) also concluded that groundwater nitrification was either generally less important than denitrification in defining N transformations or less localized than denitrification.

We then assessed the $\delta^{15}\text{N}$ signature of the NO_3^- produced by nitrification using a version of the Rayleigh equation appropriate for product formation (Eq. 3; Rayleigh Production Formation Model, Table 3.3 & Fig. 3.3(3)). Using an isotopic enrichment factor (ϵ_{nit}) of -21‰ , and a $\delta^{15}\text{N}_{\text{NH}_4\text{source}}$ value of $+1.6 \text{‰}$ for soil-derived N, and -1.7‰ for fertilizer-derived N, we calculated the $\delta^{15}\text{N}$ value of the nitrate produced via nitrification for each groundwater sample (Table 3.3). $\delta^{15}\text{N}_{\text{NO}_3^- \text{nit}}$ values ranged from -15.0 to -21.5‰ . We used these calculated $[\text{NO}_3^-]_{\text{nit}}$ and $\delta^{15}\text{N}_{\text{NO}_3^- \text{nit}}$ values in the

‘Apparent $\delta^{15}\text{NO}_3^-$ ’ Model (Table 3.4) to adjust the isotopic signature of the source nitrate ($\delta^{15}\text{NO}_3^-_{\text{source}}$) to reflect the effects of nitrification.

7.1.3. ‘Apparent $\delta^{15}\text{NO}_3^-$ ’ Model

We assumed that nitrification occurred primarily near the surface of the water table. We used the following mass balance equations to adjust the $\delta^{15}\text{NO}_3^-$ signal of nitrate near the water table ($\delta^{15}\text{NO}_3^-_{\text{source}}$) to reflect nitrification of ammonium ($\delta^{15}\text{NO}_3^-_{\text{adj}}$, Fig. 3.3(4) & Table 3.4):

$$(5) [\text{NO}_3^-]_{\text{adj}} = [\text{NO}_3^-]_{\text{source}} + [\text{NO}_3^-]_{\text{nit}}$$

$$(6) (\delta^{15}\text{NO}_3^-)_{\text{adj}} * [\text{NO}_3^-]_{\text{adj}} = (\delta^{15}\text{NO}_3^-)_{\text{source}} * [\text{NO}_3^-]_{\text{source}} + (\delta^{15}\text{NO}_3^-)_{\text{nit}} * [\text{NO}_3^-]_{\text{nit}},$$

where $[\text{NO}_3^-]_{\text{adj}}$ = the concentration of nitrate after nitrification, $[\text{NO}_3^-]_{\text{source}}$ = the concentration of nitrate at the water table, $[\text{NO}_3^-]_{\text{nit}}$ = the concentration of nitrate produced *in situ* via nitrification, $(\delta^{15}\text{NO}_3^-)_{\text{adj}}$ = the isotopic value of nitrate near the water table, adjusted for nitrification, $(\delta^{15}\text{NO}_3^-)_{\text{source}}$ = the isotopic value of nitrate at the water table, and $(\delta^{15}\text{NO}_3^-)_{\text{nit}}$ = the isotopic value of nitrate produced *in situ* via nitrification.

For soil-derived N, we used the average mass ($[\text{NO}_3^-]_{\text{nit}} = 0.37 \mu\text{M}$) and isotopic signal of the nitrate produced via nitrification ($\delta^{15}\text{NO}_3^-_{\text{nit}} = -18.3 \text{‰}$) as inputs to this model. For fertilizer-derived N, we used calculated $\delta^{15}\text{NO}_3^-_{\text{nit}}$ (-16.2 to -21.6 ‰) and $[\text{NO}_3^-]_{\text{nit}}$ (0 to 0.75 μM) for each individual sample. The $\delta^{15}\text{NO}_3^-_{\text{source}}$ value for soil-

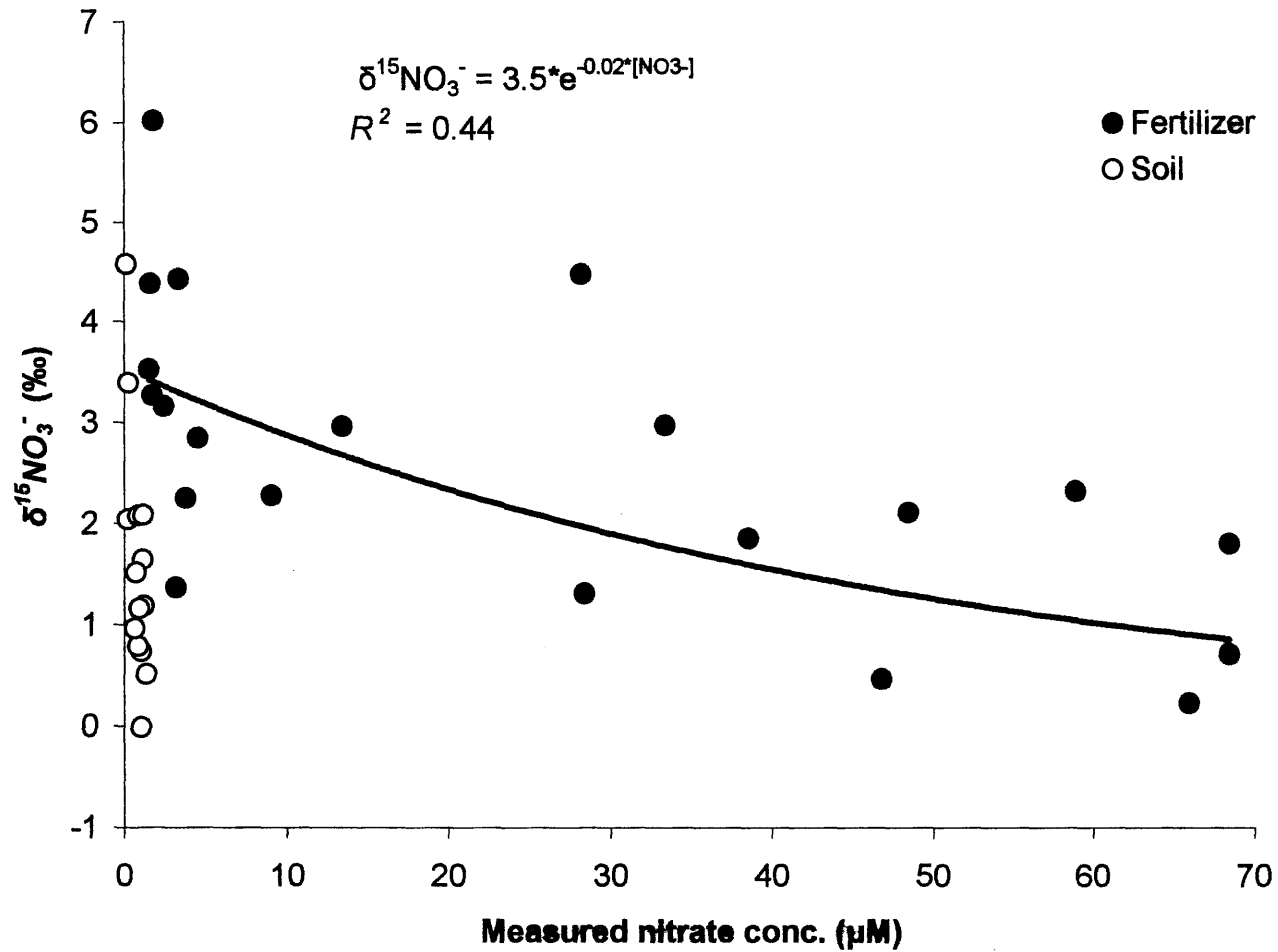
derived N was calculated from measured values in the uppermost well ports (+3.4 ‰); the $\delta^{15}\text{NO}_3^-$ source value for fertilizer-derived N was estimated from the literature (-3.2 ‰), since water table samples were not available.

Our correction resulted in a $\delta^{15}\text{NO}_3^-$ adj value for soil-derived nitrate (-1.7 ‰) that was 5.2 ‰ lower than that of the $\delta^{15}\text{NO}_3^-$ source value (+3.4 ‰). For fertilizer-derived nitrate, the correction resulted in $\delta^{15}\text{NO}_3^-$ adj values ranging from -3.2 to -3.3 ‰, only slightly lower (~ 0.1 ‰) than the $\delta^{15}\text{NO}_3^-$ source value (-3.2 ‰). The larger correction for soil-derived nitrate results from the hyperbolic nature of stable isotope mixing models (Mariotti et al. 1988, Kendall & McDonnell 1998), whereby a small increase in the quantity of one of the mixing end-members can have a significant impact on the measured $\delta^{15}\text{NO}_3^-$ values. Because $[\text{NO}_3^-]_{\text{nit}}$ is much larger relative to $[\text{NO}_3^-]_{\text{source}}$ for soil-derived nitrate (29 %) than for fertilizer-derived nitrate (< 1%), we expect a larger correction to the $\delta^{15}\text{NO}_3^-$ values for the soil-derived samples.

7.1.4. Denitrification

The $\delta^{15}\text{N}$ values of nitrate measured in our samples increased with decreasing nitrate concentrations (Fig. 3.14), suggesting that denitrification occurred in the groundwater, leaving the residual nitrate enriched relative to the nitrate delivered to the water table. We segregated these data into two populations based on NO_3^- concentration: those samples with high NO_3^- concentrations, comprising the peaks within the depth profiles and believed to represent water bearing NO_3^- derived from fertilizer ($> 1.5 \mu\text{M}$ NO_3^-); and samples with the low concentrations of NO_3^- above and below the peaks,

Figure 3.14. $\delta^{15}N$ of nitrate measured at Crane Wildlife Management Area for fertilizer- and soil-derived nitrate. $\delta^{15}N$ values increase with decreasing nitrate concentration.



presumably representing NO_3^- originating from soil organic N sources ($< 1.5 \mu\text{M NO}_3^-$), since the isotopic signature of these two nitrate sources is different (Table 3.5).

As we did for nitrification, we used the Rayleigh equation (Eq. 1; Denitrification Model, Table 3.5 & Fig. 3.3(5)) to solve for initial nitrate concentration (C_0 in Eq. 1, and $[\text{NO}_3^-]_{\text{adj}}$ in Table 3.5), and for mass balance losses of nitrate between the sampling point and the groundwater recharge point ($C - C_0$ in Eq. 1, and $[\text{NO}_3^-]_{\text{denit}}$ in Table 3.5) for each groundwater sample. In this calculation, we used the values for $\delta^{15}\text{NO}_3^-_{\text{adj}}$ calculated using the 'Apparent $\delta^{15}\text{NO}_3^-$ ' Model. The calculated nitrate loss ($[\text{NO}_3^-]_{\text{denit}}$) was divided by groundwater age (t) to produce an average denitrification rate ($d\text{NO}_3^-/dt$) for each groundwater sample over the groundwater flowpath since the time of recharge.

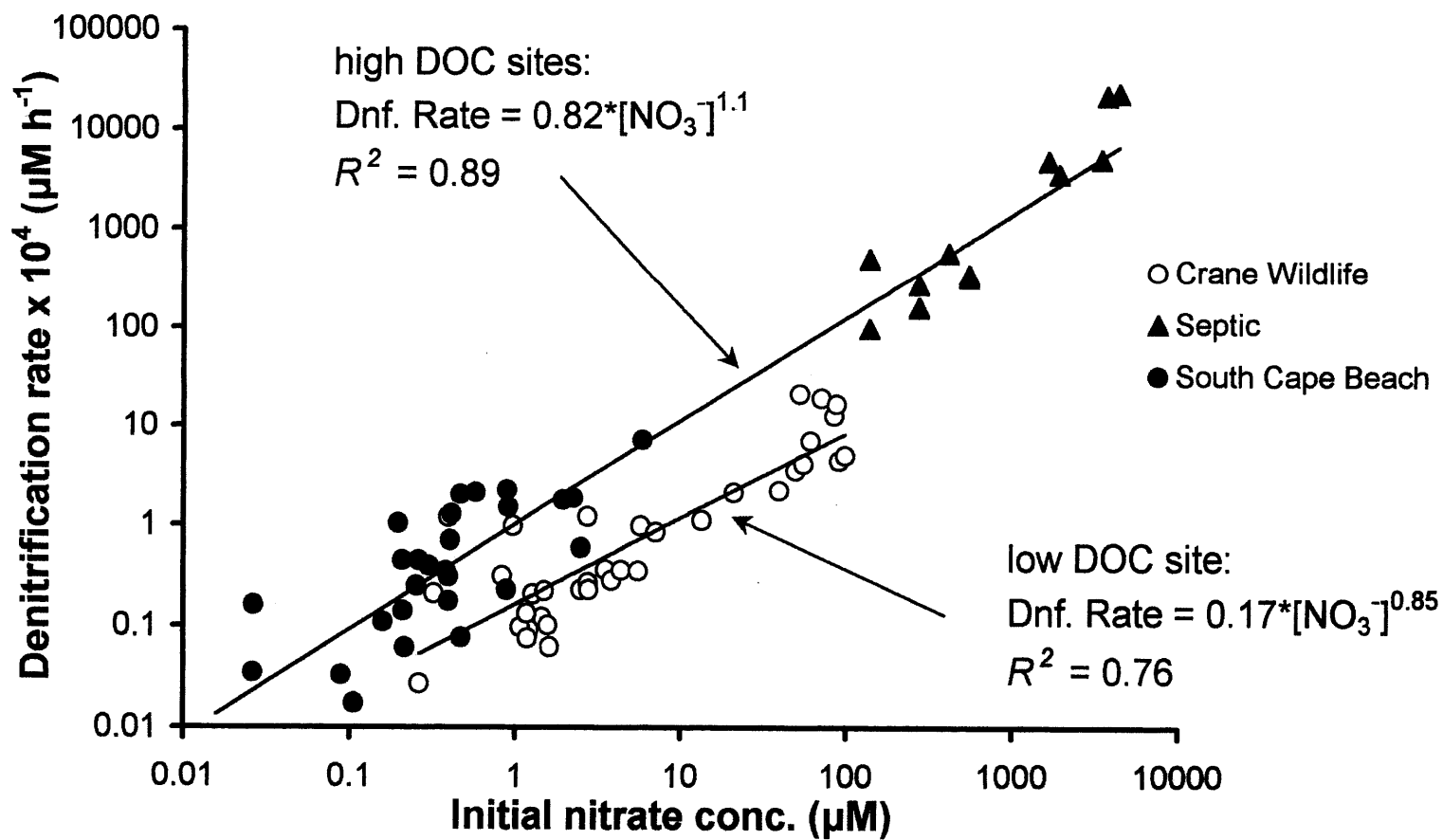
Calculated initial nitrate concentrations ($[\text{NO}_3^-]_{\text{adj}}$) for the soil-derived nitrate samples (0.3 to $1.6 \mu\text{M NO}_3^-$) were consistent with calculations we made of nitrate concentrations in groundwater beneath forest soils (0 to $2.7 \mu\text{M NO}_3^-$), using estimates of nitrate fluxes to groundwater at three sites within the Waquoit Bay watershed (Seely 1997). Initial nitrate concentrations calculated for samples containing fertilizer-derived nitrate (2.5 to $98.0 \mu\text{M}$) fell within the range of nitrate concentrations measured in groundwater beneath four Cape Cod golf courses (0 to $2,143 \mu\text{M N}$, Cohen et al. 1990), and were somewhat lower than our calculations for mean total nitrogen concentration delivered to the water table from golf course turf ($165 \mu\text{M N}$, NLM, Valiela 1997).

Average denitrification rates spanned 3 orders of magnitude (2.7×10^{-6} to $2.1 \times 10^{-3} \mu\text{M N h}^{-1}$), and increased with increasing initial nitrate concentration (0.3 to 98 μM). The data was fit with a power curve (Fig. 3.15, low DOC site, $\text{rate} = 0.17 * [\text{NO}_3^-]^{0.85}$, $R^2 = 0.76$).

To address any issues of circularity associated with using several of the same points to both parameterize the Rayleigh model (i.e., those points from which we estimated the $\delta^{15}\text{N}$ values for ammonium ($\delta^{15}\text{NH}_4^+_{\text{source}}$) and nitrate ($\delta^{15}\text{NO}_3^-_{\text{source}}$) at the water table) and to estimate denitrification rates using the model, we removed those four points from the data set and reexamined the results. We found that removing these four points does not change the calculated range in denitrification rates and increases the mean denitrification rate only slightly ($3.3 \times 10^{-4} \mu\text{M N h}^{-1}$ when we exclude the points, versus $3.0 \times 10^{-4} \mu\text{M N h}^{-1}$ when we include them).

In our analysis, we segregated the data into only two populations, those containing fertilizer-derived nitrate ($>1.5 \mu\text{M}$; $\delta^{15}\text{NO}_3^-_{\text{source}} = -3.2 \text{‰}$) and those containing soil-derived nitrate ($<1.5 \mu\text{M}$; $\delta^{15}\text{NO}_3^-_{\text{source}} = +3.4 \text{‰}$). In doing so, we neglected the impact of mixing between the two nitrate sources, which would result in a range of $\delta^{15}\text{NO}_3^-_{\text{source}}$ values lying between the two end-member $\delta^{15}\text{NO}_3^-_{\text{source}}$ values. To assess the implications of this assumption, we used the following stable isotope mixing equations to assign variable $\delta^{15}\text{NO}_3^-_{\text{source}}$ values to the fertilizer-derived nitrate samples:

Figure 3.15. Average denitrification rate versus initial nitrate concentration for two forested sites (South Cape Beach and Crane Wildlife), and for a septic plume (Ch. 4).



$$[\text{NO}_3^-]_{\text{meas}} = [\text{NO}_3^-]_{\text{soil}} + [\text{NO}_3^-]_{\text{fert}}$$

$$\delta^{15}\text{NO}_3^-_{\text{source}} * [\text{NO}_3^-]_{\text{meas}} = \delta^{15}\text{NO}_3^-_{\text{soil}} * [\text{NO}_3^-]_{\text{soil}} + \delta^{15}\text{NO}_3^-_{\text{fert}} * [\text{NO}_3^-]_{\text{fert}}$$

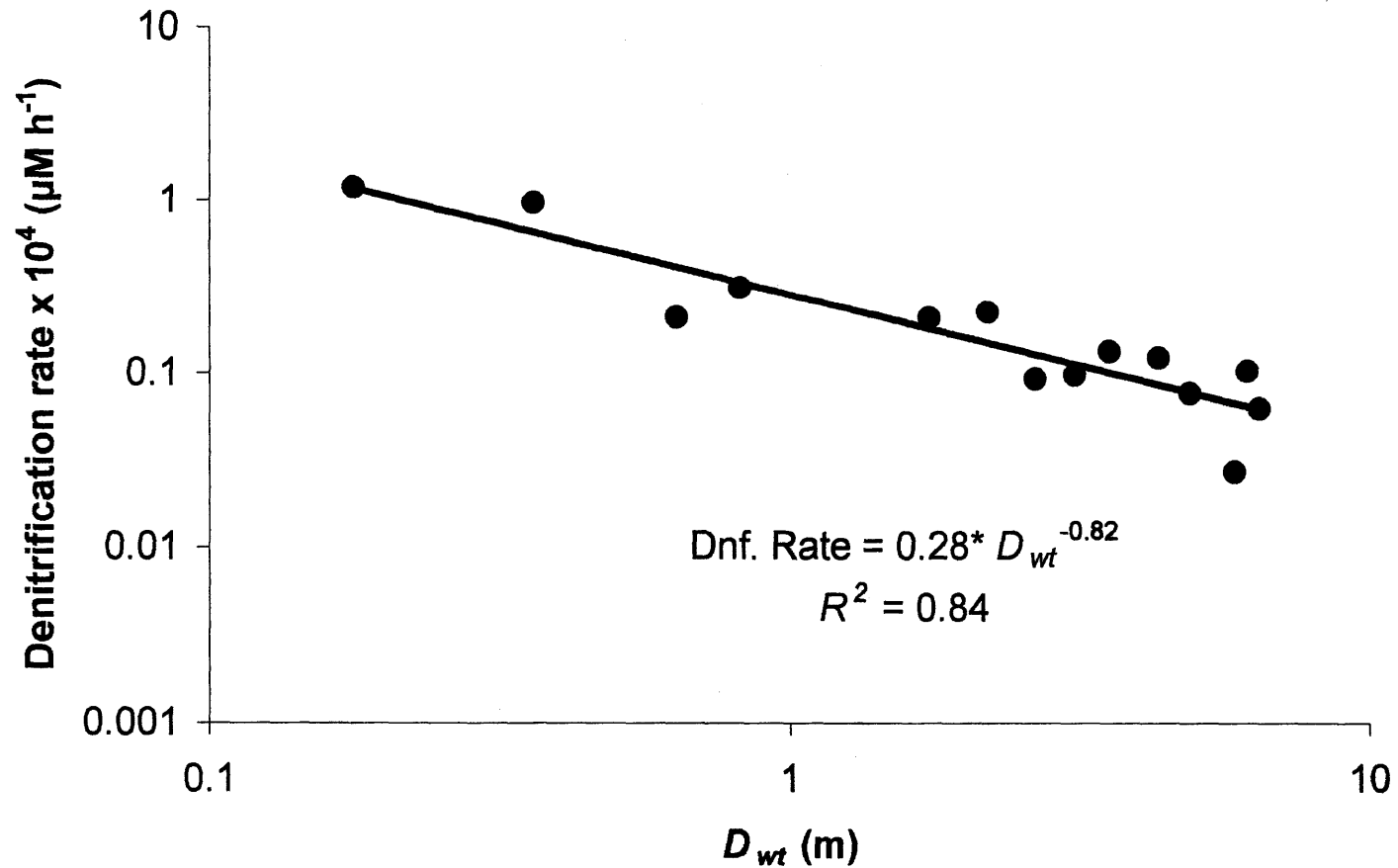
where $[\text{NO}_3^-]_{\text{meas}}$ is the nitrate concentration measured in the profile, $[\text{NO}_3^-]_{\text{soil}}$ is the concentration of the nitrate derived from soil, $[\text{NO}_3^-]_{\text{fert}}$ is the concentration of nitrate derived from fertilizer, $\delta^{15}\text{NO}_3^-_{\text{source}}$ is the $\delta^{15}\text{N}$ value of nitrate derived from the mixture of fertilizer and soil sources, $\delta^{15}\text{NO}_3^-_{\text{soil}}$ is the $\delta^{15}\text{N}$ source value for soil-derived nitrate (+3.4 ‰), and $\delta^{15}\text{NO}_3^-_{\text{fert}}$ is the $\delta^{15}\text{N}$ source value for fertilizer-derived nitrate (-3.2 ‰). Recalculating the denitrification rates for the fertilizer-derived nitrate samples using the variable $\delta^{15}\text{NO}_3^-_{\text{source}}$ values resulted, on average, in a 25% reduction in the denitrification rate. Reductions in the calculated denitrification rates were greatest (50-75%) where nitrate concentrations were lowest (1-2 μM) and negligible (< 8 %) where nitrate concentrations were higher (>10 μM).

Our calculated average denitrification rates are consistent with groundwater denitrification rates estimated by Smith and Duff (1988; 1.0×10^{-6} to 1.2×10^{-4} $\mu\text{M N h}^{-1}$) using an acetylene blockage assay on slurried aquifer core material obtained near wastewater disposal beds, located approximately 1 km to the east of the Crane Wildlife field site on the Massachusetts Military Reservation. Nitrate concentrations in the groundwater at the locations where core material was obtained ranged from 0 – 1,760 μM ; DOC concentrations were estimated to be ~ 12 mg C l^{-1} , and were found to be limiting to denitrification.

In this aquifer, DOC concentrations in groundwater decrease with increasing depth below the water table, with the majority of the attenuation occurring in the first several meters beneath the water table (Pabich et al. submitted). Based on this previous work, we hypothesized that the upper portion of the aquifer is a particularly biogeochemically active zone. If this is the case, we would expect denitrifying activity to be high near the water table, and decrease with increasing depth below the aquifer surface, as groundwater ages and labile carbon and nitrate are consumed by denitrification and other metabolic reactions. To test this hypothesis, we plotted denitrification rate against depth below the water table for those samples containing soil-derived nitrate. Denitrification rate indeed decreased with depth below the water table; $R^2 = 0.84$, Fig. 3.16), so that denitrification was fastest in the youngest water and slower in older waters.

Given the positive relationship between nitrate concentration and denitrification rate, we investigated whether the data could be modeled using both a first order rate approximation ($[\text{NO}_3^-]_{\text{meas}} = [\text{NO}_3^-]_{\text{adj}} * e^{-kt}$) and a saturating kinetics expression ($d[\text{NO}_3^-]/dt = (V_{\text{max}} * ([\text{NO}_3^-]_{\text{adj}} / (K_M + [\text{NO}_3^-]_{\text{adj}}))$; where V_{max} is the maximum reaction velocity and K_M is the half-saturation constant) with respect to nitrate. For the first order approximation, we calculated a first order rate constant ($k = [\ln([\text{NO}_3^-]_{\text{adj}} / [\text{NO}_3^-]_{\text{meas}})] / t$), or $k = [\ln(C/C_0)]/t$ from Rayleigh equation) for each individual groundwater sample, and averaged the individual values to produce a first order rate constant for the data set as a whole ($k = 2.9 \times 10^{-5} \text{ h}^{-1}$ or $.26 \text{ y}^{-1}$). Calculating a numerical average of the individual k 's provided a better fit to the data than did a graphical estimation of k (i.e., the slope of a

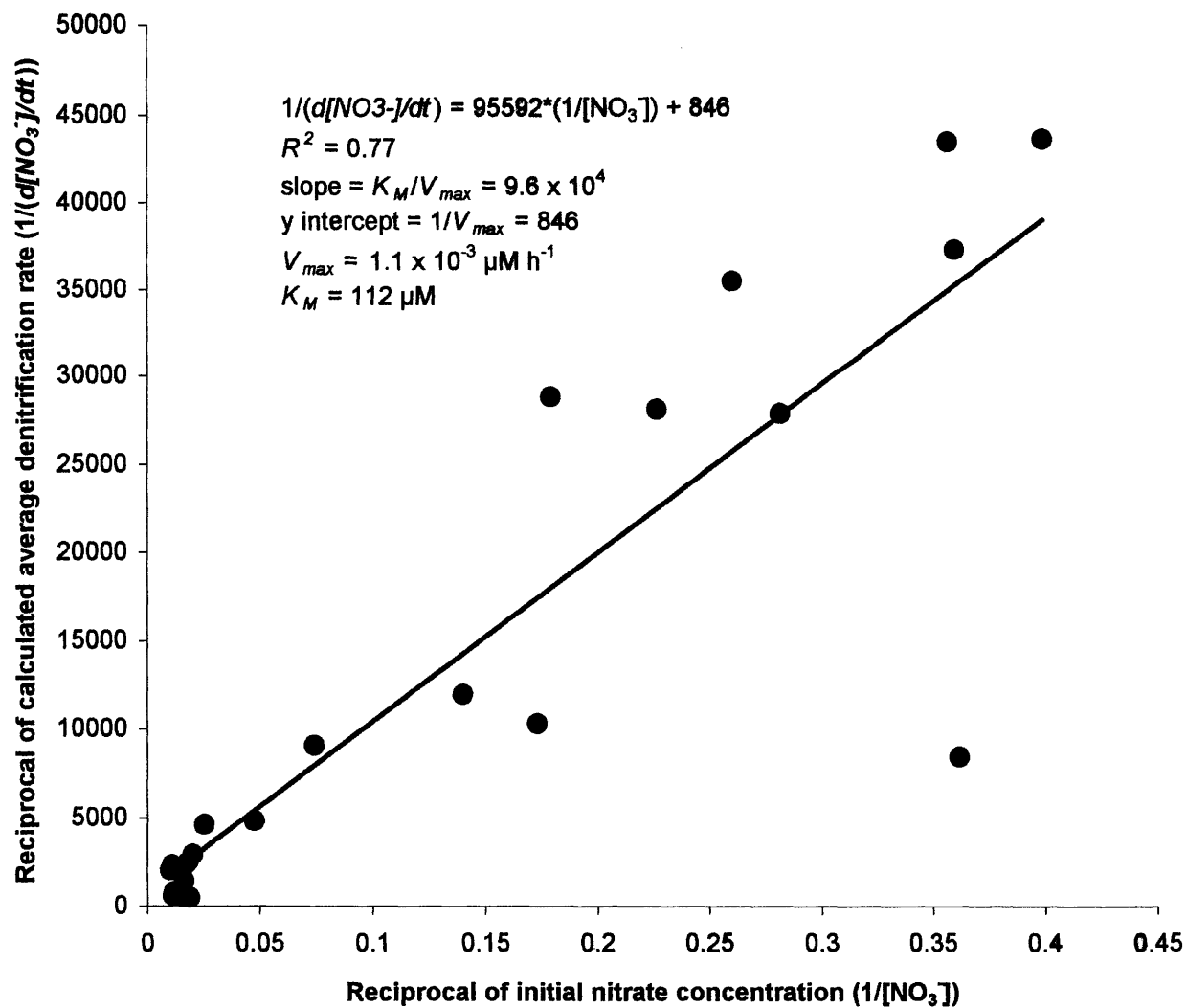
Figure 3.16. Denitrification rates decrease with increasing depth below the water table (D_{wt}) for soil-derived nitrate samples at Crane Wildlife Management Area ($R^2 = 0.84$). Axes are logarithmic.



plot of $\ln([\text{NO}_3^-]_{\text{meas}}/[\text{NO}_3^-]_{\text{adj}})$ vs. time represents k ; data not shown). The half-life for nitrate ($t_{1/2}$) given this first order rate constant, was calculated to be 2.7 years. To parameterize the saturating kinetic expression, we used a Lineweaver-Burke plot (Fig. 3.17; $1/(d[\text{NO}_3^-]/dt)$ vs. $1/[\text{NO}_3^-]_{\text{adj}}$) to calculate the half-saturation constant ($K_M = 112 \mu\text{M}$) and the maximum reaction velocity ($V_{\text{max}} = 1.1 \times 10^{-3} \mu\text{M N h}^{-1}$).

To test how well each of these three approximations (average rate over flowpath, first order rate, and saturating kinetics) represented our data, we ran simulations to estimate the total N lost in each groundwater sample over the flowpath from recharge to the downgradient well port. For the first order and saturating kinetics simulations, we discretized each groundwater flowpath into 4 time steps. For the first time step, we estimated the denitrification rate based on the initial nitrate concentration ($[\text{NO}_3^-]_{\text{adj}}$), calculated the total mass of N lost to denitrification during that time band ($[\text{NO}_3^-]_{\text{denit}}$), and subtracted the two values ($[\text{NO}_3^-]_{\text{adj}} - [\text{NO}_3^-]_{\text{denit}}$) to estimate the final nitrate concentration at the end of the time band. In each sequential time band we calculated a new denitrification rate, N loss, and final N concentration, based on the mass of nitrate remaining from the previous time band. For the simulation using the average denitrification rate, we estimated an average denitrification rate over the length of the flowpath using the power curve fit (Fig. 3.15) and either the initial or the final nitrate concentration ($[\text{NO}_3^-]_{\text{adj}}$). We multiplied this denitrification rate by the total groundwater travel time (from recharge to downgradient well port) to calculate total N lost over the flowpath ($[\text{NO}_3^-]_{\text{denit}}$); we subtracted this value from the initial nitrate concentration

Figure 3.17. Lineweaver-Burke plot using fertilizer-derived nitrate samples at Crane Wildlife to derive saturating kinetics parameters. The half-saturation constant (K_M) was estimated to be 112 μM and the maximum denitrification rate (V_{max}) was estimated to be $1.1 \times 10^{-3} \text{ h}^{-1}$.



$[\text{NO}_3^-]_{\text{adj}}$). These simulations provided approximations of the nitrate concentration expected at each downgradient well port ($[\text{NO}_3^-]_{\text{model}}$).

For each simulation, we plotted expected nitrate concentration ($[\text{NO}_3^-]_{\text{model}}$) against nitrate concentration measured at each well port ($[\text{NO}_3^-]_{\text{meas}}$; Figs. 3.18-3.20). The saturating kinetics expression provided the best approximation of measured values ($R^2 = 0.96$; Fig. 3.20). Losses estimated using the average rate (Fig. 3.19) also closely approximated the measured nitrate concentrations. For this analysis, we estimated the denitrification rate using both the nitrate concentration measured at the downgradient well port ($[\text{NO}_3^-]_{\text{meas}}$; $R^2 = 0.94$) and the estimated initial nitrate concentration ($[\text{NO}_3^-]_{\text{adj}}$; $R^2 = 0.89$). The first order rate expression was the least effective in predicting the measured downgradient nitrate concentration (Fig. 3.18; $R^2 = 0.62$). This model substantially overestimated nitrate loss due to denitrification, especially as nitrate concentration increased (data points below the 1:1 line), suggesting that the reaction becomes saturated with respect to nitrate.

7.2. *South Cape Beach*

7.2.1. Geochemistry

Dissolved oxygen concentrations at the twelve sampling stations near South Cape Beach were much more variable than at Crane Wildlife, ranging from 1.6 to 10.7 mg O₂ l⁻¹ and averaging 6.4 mg O₂ l⁻¹. This is consistent with the higher and more variable DOC concentrations at South Cape Beach (range = 0.8 to 23.4 mg C l⁻¹, mean = 7.0 mg C l⁻¹). Differences in DOC concentrations are likely to result in differences in microbial

Figure 3.18. Results of simulation predicting nitrate concentrations at downgradient well ports ($[\text{NO}_3^-]_{\text{model}}$) using a first order rate expression, versus nitrate concentrations measured at those well ports ($[\text{NO}_3^-]_{\text{meas}}$; $R^2 = 0.62$, probability $\ll 0.001$).

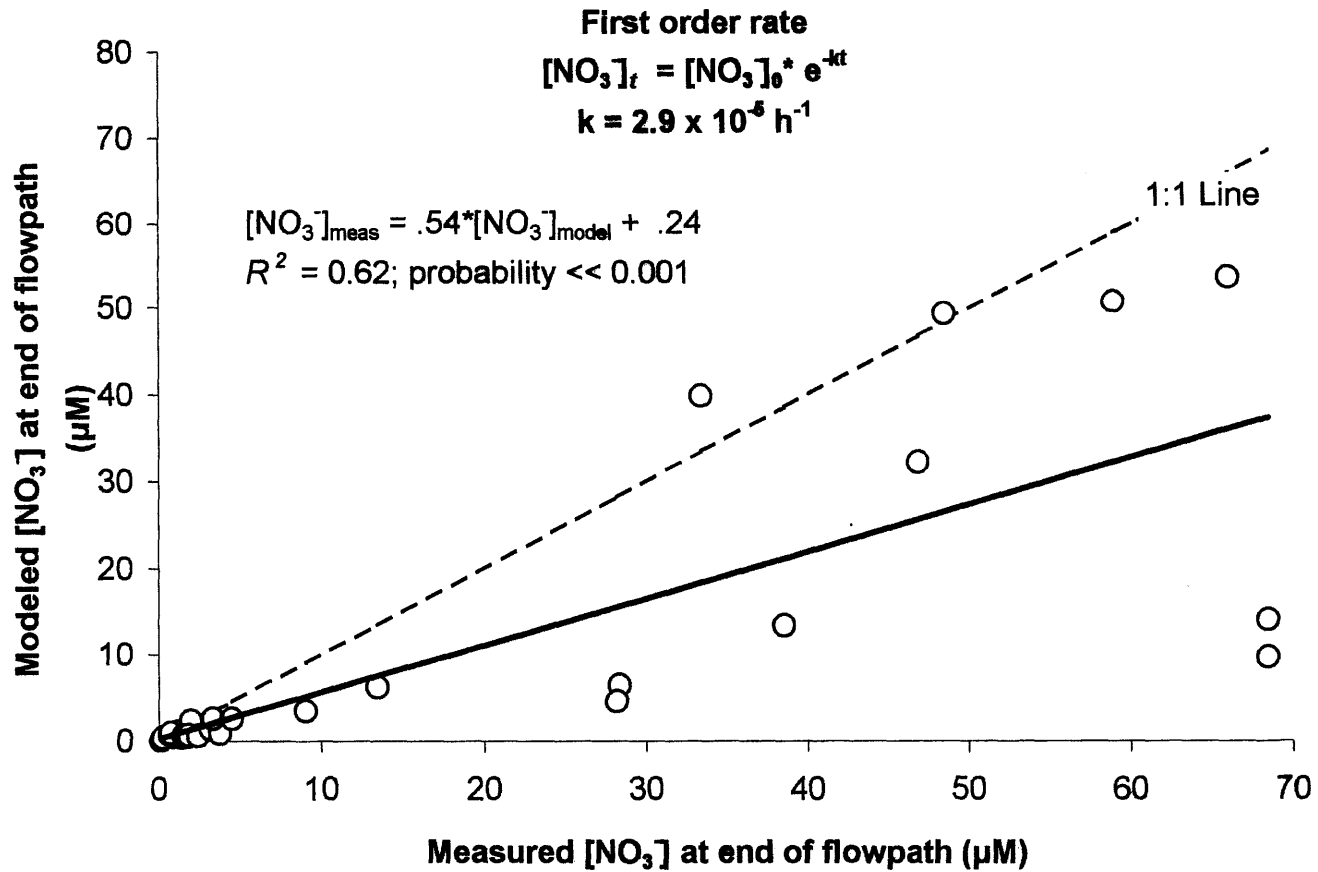


Figure 3.19. Results of simulation predicting nitrate concentrations at downgradient well ports ($[\text{NO}_3^-]_{\text{model}}$) using average denitrification rates over the flowpaths (calculated from both initial and final nitrate concentrations) versus nitrate concentrations measured at those well ports ($[\text{NO}_3^-]_{\text{meas}}$; $R^2 = 0.89$ and 0.94 , probability $\ll 0.001$).

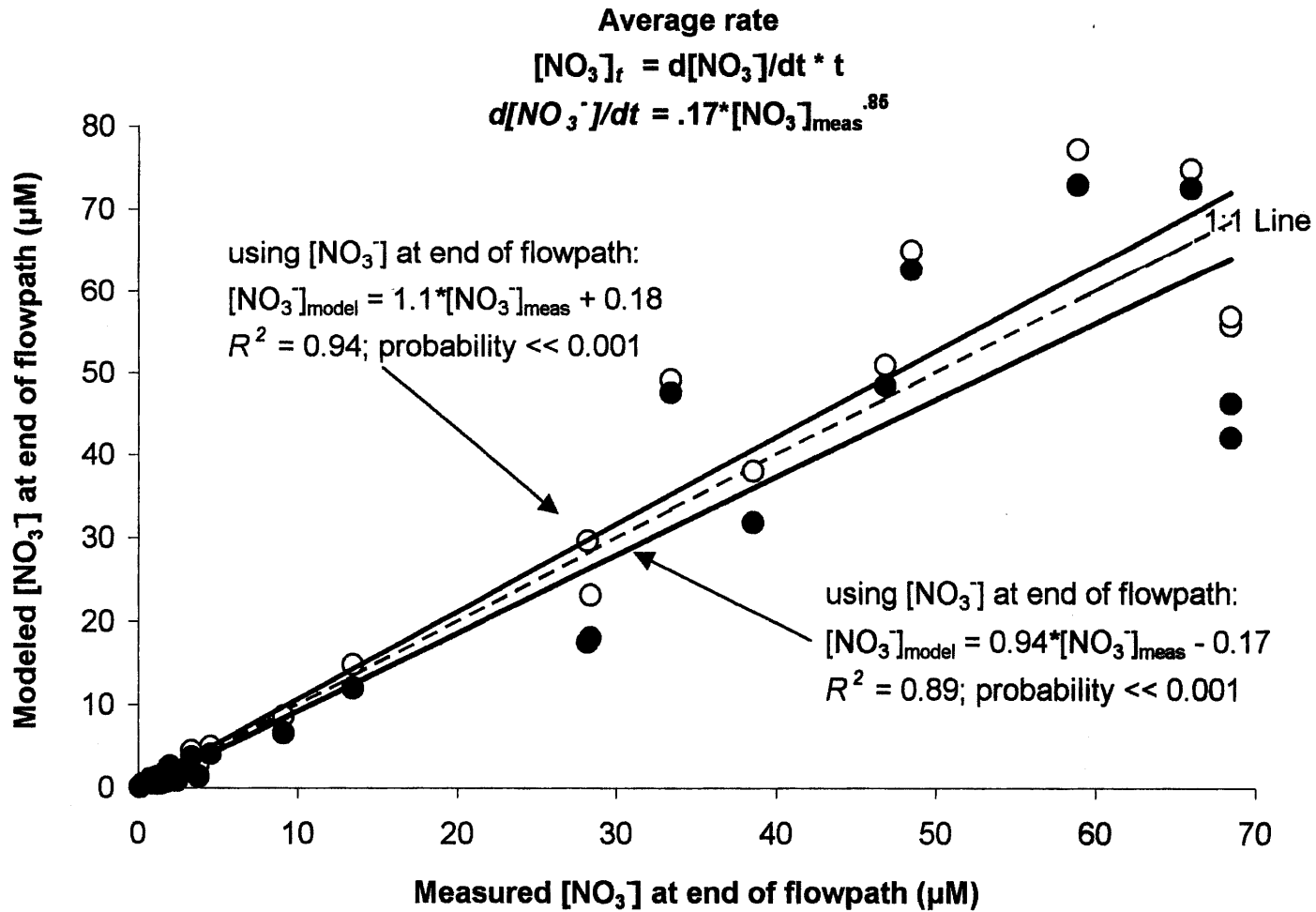
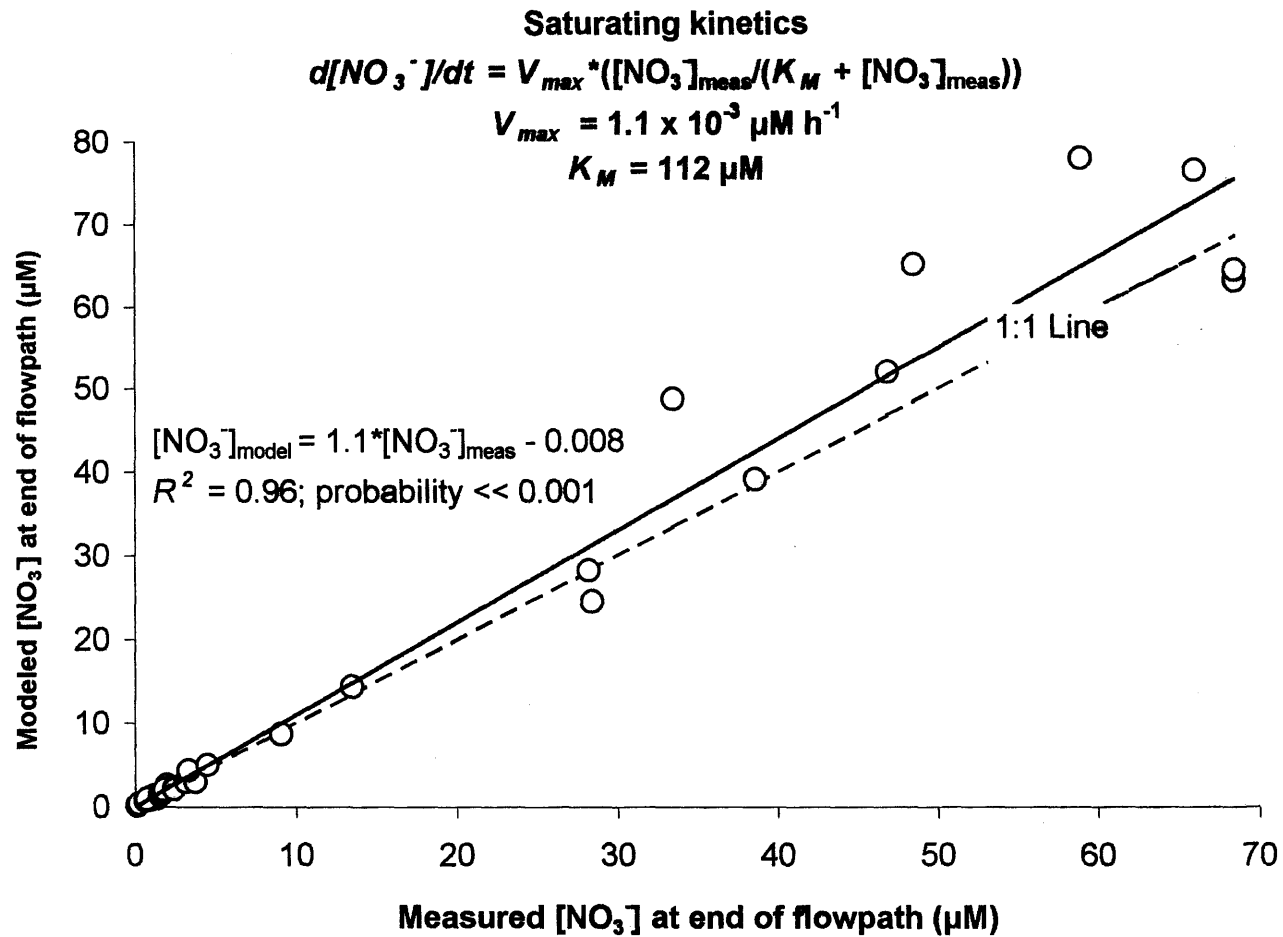


Figure 3.20. Results of simulation predicting nitrate concentrations at downgradient well ports ($[\text{NO}_3^-]_{\text{model}}$) using saturating kinetics expression with respect to nitrate versus nitrate concentrations measured at those well ports ($[\text{NO}_3^-]_{\text{meas}}$; $R^2 = 0.96$; probability $\ll 0.001$).



metabolism between the two sites; where DOC supply is high, greater microbial activity is likely to reduce dissolved oxygen concentrations.

Nitrate concentrations at the South Cape Beach stations ranged from 0.01 to 4.0 μM , and averaged 0.6 μM , which were low relative to those at Crane Wildlife and to other more residential areas in the Waquoit Bay watershed (up to 1000 μM ; Kroeger et al. 1999, Valiela et al. 1992). Ammonium concentrations were similarly low, ranging from 0 to 3.9 μM , and averaging 0.8 μM , consistent with inputs of ammonium derived solely from soil organic matter (Seely 1997). $\delta^{15}\text{N}$ of nitrate ranged from -4.9 to $+4.5$ ‰, and averaged -3.0 ‰; the modal $\delta^{15}\text{NO}_3^-$ value (~ -2 ‰) was ~ 4 ‰ lower than at Crane Wildlife Management Area ($\sim +4$ ‰; Fig. 3.9). Like at Crane Wildlife, temporal variability in groundwater chemistry was much less than spatial variability (Table 3.6).

7.2.2. Nitrification

Because we did not measure $\delta^{15}\text{N}$ of ammonium at South Cape Beach, we could not estimate nitrification rates directly as we did at the Crane Wildlife site. Instead, we assumed that the lowest measured $\delta^{15}\text{NO}_3^-$ value (-4.9 ‰) was representative of the impact of nitrification on the stable isotopic signature of nitrate near the water table, and assigned this value to $\delta^{15}\text{NO}_3^-_{adj}$.

7.2.3. Denitrification

To model denitrification at South Cape Beach, we used the same enrichment factor (ϵ) as at Crane Wildlife (-13.9 ‰), and -4.9 ‰ for the source nitrate adjusted for

nitrification ($\delta^{15}\text{NO}_3^-_{\text{adj}}$), as discussed above. Measured $\delta^{15}\text{N}$ values at South Cape Beach were consistently lower than those at Crane Wildlife (Fig. 3.9), suggesting that less complete nitrification (greater fractionation) occurred at South Cape Beach. Ammonium made up a much larger fraction, on average, of the total inorganic nitrogen ($\text{NH}_4 + \text{NO}_3^-$, 57%) than at Crane Wildlife (13 %), supporting the idea that nitrification was less complete at South Cape Beach, and therefore played a more important role in determining groundwater $\delta^{15}\text{N}$ signals.

Consistent with our findings at Crane Wildlife, average denitrification rates at South Cape Beach increased with increasing initial nitrate concentration, from $9.2 \times 10^{-9} \mu\text{M NO}_3^- \text{ h}^{-1}$ to $7.2 \times 10^{-4} \mu\text{M NO}_3^- \text{ h}^{-1}$ as initial nitrate increased from 0.2 to 5.9 $\mu\text{M NO}_3^-$. However, denitrification rates at this site were higher for any given initial nitrate concentration than in the lower DOC environment of Crane Wildlife. This is illustrated by a power curve fit through a plot of average denitrification rate versus initial nitrate concentration (Fig. 3.15), where the regression slope is similar for both the high and the low DOC populations, but the curve has been shifted such that the value of the y-intercept is higher for the higher DOC population. This suggests that DOC concentration is an important determinant of denitrification rate. In fact, the mean of the first order rate constants ($k = [\ln([\text{NO}_3^-]_{\text{adj}}/[\text{NO}_3^-]_{\text{meas}})]/t$) calculated for the individual samples at South Cape Beach was 6 times higher ($1.8 \times 10^{-4} \text{ h}^{-1}$ or 1.5 y^{-1} ; $t_{1/2} = 0.45 \text{ y}$) than that calculated for the Crane Wildlife samples. This suggests that, independent of nitrate concentration, denitrification rates are higher at the higher DOC site.

In Chapter 4, we calculated denitrification rates in excess of dilution in a septic system plume outfitted with 9 multilevel sampling wells along a downgradient transect. Losses of nitrate were assessed with respect to boron, a conservative tracer; rates were calculated for each water sample by dividing the mass of nitrate lost between the septic system leach field and the downgradient well sampling port, by groundwater age at that port calculated using the Vogel (1967). Denitrification rates in the septic system (0.01 to $2.23 \mu\text{M NO}_3^- \text{ h}^{-1}$) also increased with increasing initial nitrate concentration (137 to $4,396 \mu\text{M}$). We assumed that DOC concentrations in the septic plume were similar to those measured in other plumes of this age (Ch. 4, $\sim 26 \text{ mg C l}^{-1}$ from Robertson et al. (1998)).

We add this data here (Fig. 3.15) to illustrate that denitrification rates, both assessed using a different method (mass balance instead of stable isotopes), and in a very different system (higher DOC and nitrate concentrations, and presumably a larger and more active microbial population), follow the same general trend as observed in the natural forested sites. The addition of the septic system data to Figure 3.15 supports the conclusion that denitrification rates are higher for any given nitrate concentration in the two systems with higher DOC concentrations (South Cape Beach (0.8 to 23.4 mg C l^{-1}), and the septic plume ($\sim 26 \text{ mg C l}^{-1}$); denitrification rate = $0.82 * [\text{NO}_3^-]^{1.1}$, $R^2 = 0.89$) than in the system with low DOC (Crane Wildlife ($< 2 \text{ mg C l}^{-1}$); denitrification rate = $0.17 * [\text{NO}_3^-]^{0.85}$, $R^2 = 0.76$). Further, the mean of the first order rate constants (Table 3.8) calculated for the individual septic plume samples ($k = 3.1 \times 10^{-4} \text{ h}^{-1}$ or 2.7 y^{-1} ;

Table 3.8. First order rate constants for denitrification in groundwater at three field sites increase with increasing DOC concentration (e.g. septic plume > South Cape Beach > Crane Wildlife). The half-life for nitrate, and the groundwater travel distance required for nitrate to be attenuated to 1/2 its initial concentration, are shown for each site.

Field site	[DOC] (mg l ⁻¹)	[NO ₃] (μM)	First order rate constant k (y ⁻¹)	Half-life for nitrate, t _{1/2} (y ⁻¹)	Travel distance to t _{1/2} (m)
Crane Wildlife Management Area	< 2	0 - 68	0.26	2.8	409
South Cape Beach	0.8 - 23	0 - 4	1.5	0.45	66
Septic system plume	~ 26	up to 4,000	2.7	0.25	37

$t_{1/2} = 0.25$ y) was 11 times higher than at Crane Wildlife ($k = 2.9 \times 10^{-5} \text{ h}^{-1}$ or $.26 \text{ y}^{-1}$; $t_{1/2} = 2.8$ y), but only twice as high as the first order rate for South Cape Beach ($k = 1.8 \times 10^{-4} \text{ h}^{-1}$ or 1.5 y^{-1} , $t_{1/2} = 0.45$ y), presumably because the DOC concentrations in the septic plume are similar to the high end of the range of DOC concentrations measured at South Cape Beach (0.8 to 23.4 mg C l⁻¹), but are significantly higher than those found at Crane Wildlife (0.1 to 1.9 mg C l⁻¹). In Chapter 5, we pursue the idea that denitrification rates are controlled by both nitrate and DOC concentrations by modeling denitrification rates at the three sites using a saturating kinetics model where denitrification rate is substrate-limited by both nitrate and DOC concentrations.

7.3. Sensitivity Analysis

To test the robustness of our model, we varied the values of the input parameters ($\delta^{15}\text{NO}_3^-$ source, $\delta^{15}\text{NH}_4^+$ source, ϵ_{denit} , ϵ_{nit}) across a range of reasonable values for each and compared the results to those generated using the input parameters defined in this paper. We conducted this analysis for both soil-derived nitrate (Fig. 3.21) and fertilizer-derived nitrate (Fig. 3.22) at Crane Wildlife. For soil-derived nitrate, we varied the value of $\delta^{15}\text{NO}_3^-$ source across the range of values that might reasonably be interpolated from our measurements of $\delta^{15}\text{NO}_3^-$ in the near water table samples (Fig. 3.8). We used the regression line through the two measurements in well F606 to interpolate a water table value for $\delta^{15}\text{NO}_3^-$ and used this to represent the low end of the range for $\delta^{15}\text{NO}_3^-$ source (+ 1.9 ‰); similarly, we used the regression through the measured values for F605 to extrapolate a higher $\delta^{15}\text{NO}_3^-$ source value (+ 3.9 ‰). In an alternative interpretation, we

Figure 3.21. Results of sensitivity analysis of denitrification model for soil-derived nitrate. Input parameters ($\delta^{15}NH_4^+$ source, $\delta^{15}NO_3^+$ source, ϵ_{denit} , and ϵ_{nit}) were varied across a reasonable range of values; dashed lines represent the modeled denitrification rates used in this paper.

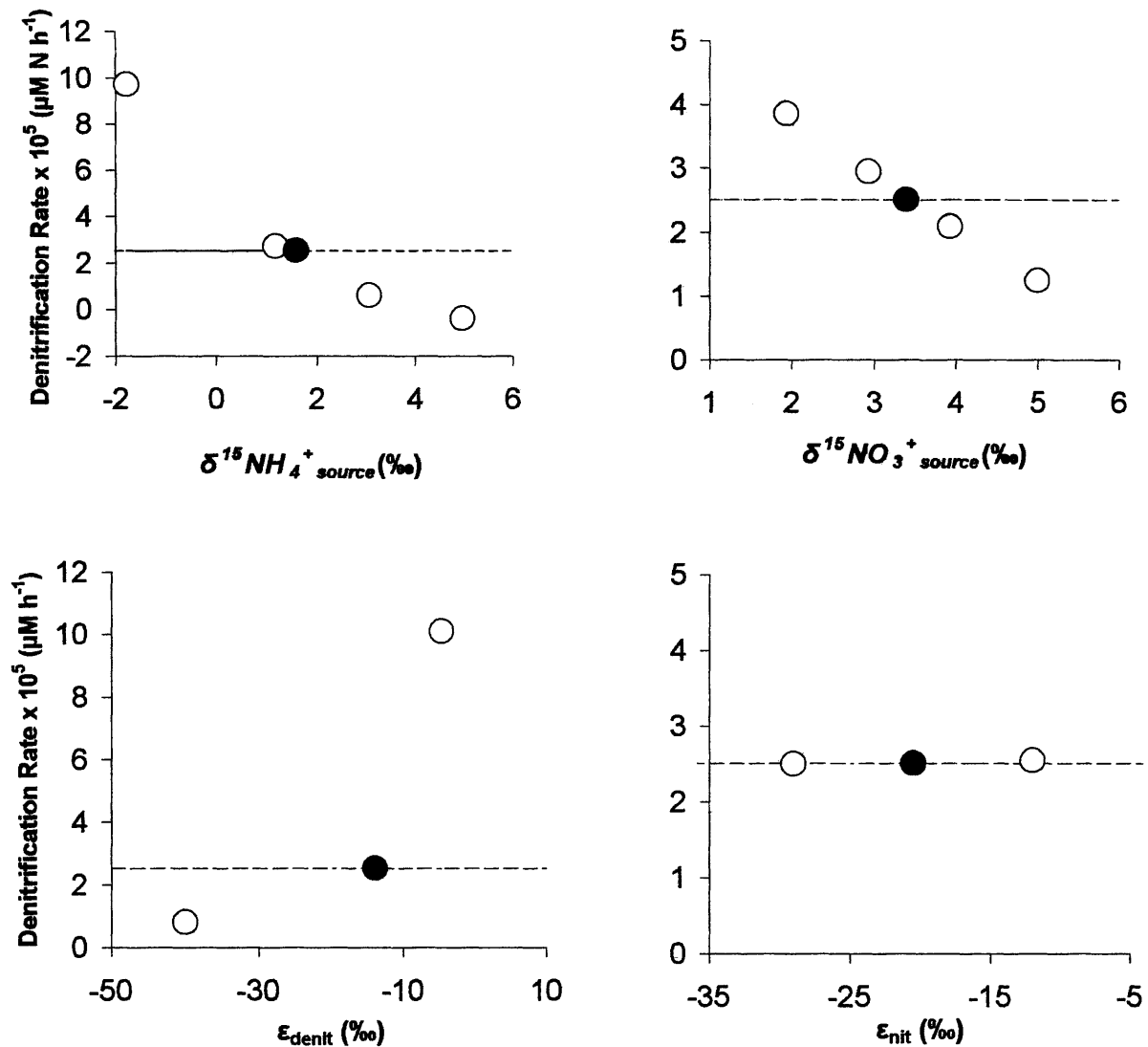
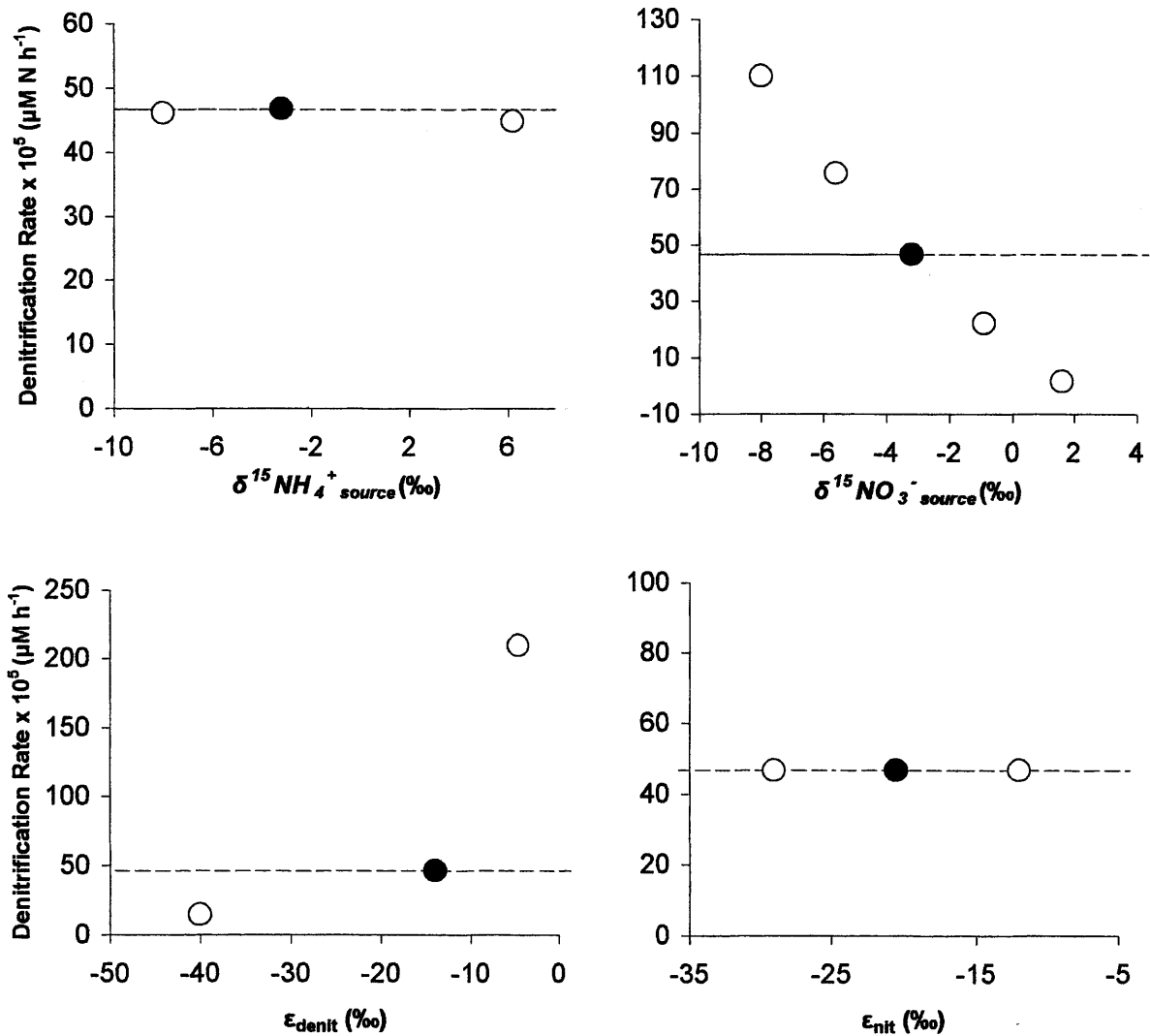


Figure 3.22. Results of sensitivity analysis of denitrification model for fertilizer-derived nitrate. Input parameters ($\delta^{15}\text{NH}_4^+$, $\delta^{15}\text{NO}_3^-$, ϵ_{denit} , and ϵ_{nit}) were varied across a reasonable range of values: dashed lines represent the modeled denitrification rates used in this paper.



used an average of the two regression lines (as opposed to the regression through all four points as used in our previous calculations) to interpolate a value for the mean water table $\delta^{15}NO_3^-$ (+ 2.9 ‰). Since the value used in our model (+ 3.4‰) was near the high end of the range defined by these other regressions, we tested a higher value (+ 5 ‰), placing our model value in the middle of the range used in the sensitivity analysis.

We used a similar analysis of our measured $\delta^{15}NH_4^+$ values near the water table (Fig. 3.8) to define a range of $\delta^{15}NH_4^+_{source}$ values for the sensitivity analysis. The regression through the $\delta^{15}NH_4^+$ measurements for F606 gave us the high end of the range (+ 5.0 ‰); the regression through the $\delta^{15}NH_4^+$ measurements for F605 produced a lower value (+ 1.2 ‰). The average of these two regressions produced an intermediate value for $\delta^{15}NH_4^+_{source}$ (+ 3.1 ‰). We rounded out the analysis by using another lower value (-1.8 ‰), again placing our model value (+ 1.6 ‰) in the middle of the range used in the sensitivity analysis.

For fertilizer-derived nitrate, we varied the value for $\delta^{15}NO_3^-_{source}$ from the low end of the range of $\delta^{15}N$ measured for fertilizer reported in the literature (-8.0 ‰, Freyer and Aly 1974, Kohl et al. 1971, Kreitler 1977, Mariotti and Letolle 1977) through +2 ‰, or 4.8 ‰ in either direction of our model value (-3.2 ‰). While fertilizer values can range as high as + 6.2 ‰ (Freyer and Aly 1974, Kohl et al. 1971, Kreitler 1977, Mariotti and Letolle 1977), the fertilizer applied on Falcon golfcourse was primarily urea. Because nitrate in the underlying groundwater was likely produced via nitrification of urea, a significantly positive $\delta^{15}NO_3^-_{source}$ signal is unlikely. We similarly varied the

$\delta^{15}NH_4^+$ *source* value for fertilizer-derived N through the full range reported in the literature (-8 to + 6.2 ‰), with our model value falling in between the two end-members (-3.2 ‰).

For both soil-derived and fertilizer-derived N, we varied the enrichment factors for nitrification and denitrification (ϵ_{denit} and ϵ_{nit} , respectively) across the full range reported in the literature, or from -5 to -40 ‰ for ϵ_{denit} , and from -12 to -29 ‰ for ϵ_{nit} . In both cases, our model value was the mean of the literature range.

The sensitivity analysis suggested that our results are highly insensitive to the value used for ϵ_{nit} for both soil-derived (Fig. 3.21) and fertilizer-derived (Fig. 3.22) nitrate, and to the value used for $\delta^{15}NH_4^+$ *source* in the case of fertilizer-derived N. Mean denitrification rate calculated for the Crane Wildlife groundwater samples changed, at most, only 1.4 % over the range of ϵ_{nit} values used in the sensitivity analysis (lower right panels in Figs. 3.21 & 3.22). For the fertilizer-derived N samples, mean denitrification rate changed only 3.9 %, at most, when the value of $\delta^{15}NH_4^+$ *source* was varied across the entire of the literature range (Fig. 3.22, upper left panel).

Calculated denitrification rates were more sensitive to the values used for $\delta^{15}NH_4^+$ *source* in the case of soil-derived N, and to the values used for $\delta^{15}NO_3^-$ *source* and ϵ_{denit} for both soil-derived and fertilizer-derived N. In all cases, the results were within the same order of magnitude as those used in this paper. In the case of soil-derived N, mean denitrification rate increasing almost 3 fold when the $\delta^{15}NH_4^+$ *source* value was decreased to the lowest end of the range (-1.2 ‰; Fig. 3.21, upper left panel). The model

produced negative denitrification rates when the highest $\delta^{15}NH_4^+$ *source* value was used (+5.0 ‰). Over the range of input values for $\delta^{15}NO_3^-$ *source*, mean denitrification rate changed by a maximum of +54% for soil-derived nitrate (Fig. 3.21, upper right panel), and +136% for fertilizer-derived nitrate (Fig. 3.22, upper right panel), when the lowest $\delta^{15}NO_3^-$ *source* values were used (+1.9 and -8 ‰, for soil- and fertilizer-derived N, respectively).

An interesting result of the sensitivity analysis was that denitrification rates were only somewhat sensitive to a *decrease* in the value of the enrichment factor for denitrification (ϵ_{denit}) from that used in our calculations, but much more sensitive to an *increase* in ϵ_{denit} . Mean denitrification rate decreased by 69% when ϵ_{denit} was decreased from -14 to -40 ‰ (lower left panels in Figs. 3.21 & 3.22). In contrast, mean denitrification rate increased to a much greater extent (3.5-fold) when the value of ϵ_{denit} was increased from -14 to -5 ‰. The sensitivity of our calculations to the enrichment factor, particularly as ϵ_{denit} becomes less negative, points to the importance of understanding what controls the degree of fractionation during denitrification, and to what degree fractionation in groundwater is site-specific.

Researchers have observed that ϵ_{denit} values measured *in situ* (Mariotti et al. 1988, Smith et al. 1991) are lower than those measured in laboratory incubations (Delwiche and Steyn 1970). Mariotti et al. (1988) suggested that groundwater denitrification may proceed in dead-end or “cul-de-sac” pores in the aquifer, within which reduction may go to completion with no net fractionation; diffusion of nitrate into those pores may then be

what controls the degree of fractionation. Thus, what we measure in groundwater may be an “apparent” enrichment factor. A similar effect might be observed where denitrification is otherwise transport-limited (i.e., in organic clusters or sediment-water interfaces, J.K. Bohlke, personal communication), or rate-limited at the enzymatic or cellular level. In an aquifer system such as ours, characterized by oxygenated groundwater and relatively low NO_3 concentrations, denitrification is likely to proceed primarily in anaerobic microsites (Koba et al. 1997, Parkin 1987, Højberg et al. 1994) within the aquifer matrix or within areas of restricted flow where oxygen concentrations may be reduced and carbon substrate accumulated. The progress of the denitrification reaction in such environments would necessarily be diffusion-limited. An interesting question for future research is to what degree do the physical characteristics of the aquifer system effect the measured enrichment factor (ϵ_{denit}).

8. Conclusions

Our results have important implications for interpretation of natural variability in groundwater denitrification, and suggest that both DOC and nitrate concentrations exert important controls on denitrification rates. First order denitrification rate constants with respect to nitrate were highest where groundwater DOC concentrations were highest: $k = 2.8 \text{ y}^{-1}$ in the septic plume ($\sim 26 \text{ mg C l}^{-1}$), $k = 1.6 \text{ y}^{-1}$ at South Cape Beach (DOC = 0.8 to 23.4 mg C l^{-1}), and $k = .25 \text{ y}^{-1}$ at Crane Wildlife (0.1 to 1.9 mg C l^{-1}), suggesting that denitrification rates in all cases increase with increasing nitrate, and that, independent of nitrate concentration, DOC concentrations exert a significant control on denitrification rates. A simulation of N losses along groundwater flowpaths at Crane Wildlife suggests

that a saturating kinetics expression with respect to nitrate best predicts nitrate concentrations measured at the downgradient well ports ($R^2 = 0.96$ for $[\text{NO}_3^-]_{\text{model}}$ vs. $[\text{NO}_3^-]_{\text{meas}}$). In Chapter 5, we further explore the use of a saturating kinetics expression that incorporates both nitrate and DOC concentrations to model denitrification rates.

Our findings have relevance for land use and planning decisions related to nitrogen loading. The distance-dependent nature of N losses resulting from aquifer denitrification suggests that while denitrification occurs at relatively low rates within the Waquoit Bay aquifer, when integrated over long flow path lengths, substantial natural attenuation of N can occur. In assessing the potential N loads from various sources, it is critical to consider the magnitude of individual NO_3^- sources, travel distances to shore, and the DOC concentrations in groundwater in determining options for reducing N loads. For example, if we consider two nitrate sources, both located 100 m from a downgradient receiving water body, one a fertilizer plume containing $500 \mu\text{M NO}_3^-$ (where $\text{DOC} < 2 \text{ mg C l}^{-1}$ and $k = 0.26 \text{ y}^{-1}$), and the other, a septic system plume containing $4,000 \mu\text{M NO}_3^-$ (where $\text{DOC} \sim 26 \text{ mg C l}^{-1}$ and $k = 2.7 \text{ y}^{-1}$), we find that by the time these plumes have reached the downgradient water body, nitrate concentrations within the fertilizer plume have been reduced by denitrification to about $430 \mu\text{M NO}_3^-$, while nitrate concentrations in the plume have been reduced to about $1100 \mu\text{M}$. In this case, the septic-derived N clearly constitutes a larger fraction of the total N load from these two sources. However, if we then institute a 200 m setback limit from the receiving water body for all N sources, we find that by the time these two plumes have reached the downgradient water body, the nitrate concentration in the septic plume has been reduced

by groundwater denitrification to approximately $100 \mu\text{M NO}_3^-$, while the fertilizer plume, given its lower DOC concentration, still contributes about $350 \mu\text{M NO}_3^-$, making it the dominant N source. The principles outlined in this paper should be applied to the design of setback limits for septic systems, in assessing the value of open spaces for N load reduction, in regulating wastewater disposal, and in watershed-wide land use planning.

9. Acknowledgements

We thank staff at the Waquoit Bay National Estuarine Research Reserve for general support. This work could not have been done without the generous contributions of expertise and resources by Denis LeBlanc of the US Geological Survey, Marlborough, MA; his help with well construction, installation, and site access, and his worthy advice were invaluable. Paul Barlow at the USGS was also an essential contributor by running a MODFLOW simulation of groundwater flow at Crane Wildlife. We thank Gabrielle Tomasky, at the Boston University Marine Program, for field and lab assistance; Amy Watson at MIT, who helped analyze our NH_4 samples as part of her summer internship; and Anne Giblin and Kathy Regan at MBL for use of and technical support with an ion chromatograph. MIT Sea Grant (# 65591) and a National Estuarine Research Reserve (NERRS) Graduate Fellowship from the National Oceanic and Atmospheric Administration (NA77OR024) supported this work.

10. References

- Barlow PM & Hess KM (1993) Simulated Hydrologic Responses of the Quashnet River Stream-Aquifer System to Proposed Ground-Water Withdrawals, Cape Cod, Massachusetts. U.S. Geological Survey, Water-Resources Investigations Report 93-4-64, Marlborough.
- Bengtsson G & Annadotter H (1989) Nitrate reduction in a groundwater microcosm determined by ^{15}N gas chromatography-mass spectrometry. *Appl. Environ. Microbiol.* 55: 2861-2870.
- Bottcher J, Strebel O, Voerkelius S, & Schmidt HL (1990) Using isotope fractionation of nitrate-nitrogen and nitrate-oxygen for evaluation of microbial denitrification in a sandy aquifer. *J. Hydrol.* 114: 413-424.
- Bragan RJ, Starr JL, & Parkin TB (1997) Shallow groundwater denitrification rates measured by acetylene block. *J. Environ. Qual.* 26: 1531-1538.
- Bragan RJ, Starr JL & Parkin TB (1997a) Acetylene transport in shallow groundwater for denitrification rate measurement. *J. Environ. Qual.* 26: 1524-1530.
- Brenner A & Argaman Y (1990) Effect of feed composition, aerobic volume fraction and recycle rate on nitrogen in the single-sludge system. *Wat. Res.* 24: 1041-1049.
- Cambareri TC & Eichner EM (1998) Watershed delineation and ground water discharge to a coastal embayment. *Ground Water* 36: 626-634.
- Chapelle FH (1992) *Ground-Water Microbiology & Geochemistry*. John Wiley & Sons, Inc. New York.
- Clay DE, Clay SA, Moorman TB, Brix-Davis K, Scholes KA & Bender AR (1996) Temporal variability of organic C and nitrate in a shallow aquifer. *Water Res.* 30: 559-568.
- Cline JD and Kaplan IR (1975) Isotopic fractionation of dissolved nitrate during denitrification in the eastern tropical North Pacific Ocean. *Mar. Chem.* 3:271-299.
- Cohen S, Nickerson S, Maxey R, Dupuy A Jr. & Senita JA (1990) A ground water monitoring study for pesticides and nitrates associated with golf courses on Cape Cod. *Ground Wat. Monit. Rev.* Winter 1990: 160-173.
- Costa JE (1988) Distribution, production, and historical changes in abundance of eelgrass (*Zostera marina*) in southeastern Massachusetts. Ph.D. Thesis. Boston University, 352 p.

- D'Angelo EM & Reddy KR (1993) Ammonium oxidation and nitrate reduction in sediments of a hypereutrophic lake. *Soil Sci. Soc. Amer. J.* 57: 1156-1163.
- D'Elia CF, Steudler PA and Corwin N (1977) Determination of total nitrogen in aqueous samples using persulfate digestion. *Limnol. Oceanogr.* 22:760-764.
- Engberg DJ & Schroeder ED (1975) Kinetics and stoichiometry of bacterial denitrification as a function of cell residence time. *Wat. Res.* 9: 1051-1054.
- Fiebig D, Lock MA & Neal C (1990) Soil water in the riparian zone as a source of carbon for a headwater stream. *J. Hydrol.* 116: 217-237.
- Fiebig D (1995) Groundwater discharge and its contribution of dissolved organic carbon to an upland stream. *Arch. Hydrobiol.* 134: 129-155.
- Fogg GE, Rolston DE, Decker DL, Louie DT, & Grismer ME (1998) Spatial variation in nitrogen isotope values beneath nitrate contamination sources. *Ground Water* 36:418-426.
- Ford T & Naiman RJ (1989) Groundwater-surface water relationships in boreal forest watersheds: dissolved organic carbon and inorganic nutrient dynamics. *Can. J. Fish. Aquat. Sci.* 46: 41-49.
- Freyer HD & Aly AIM (1974) Nitrogen-15 variations in fertilizer nitrogen. *J. of Env. Qual.* 3: 405-406.
- Fustec E, Mariotti A, Grillo X, & Sajus J (1991) Nitrate removal by denitrification in alluvial groundwater: Role of a former channel. *J. of Hydrol.* 123: 337-354.
- Garten CT, Jr. (1993) Variability in foliar ¹⁵N abundance and the availability of soil nitrogen on the Walker Branch Watershed. *Ecology* 74:2098-2113.
- Gelda, R., Brooks, CM, Effler SW, & Auer MT (2000). Interannual variations in nitrification in a hypereutrophic urban lake: occurrences and implications. *Wat. Res.* 34: 1107-1118.
- GESAMP (1990) State of the Marine Environment: Rep. Stud. No. 39, Joint Group of Experts on the Scientific Aspects of Marine Pollution. United Nations Environment Programme. 111 p.
- Gillham RW (1991) Nitrate contamination of groundwater in Southern Ontario and the evidence for denitrification. NATO ASI SERIES, V G 30 Nitrate Contamination, (edited by Bogardi I and Kuzelka RD) p. 182-198.
- Gold AJ, Jacinthe PA, Groffman PM, Wright WR, & Puffer PH (1998) Patchiness in groundwater nitrate removal in a riparian forest. *J. of Env. Qual.* 27: 146-155.

Groffman PM, Howard G, Gold AJ & Nelson WM (1996) Microbial nitrate processing in shallow groundwater in a riparian forest. *J. of Env. Qual.* 25: 1309-1316.

Heaton THE (1986) Isotopic studies of nitrogen pollution in the hydrosphere and atmosphere: A review. *Chem. Geol. (Isot. Geosci. Sect.)* 59: 87-102.

Hedin LO, von Fischer JC, Ostrom NE, Kennedy BP, Brown MG, and Robertson GP (1998) Thermodynamic constraints on nitrogen transformations and other biogeochemical processes at soil-stream interfaces. *Ecology* 79: 684-703.

Herbel MJ, & Spalding RF (1993) Vadose zone fertilizer-derived nitrate and $\delta^{15}N$ extracts. *Groundwater.* 31:376-382.

Højberg O, Revsbech NP and Tiedje JM (1994) Denitrification in soil aggregate analyzed with microsensors for nitrous oxide and oxygen. *Soil Sci. Soc. Amer. J.* 58: 1691-1698.

Holmes RM, Aminot A, Kerouel R, Hooker BA and Peterson BJ (1999) A simple and precise method for measuring ammonium in marine and fresh water. *Can. J. Fish. Aquat. Sci.* 56: 1801-1808.

Howarth RW, Billen G, Swaney D, Townsend A, Jaworski N, Lajtha K, Downing JA, Elmgren R, Caraco N, Jordan T, Berendse F, Freney J, Kudeyarov V, Murdoch P, & Zhao-Liang Z (1996) Regional nitrogen budgets and riverine nitrogen and phosphorus fluxes for the drainages to the North Atlantic Ocean: natural and human influences. *Biogeochemistry* 35:75-79.

Hübner H (1986) Isotope effects of nitrogen in the soil and biosphere. In: Fritz P & Fontes JC (Eds.). *Handbook of Environmental Isotope Geochemistry*, vol. 2b, The Terrestrial Environment, Elsevier, pp. 361-425.

Iqbal MZ, Krothe NC, & Spalding, RF (1997) Nitrogen isotope indicators of seasonal source variability in groundwater. *Environmental Geology.* 32:210-218.

Jacinthe PA, Groffman PM, Gold AJ, & Mosier A (1998) Patchiness in microbial nitrogen transformations in groundwater in a riparian forest. *J. of Env. Qual.* 27: 156-164.

Kendall C & McDonnell JJ (eds) (1998) *Isotope Tracers in Catchment Hydrology*. Elsevier Science B.V., Amsterdam, 839 pp.

Koba K, Tokuchi N, Yoshioka T, Hobbie EA, & Iwatsubo G (1998). Natural abundance of nitrogen-15 in a forest soil. *Soil Sci. Soc. Am. J.* 62: 778-781.

Koba K, Tokuchi N, Wada E, Nakajima T, & Iwatsubo G (1997) Intermittent denitrification: The application of a ^{15}N natural abundance method to a forested ecosystem. *Geochim. Cosmochim. Acta* 61: 5043-5050.

- Kohl D, Shearer GB & Commoner B (1971) Fertilizer nitrogen: Contribution to nitrate in surface water in a corn belt watershed. *Science* 174: 1331-1334.
- Kookana RS, & Naidu R (1998) Hydrologic control of aluminum chemistry in an acidic headwater stream. *Water Resources Res.* 24: 659-669.
- Korom SF (1991) Denitrification in the unconsolidated deposits of the Heber Valley aquifer, PhD thesis, Utah State University, Logan, Utah. 176 pp.
- Korom SF (1992) Natural denitrification in the saturated zone: A review. *Water Resources Res.* 28: 1657-1668.
- Kreitler CW (1977) Nitrogen isotopes of soil and groundwater nitrate, Lockhart and Taylor alluvial fans, central Texas. (Abs.). *Geol. Soc. Amer.* 97: 1058-1059.
- Kroeger KD, Bowen JD, Corcoran D, Moorman J, Michalowski J, Rose C, & Valiela I (1999) Nitrogen loading to Green Pond, Falmouth, MA: Sources and evaluation of management options. *Environ. Cape Cod* 2: 15-26.
- LeBlanc DR, Garabedian SP, Hess KM, Gelhar LW, Quadri RD, Stollenwerk KG, & Wood WW (1991) Large-scale natural gradient tracer test in sand and gravel, Cape Cod, Massachusetts 1. Experimental design and observed tracer. *Water Resources Res.* 27:895-910.
- LeBlanc DR (1984) Sewage plume in a sand and gravel aquifer, Cape Cod, Massachusetts. U.S. Geological Survey, Water-Supply paper 2218, Washington.
- LeBlanc DR, Guswa JH, Frimpter MH & Londquist CJ (1986) Ground-water resources of Cape Cod, Massachusetts: U.S. Geological Survey Hydrologic Atlas 692.
- Ledgard SF, Treney JR & Simpson JR (1984) Variations in natural enrichment of ^{15}N in the profiles of some Australian pasture soils. *Aust. J. Soil Res.* 22:155-164.
- Lee V & Olson S (1985) Eutrophication and management initiatives for the control of nutrient inputs to Rhode Island coastal lagoons. *Estuaries* 8: 191-202.
- Leenheer J, Malcolm RL, McKinley PW, & Eccles LA (1974) Occurrence of dissolved organic carbon in selected ground-water samples in the United States. *J. Res. U.S. Geol. Survey* 2: 361-369.
- Mariotti A, Pierre D, Vedy JC, & Bruckert S (1980) The abundance of natural N-15 in the organic matter of soils along an altitudinal gradient (Chablais, Haute-Savoie). *Catena* 7:293-300.

Mariotti A, Germon JC, Hubert P, Kaiser P, Letolle R, Tardieux A, & Tardieux P (1981) Experimental determination of nitrogen kinetic isotope fractionation: some principles; illustration for the denitrification and nitrification processes. *Plant and Soil* 62: 413-430.

Mariotti A, Landreau A, & Simon B (1988) ^{15}N isotope biogeochemistry and natural denitrification process in groundwater: Application to the chalk aquifer of northern France. *Geochim. Cosmochim. Acta* 52: 1869-1878.

Mariotti A, & Letolle R (1977) Application de l'etude isotopique de l'azote en hydrologie et en hydrogeologie - Analyse des resultants obtenus sur un exemple precis: Le Bassin de Melarchez (Seine-et-Marne, France). *J. Hydrol.* 33: 157-172.

Masterson JP, Walter, DA, Savoie, J. (1997) Use of particle tracking to improve numerical model calibration and to analyze ground-water flow and contaminant migration, Massachusetts Military Reservation, western Cape Cod, Massachusetts, USGS W 2482, 50 pp.

McClelland JW, & Valiela I (1998) Linking nitrogen in estuarine producers to land-derived sources. *Limnol. Oceanogr.* 43: 577-585.

McDonnell K, Rudy M, Valiela I, & Foreman K (1994) The effects of coastal land use on inorganic nutrient concentrations in groundwater entering estuaries of Waquoit Bay, Massachusetts. *Biol. Bull.* 187:276-277.

Nadelhoffer KJ, & Fry B (1988) Controls on natural nitrogen-15 and carbon-13 abundances in forest soil organic matter. *Soil Sci. Soc. Am J.* 52:1633-1640.

National Research Council (NRC) (2000) Clean Coastal Waters: Understanding and Reducing the Effects of Nutrient Pollution. National Academy Press, Washington D.C. 405 p.

National Research Council (NRC) (1994) Priorities for Coastal Science, National Academy Press, Washington D.C. 88 p.

Nixon S, Oviatt CA, Frithsen J, & Sullivan B (1986) Nutrients and the productivity of estuarine and coastal marine ecosystems. *J. Limnol. Soc. S. Africa* 12: 43-71.

Pabich WJ, Valiela I, & Hemond HF (submitted) The effect of vadose thickness and depth below the water table on DOC concentration in groundwater on Cape Cod, U.S.A. *Biogeochemistry*.

Parkin TB (1987) Soil microsite as a source of denitrification variability. *Soil Sci. Soc. Amer. J.* 51: 1194-1199.

- Peterjohn WT, & DL Correll (1984) Nutrient dynamics in an agricultural watershed: Observations on the role of riparian forest. *Ecology* 65: 256-268.
- Robertson WD, Schiff SL, & Ptacek CJ (1998) Review of phosphate mobility and persistence in 10 septic system plumes. *Ground Water* 36:1000-1010.
- Savoie J & LeBlanc DR (1998) Water-Quality Data and Methods of Analysis for Samples Collected Near a Plume of Sewage-Contaminated Ground Water, Ashumet Valley, Cape Cod, Massachusetts, 1993-94. U.S. Geological Survey, Marlborough, MA.
- Schulze E -D, Chapin FS, III & Gebauer G (1994) Nitrogen nutrition and isotope differences among life forms in the northern treeline of Alaska. *Oecologia* 100:406-412.
- Seely BA (1997) Atmospheric Deposition and Flux Dynamics of Nitrogen in the Coastal Forests of the Waquoit Bay Watershed, Cape Cod, MA. PhD dissertation, Boston University.
- Short FT, & Burdick DM (1996) Quantifying eelgrass habitat loss in relation to housing development and nitrogen loading in Waquoit Bay, Massachusetts. *Estuaries* 19:730-739.
- Sigman DM, Altabet MA, Michener RH, McCorkle D, Fry B & Holmes RM (1997) Natural abundance-level measurement of the nitrogen isotopic composition of oceanic nitrate: An adaptation of the ammonium diffusion method. *Mar. Chem.* 57: 227-242.
- Smith RL, Howes BL, & Duff JH (1991) Denitrification in nitrate-contaminated groundwater: Occurrence in steep vertical geochemical gradients. *Geochim. Cosmochim. Acta* 55: 1815-1825.
- Solomon DK, P.R., Cook PG & Hunt A (1995) Site characterization using $^3\text{H}/^3\text{He}$ ground-water ages, Cape Cod, MA. *Ground Water* 33: 988-996.
- Spalding RF, Exner ME, Lindau CW, & Eaton DW (1982) Investigation of sources of groundwater nitrate contamination in the Burbank-Wallula area of Washington, U.S.A. *J. Hydrol.* 58:307-324.
- Stollenwerk KG (1996) Simulation of phosphate transport in sewage-contaminated groundwater, Cape Cod, Massachusetts. *Appl. Geochem.* 11: 317-324.
- Thurman EM (1985) *Organic Geochemistry of Natural Waters*. Martinus Nijhoff/DR W. Junk Publishers, Dordrecht.
- Trudell MR, Gillham RW, & Cherry JA (1986) An in-situ study of the occurrence and rate of denitrification in a shallow unconfined sand aquifer. *J. Hydrol.* 83: 251-268.

- Valiela I, Geist M, McClelland J, & Tomasky G (2000) Nitrogen loading from watersheds to estuaries: Verification of the Waquoit Bay Nitrogen Loading Model. *Biogeochemistry* 49:277-293.
- Valiela I, Collins G, Kremer J, Lajtha K, Geist M, Seely B, Brawley J, & Sham CH (1997) Nitrogen loading from coastal watersheds to receiving estuaries: New method and application. *Ecol. Appl.* 7: 358-380.
- Valiela I, & Costa J (1988) Eutrophication of Buttermilk Bay, a Cape Cod coastal embayment: Concentrations of nutrients and watershed nutrient budgets. *Environ. Management* 12: 539-553.
- Valiela I, Foreman K, LaMontagne M, Hersh D, Costa J, Peckol P, DeMeo-Anderson B, D'Avanzo C, Babione M, Sham CH, Brawley J, & Lajtha K (1992) Couplings of watersheds and coastal waters: Sources and consequences of nutrient enrichment in Waquoit Bay, Massachusetts. *Estuaries* 15: 443-457.
- Verchot LV, Franklin EC, & Gilliam JW (1997) Nitrogen cycling in Piedmont vegetated filter zones: II. Subsurface nitrogen removal. *J. Environ. Qual.* 26: 337-347.
- Vitousek P, Shearer G, & Kohl DH (1989) Foliar ^{15}N natural abundance in Hawaiian rainforest: Patterns and possible mechanisms. *Oecologia* 78:383-388.
- Vogel JC (1967) Investigation of groundwater flow with radiocarbon. In: *Isotopes in Hydrology* (pp. 355-369). IAEA-SM-83/24, Vienna.
- Vogel JC, Talma AS, & Heaton THE (1981) Gaseous nitrogen as evidence for denitrification in groundwater. *J. Hydrol.* 50: 191-200.
- Wada E, Imaizumi R, & Takai Y (1984) Natural abundance of ^{15}N in soil organic matter with special reference to paddy soils in Japan; biogeochemical implications on the N cycle. *Geochem. J.* 18:109-123.
- Wan J, & Tokunaga TK (1997) Film straining of colloids in unsaturated porous media: conceptual model and experimental testing. *Environ. Sci. Technol.* 31: 2413-2420.
- Wells ER, & Krother NC (1989) Seasonal fluctuation in $\delta^{15}\text{N}$ of groundwater nitrate in a mantled karst aquifer due to macropore transport of fertilizer-derived nitrate. *J. Hydrol.* 112: 191-201.

CHAPTER 4.

FATE OF NITROGEN FROM A SEPTIC SYSTEM IN A NEARSHORE CAPE COD AQUIFER

1. Introduction

The largest source of anthropogenic nitrogen to Cape Cod groundwater is wastewater (1,2,3). The following paper examines mass balance losses of nitrogen from a single private septic system, located near the banks of the Moonakis River in Falmouth, near the head of Waquoit Bay. The septic system had been in operation approximately twenty years for two household occupants at the time of sampling, and the associated flows and nutrient concentrations were presumed to be at steady state. The septic tank and leach field were located approximately 60 m from the bank of the river. The site was outfitted with 11 multi-level sampling wells, 9 in the plume downgradient from the septic tank and leach field, and 2 outside the plume, spanning a 50 m transect.

The high concentration of ions in wastewater make it more conductive than ambient groundwater. This property of wastewater allowed us to conduct a ground conductivity survey using a Geonics EM31 ground conductivity meter to roughly delineate the contours of the septic plume prior to well installation. We augmented this data with nitrate and ammonium measurements on groundwater samples obtained at the seepage face of the site using a piezometer; these measurements showed the location of the plume as it passed through the seepage face into the Moonakis River, and guided our placement of multi-level sampling wells upgradient.

In the following paper, we present data on nitrate loss as a function of groundwater age, and show that 50% of the nitrogen attenuation in the septic plume occurs within the first 0.2 yrs of travel time, and that reduction rates decline with time. I

augment this paper with a presentation of denitrification rates, which range from 0.01 to $2.23 \mu\text{M NO}_3^- \text{ h}^{-1}$; these reduction rates are 4 to 7 orders of magnitude higher than those measured in ambient groundwater using N stable isotopes at two forested sites, Crane Wildlife Management Area and South Cape Beach (Ch. 3). Denitrification rates in the plume increased with increasing initial nitrate concentration ($R^2 = 0.86$, Fig. 4.3) in a manner similar to what we found at South Cape Beach, suggesting that the higher DOC concentrations typically found in septic plumes (Robertson et al. 1988) and those found at South Cape Beach (relative to Crane Wildlife) allow for faster rates of denitrification for a given nitrate concentration. In Chapter 5, we model these rates using a Monod kinetic expression, where denitrification rates are both nitrate- and DOC-limited.

2. Fate of Anthropogenic Nitrogen in a Nearshore Cape Cod Aquifer

Elizabeth J. Westgate¹, Kevin D. Kroeger, Wendy J. Pabich, and Ivan Valiela (Boston University Marine Program, Marine Biological Laboratory, Woods Hole, Massachusetts 02543)

Nitrogen loading from land is a principal cause of eutrophication of shallow estuaries (1,2,3). In regions such as Cape Cod, Massachusetts, which are underlain by unconsolidated sands, the major mechanism that transports nitrogen to estuaries is groundwater flow, and the major nitrogen source (primarily in the form of nitrate, NO₃⁻) is often wastewater from septic systems (1,2,3). Wastewater nitrate concentrations decrease during travel in groundwater due to dilution with clean groundwater and to loss by denitrification (4). The loss of nitrogen during flow between a septic tank and receiving estuary can be calculated by determining the reduction in concentration of dissolved inorganic nitrogen relative to the change in concentration of a passive tracer that accounts for dilution.

We investigated losses of nitrate for a domestic septic system in the watershed of Quashnet River, Cape Cod. Effluent from septic systems moves downgradient, forming plumes containing high concentrations of nitrate. In addition, the study area has plumes derived from fertilized turf or fields. To sort out the different plumes, we measured

¹ Lafayette College, Easton, PA 18042

boron (B, a passive tracer derived from laundry detergents and associated with wastewater sources (5, 6, 7)) and potassium (K, associated with both wastewater and fertilizer sources (8, 9)) in the samples of groundwater.

To calculate loss of nitrate along the plumes, we collected samples from nine wells downgradient from the septic system. Each well was furnished with 14 ports that allowed us to sample groundwater at intervals of 1-2 m. We collected 300 mL of water from 129 ports during June and July 2000 and measured concentrations of nitrate ($\text{NO}_3^- + \text{NO}_2^-$) and ammonium (NH_4^+) using colorimetric and fluorometric techniques, respectively. We selected samples with nitrate concentrations above 8 μM and conductivities less than 4,000 $\mu\text{S}/\text{cm}$ for measurements of B and K. These samples were analyzed by Ward Laboratories (Kearney, NE).

Examination of vertical and horizontal profiles of nitrate and ammonium suggested that there were three distinct plumes within our well field (Fig. 4.1). The upper plume moved along near the surface of the water table and contained the highest nitrate concentration of the three plumes; at nearly 3000 μM , it was similar to literature values (8) for septic effluent that has just left the leaching field. The nitrate, B, and K concentrations in this plume differed considerably from those of the other plumes (Fig. 4.2, A and B).

In contrast, the lower plume showed no increase in nitrate relative to increase in B (Fig. 4.2, A). It did, however, show a positive relationship to K, and at a given K

concentration, had a much higher nitrate concentration than did the upper plume (Fig. 4.2, B). This evidence suggests that the lower plume might be due to fertilizer use upgradient of our septic system.

The middle plume had no significant relationships between nitrate and B or K, perhaps because of the small number of samples and the low concentrations. The concentrations of nitrate, B, and K from the middle plume do, however, fit on the lower portions of the curves for the upper plume (Fig. 4.2, A and B). These circumstances lead us to think that the middle plume was probably the leading edge of a plume from a septic system located farther upgradient from our septic system. We therefore used data for the upper and middle plumes in our examination of the fate of septic system nitrogen in this watershed.

Concentrations of nitrate and B diminished as water parcels aged (age, Fig. 4.2, C and D, calculated from the Vogel equation (10)), which predicts groundwater age as a function of position in the aquifer. To allow for dilution, we normalized the data by expressing concentrations as NO_3^-/B (Fig. 4.2, E). We estimated the NO_3^-/B in the effluent that had just left the septic system (age 0) by using a literature value (8) (Fig. 4.2, E, upper dashed line). The NO_3^-/B values we used came from a Cape Cod site near our study area, and the data dated from 1992, only a 7-8 year difference from our date of collection. We presume that differences in B were therefore a reasonable proxy for those in our study system. We calculated losses of NO_3^- as the difference between the age 0 nitrate concentration, allowing for dilution, and the measured nitrate concentration.

Losses of nitrate in excess of dilution were quite rapid, with rates reaching 50% loss at 0.2 years (Fig. 4.2, F). The loss rates diminished with time, which suggests that, if these data are representative of losses elsewhere, N losses by denitrification and retention take place primarily near the septic system source. Extrapolating the curve of Figure 4.2 (F), we find that near-complete losses may be reached at 4.8 years, which is equivalent to 480-730 m from the septic system, assuming a travel rate of 100-150 m per year (11).

As a minimum estimate of loss, we also calculated loss relative to our highest measured NO_3^-/B ratio (Fig. 4.2, E, lower dashed line). If our initial NO_3^-/B ratio were closer to this measured value, our estimate of time to 50% NO_3^- loss would increase to 0.6 years, but the estimate of time to 100% loss would not be affected. The extrapolation to 100% loss assumes that the relationship between % loss NO_3^- and age continues to hold beyond our oldest sample. This would not be the case if the availability of labile organic carbon were to limit NO_3^- loss before 100% loss is achieved.

If coastal zone managers wish to regulate septic nitrogen loads, they could concentrate on management of septic systems that lie within 480-730 m of the shore, since these appeared to be the major contributors of nitrate to receiving estuaries. Septic sources farther upgradient probably contribute less significantly.

This research was supported by an internship from the Woods Hole Marine Science Consortium to Elizabeth Westgate, an MIT Sea Grant (#65591) awarded to Ivan

Valiela and Harold Hemond, and National Estuarine Research Reserve Fellowships to
Wendy Pabich and Kevin Kroeger.

Figure 4.1. Vertical cross section from the soil surface, water table, and aquifer through our field of multiple sampling wells (elevation relative to mean low water (MLW)). The numbers are concentrations of NO_3^- (μM) for water samples collected from each of the 14 ports in each of the 9 wells. Although the wells were not all in one plane, they are shown as if they were for simplicity. Contour lines are drawn to indicate NO_3^- concentrations of 32, 128, 512, and 2048 μM . Position of salty water determined from salinity of water samples.

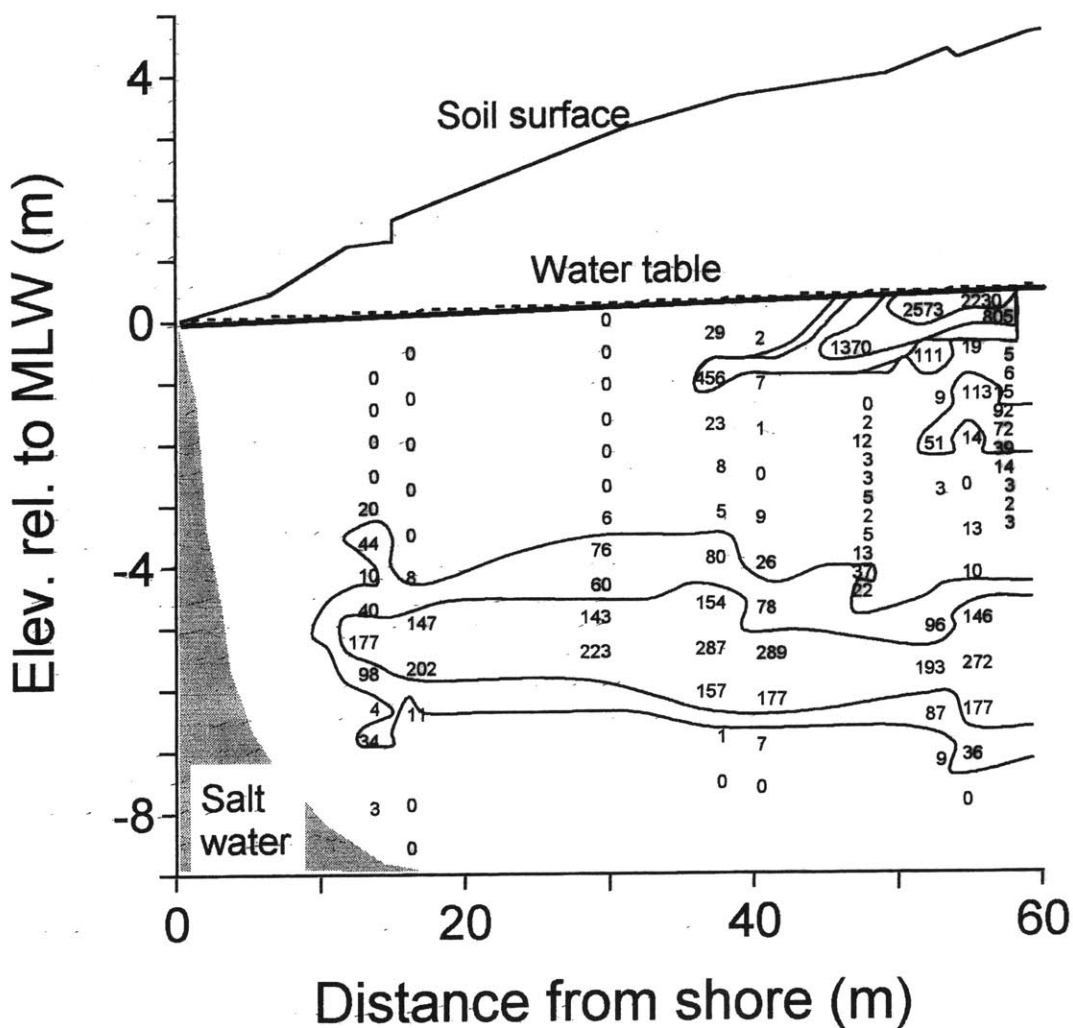
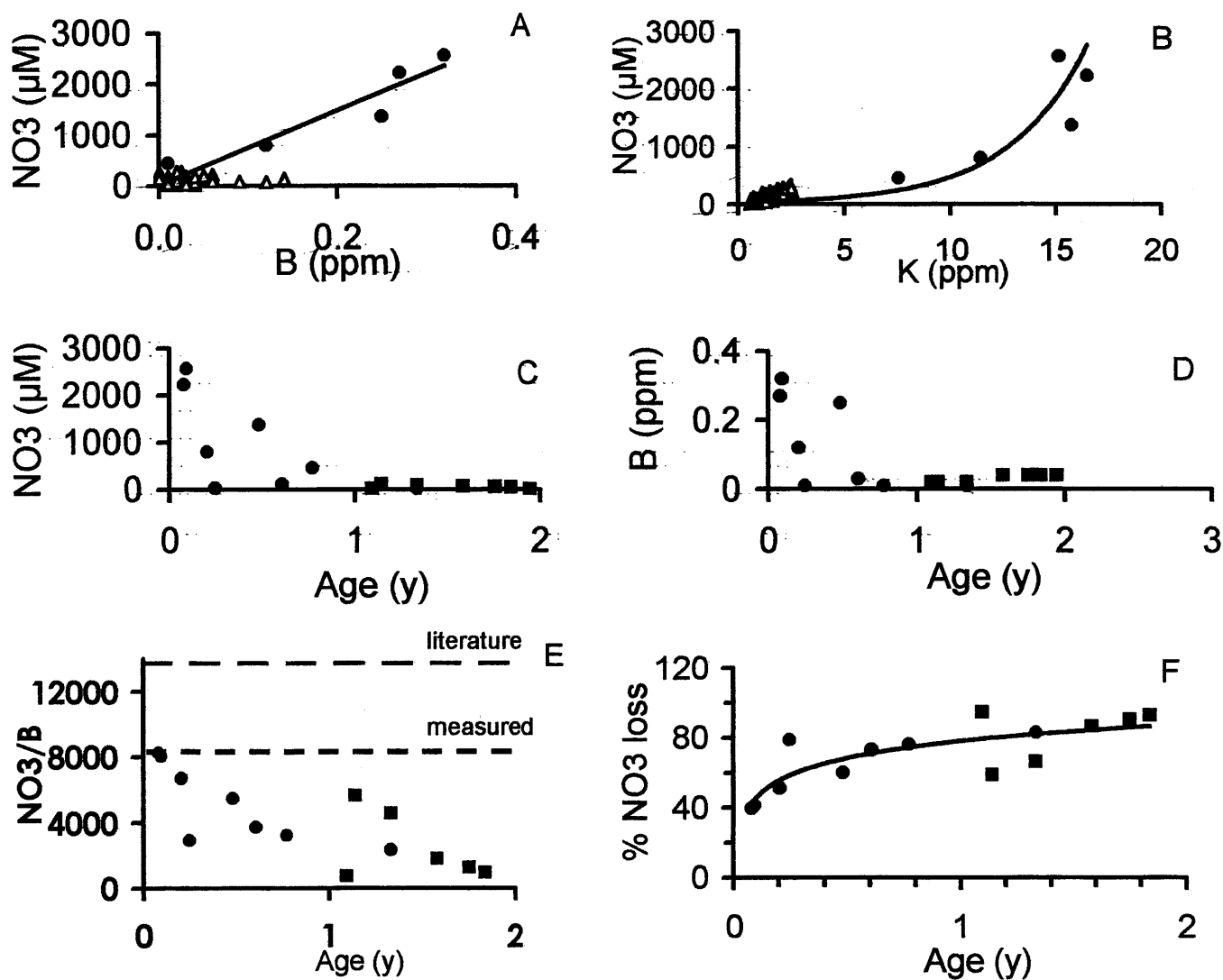


Figure 4.2. A: NO_3^- concentration versus B concentration for samples collected from upper (\bullet), middle (\blacksquare), and lower (\triangle) plumes. B: NO_3^- concentration versus K concentration for all three plumes. C: NO_3^- concentration versus age for upper and middle plumes. D: B concentration versus age for upper and middle plumes. E: NO_3^- to B ratio versus age for upper and middle plumes. F: % Loss of NO_3^- versus age for upper and middle plumes.



3. Denitrification Rates in Groundwater Containing Septic Effluent

Denitrification rates were calculated for each water sample by dividing the mass of nitrate lost between the septic system leach field and the downgradient well sampling port, by groundwater age at that port. Mass balances losses of nitrate in excess of dilution were assessed using the following equations:

$$[\text{NO}_3^-]_{\text{exp}} = R * [\text{B}]_{\text{meas}}$$

$$[\text{NO}_3^-]_{\text{denit}} = [\text{NO}_3^-]_{\text{exp}} - [\text{NO}_3^-]_{\text{meas}}$$

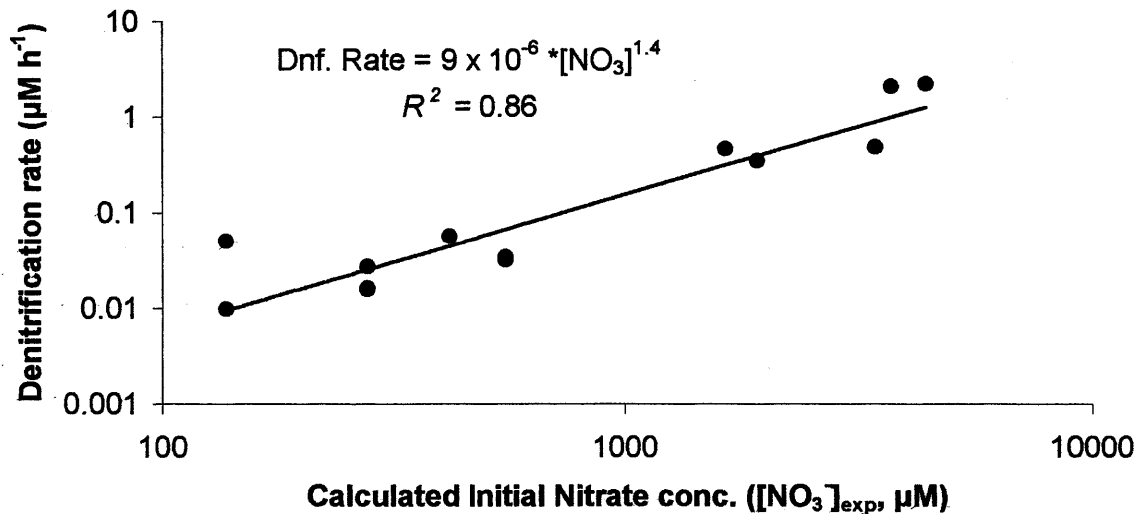
$$\text{(or } [\text{NO}_3^-]_{\text{denit}} = R * [\text{B}]_{\text{meas}} - [\text{NO}_3^-]_{\text{meas}}\text{)}$$

where $[\text{NO}_3^-]_{\text{exp}}$ is the concentration of nitrate expected in the absence of denitrification, corrected for dilution; R is the ratio of nitrate concentration to boron concentration ($[\text{NO}_3^-]/[\text{B}]$ ($\mu\text{M}/\text{mg l}^{-1}$)) expected in septic system effluent leaving the leaching field (assumed to be constant = 14,000; (8)); $[\text{B}]_{\text{meas}}$ is the measured boron concentration at the downgradient well port; $[\text{NO}_3^-]_{\text{denit}}$ is the mass balance loss of nitrate between the leach field and the sampling port attributed to denitrification; and $[\text{NO}_3^-]_{\text{meas}}$ is the concentration of nitrate measured at the well port.

Denitrification rates were calculated by dividing the mass of nitrate lost ($[\text{NO}_3^-]_{\text{denit}}$) by groundwater age (y), calculated using the Vogel model (Ch. 3, Eq. 1). Calculated initial nitrate concentrations ($[\text{NO}_3^-]_{\text{exp}}$) ranged from 140 to 4,400 μM , while denitrification rates ranged from 0.01 to 2.2 $\mu\text{M NO}_3^- \text{ h}^{-1}$, and averaged

0.42 $\mu\text{M NO}_3^- \text{ h}^{-1}$. These rates are 4 to 7 orders of magnitude higher than those measured in groundwater at our two forested sites, Crane Wildlife Management Area and South Cape Beach (0 to $2.1 \times 10^{-4} \mu\text{M NO}_3^- \text{ h}^{-1}$), where N was derived from either from soils or from fertilizer, with concentrations of nitrate $< 1.5 \mu\text{M}$ and 1.5 to $< 100 \mu\text{M}$, respectively. Denitrification rates in the septic plume increased with increasing initial nitrate concentration ($[\text{NO}_3^-]_{\text{exp}}$), and could be fit with a power curve (Fig. 4.3, $R^2 = 0.86$ at $p < .0002$), similar to our findings at the two forested sites, Cranes Wildlife Management Area and South Cape Beach (Ch. 3).

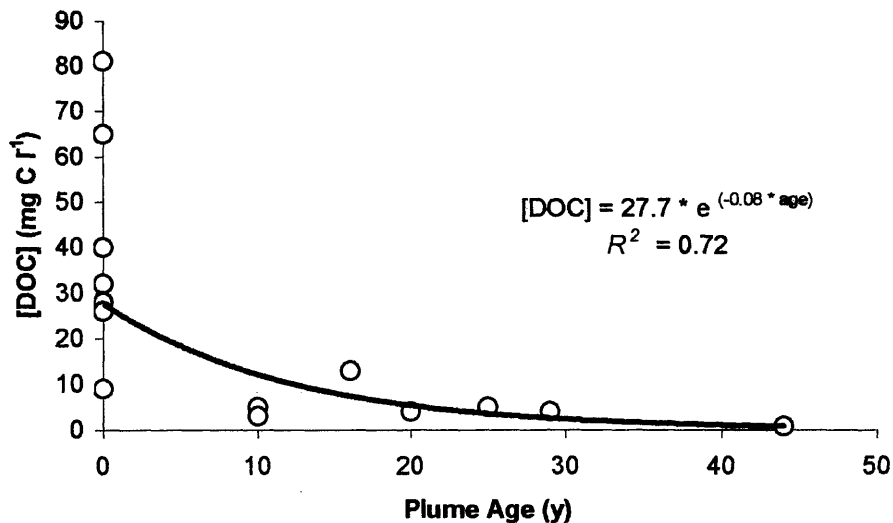
Figure 4.3. Denitrification rates in groundwater containing septic effluent as a function of calculated initial nitrate concentration corrected for dilution. Axes are logarithmic.



The relationship between denitrification rate and nitrate concentration exhibited in the septic plume samples is similar to that found at South Cape Beach (Ch. 3, Fig. 3.15),

where DOC concentrations were higher (0.8 to 24 mg C l⁻¹; mean = 7.0 mg C l⁻¹) than at Crane Wildlife Management Area (0 to 1.9 mg C l⁻¹; mean = 0.4 mg C l⁻¹). While we did not measure DOC concentrations at the septic system site, the similarity of the septic system and South Cape Beach trends suggests that DOC concentrations at the septic system are likely to be similar. Robertson et al. (12) measured DOC in 10 mature septic system groundwater plumes in a sand aquifer in central Canada. We used their data to plot DOC concentrations against plume age (Fig. 4.4; $R^2 = 0.72$).

Figure 4.4. Dissolved organic carbon concentrations (DOC) in groundwater as a function of septic system plume age. Data from Robertson et al. (12).



Using this relationship, we estimated DOC concentrations for each of our septic plume samples, based on calculated groundwater age (mean age = 0.90 yrs, mean DOC = 26 mg l⁻¹). Estimated this way, DOC concentrations in the septic system samples fall just

outside the high end of the range measured at SCB (range = 0.8 to 23.4 mg C l⁻¹, mean = 7.0 mg C l⁻¹), clearly higher than DOC concentrations at Crane Wildlife (mean = 0.4 mg C l⁻¹). Higher DOC concentrations in the septic plume and at South Cape Beach appear to have allowed for faster rates of denitrification, relative to those in the low DOC environment of Crane Wildlife for any given initial nitrate concentration.

The relationship between denitrification rate and DOC concentration is reflected in a comparison the first order rate constants calculated for each site. We calculated a first order rate constant ($k = [\ln([\text{NO}_3^-]_{\text{adj}}/[\text{NO}_3^-]_{\text{meas}}) / t]$, or $k = [\ln(C/C_0)]/t$ from Rayleigh equation) for each individual groundwater sample from the septic plume, and averaged the individual values to produce a first order rate constant for the data set as a whole ($k = 3.1 \times 10^{-4} \text{ h}^{-1}$ or 2.7 y^{-1}). The half-life for nitrate ($t_{1/2}$) in the plume, given this first order rate constant, was calculated to be 0.25 years. This first order rate was 11 times higher than at Crane Wildlife ($k = 2.9 \times 10^{-5} \text{ h}^{-1}$ or $.26 \text{ y}^{-1}$; $t_{1/2} = 2.8 \text{ y}$), but only twice as high as the first order rate for South Cape Beach ($k = 1.8 \times 10^{-4} \text{ h}^{-1}$ or 1.5 y^{-1} , $t_{1/2} = 0.45 \text{ y}$), presumably because the DOC concentrations in the septic plume are similar to the high end of the range of DOC concentrations measured at South Cape Beach (0.8 to 23.4 mg C l⁻¹), but are significantly higher than those found at Crane Wildlife (0.1 to 1.9 mg C l⁻¹). Higher rates in the septic plume and at South Cape Beach lead us to hypothesize that denitrification in this groundwater system is controlled by both nitrate and DOC concentrations, and could be modeled using a saturating kinetics expression with double substrate limitation by nitrate and DOC (Ch. 5).

4. Conclusions

Denitrification rates measured in groundwater at our septic system site ranged from 0.01 to 2.23 $\mu\text{M NO}_3^- \text{ h}^{-1}$, and averaged 0.42 $\mu\text{M NO}_3^- \text{ h}^{-1}$. Rates increased with increasing initial nitrate concentration (137 to 4,396 μM), and could be fit with a power curve ($R^2 = 0.86$ at $p < .0002$). The calculated septic system denitrification rates ($k = 3.1 \times 10^{-4} \text{ h}^{-1}$) were several orders of magnitude higher than those measured in groundwater at both the South Cape Beach ($k = 1.8 \times 10^{-4} \text{ h}^{-1}$) and Crane Wildlife sites ($k = 2.9 \times 10^{-5} \text{ h}^{-1}$), where nitrate concentrations were significantly lower (0 to 91 μM). The relationship between denitrification rate and nitrate concentration in the septic plume was similar to that found at South Cape Beach, suggesting that higher DOC concentrations in these two environments allowed for faster rates of denitrification for any given nitrate concentration relative to the low DOC environment at Crane Wildlife.

5. References

1. Valiela et al. 1992. Estuaries 15: 443-457.
2. Valiela et al. 1997. Ecol. Appl. 7: 358-380.
3. Valiela et al. 2000. Biogeochemistry 49: 277-293.
4. Wilhelm, S.R., S.L. Schiff and J.A. Cherry. 1994. Ground Water 32: 905-916.
5. Barth, S. 1998. Wat. Res. 32: 685-690.
6. LeBlanc, D.R. 1984. U.S. Geological Survey Water-Supply Paper 2218, 28 pp.
7. Barber, LB II, E.M. Thurman, M.P. Schroeder, and D.R. LeBlanc. 1988. Environ. Sci. Technol. 22: 205-211.
8. DeSimone, L.A., P.M. Barlow, B.L. Howes. Open-File Rep.- U.S. Geol. Surv. 1995, No. 95-290.
9. Bjerg, P.L., T.H. Christensen. 1992. J. Hydrol. 131: 133-149.
10. Vogel, J.C. 1967. Pp. 355-369 in Isotopes in Hydrology, Proceedings of IAEA-SM-83/24, Vienna.
11. LeBlanc, D.R., et al. 1991. Wat. Res. 27: 895-910.
12. Robertson WD, Schiff SL & Ptacek CJ. 1998. Ground Water. 36:1000-1010.

CHAPTER 5.

**AN EMPIRICAL MODEL TO PREDICT GROUNDWATER
DENITRIFICATION RATES, CAPE COD, USA: SUBSTRATE
LIMITATION BY DOC AND**

Running head: Groundwater denitrification model

Article type: General research

Title: An empirical model to predict groundwater denitrification rates, Cape Cod, USA: Substrate limitation by DOC and NO_3^-

Authors: Wendy J. Pabich^{1*}, Harold F. Hemond¹, and Ivan Valiela².

Affiliations: 1) Massachusetts Institute of Technology, Department of Civil and Environmental Engineering, Ralph M. Parsons Laboratory, Cambridge, MA 02138, U.S.A.

2) Boston University Marine Program, Marine Biological Laboratory, Woods Hole, MA 02543, U.S.A.

Corresponding author: Wendy J. Pabich
c/o Boston University Marine Program
Marine Biological Laboratory
Woods Hole, MA 02543
USA
Telephone: (508) 289-7615
Fax: (508) 289-7949
Email: wjpabich@mit.edu

Key words: Cape Cod, denitrification, groundwater, kinetics, modeling

Abstract. An empirically-based saturating kinetics model describing groundwater denitrification under carbon and nitrate-limited conditions was developed. Denitrification rates were described using a kinetic expression with double substrate limitation (with nitrate as the terminal electron acceptor and dissolved organic carbon (DOC) as the electron donor). The kinetic parameters were estimated from our field data (half saturation constant for NO_3^- (K_{NO_3})) and USGS field data (bacterial population [B]), and from data available in the literature (maximum bacterial growth rate (μ_{max}), half saturation constant for DOC (K_{DOC}), and bacterial yield constant (Y)). The proposed model is able to reasonably predict N losses along groundwater flow paths, measured at two forested sites (Ch. 3), where DOC ranged from 0 to 23 mg C l^{-1} and nitrate ranged from <1 to 91 μM . Using higher values for the bacterial population ($[B]$) and the half-saturation constant (K_{NO_3}), we were also able to predict N losses due to denitrification within the very different biogeochemical conditions of a septic system plume ($[\text{NO}_3^-]_{\text{max}} \sim 4,400 \mu\text{M}$, $[\text{DOC}] \sim 26 \text{ mg C}^{-1}$, and presumably a larger and more active bacterial population). The model performs well over the wide range of geochemical conditions found at the three sites within this ($R^2 = 0.96$, $m = 0.96$ for measured vs. modeled). Eliminating the DOC term from the saturating kinetics expression, so that denitrification is limited only by nitrate concentration, results in an overprediction of nitrate losses along groundwater flowpaths, particularly where DOC concentration are low. These results further confirm our previous conclusion (Ch. 3) that DOC concentrations exert a significant control on groundwater denitrification rates.

1. Introduction

Eutrophication by land-derived anthropogenic nitrogen (N) is the major cause of alterations to coastal ecosystems worldwide (GESAMP 1990, NRC 1994, Nixon 1986). In coastal areas underlain by unconsolidated sands, such as Cape Cod, the majority of land-derived N delivered to the coastal zone is transported by groundwater (Valiela et al. 1992). Many studies show that some portion of groundwater nitrogen is lost via denitrification within aquifers (Bengtsson and Annadotter 1989, Bottcher et al. 1990, Bragan et al. 1997a, Bragan et al. 1997b, Clay et al. 1996, Gillham 1991, Gold et al. 1998, Groffman et al. 1996, Jacinthe et al. 1998, Korom 1992, Peterjohn and Correll 1984, Valiela et al. 1992, Valiela et al. 2000, Verchot et al. 1997). Accurate estimation of land-derived nitrogen loads delivered to estuaries requires that significant losses occurring during transport, notably denitrification, be incorporated into models of nitrogen loading.

Our measurements of denitrification rates in the Waquoit Bay aquifer on Cape Cod, Massachusetts (Chs. 3 & 4), suggest that groundwater denitrification rates increased with increasing nitrate and dissolved organic carbon (DOC) concentrations. N losses along groundwater flowpaths at Crane Wildlife Management Area, where nitrate concentrations ranged from 0.2 to 68 μM , but DOC was consistently low ($< 2 \text{ mg C l}^{-1}$), could be best predicted using a saturating kinetics expression with respect to nitrate ($R^2 = 0.96$; Ch. 3, Fig. 3.20). Denitrification rates in the higher DOC environments of South Cape Beach (up to 24 mg C l^{-1}), and a septic plume ($\sim 26 \text{ mg C l}^{-1}$), were higher for any

given nitrate concentration than in the low DOC environment of Crane Wildlife. These results are consistent with other studies that demonstrate the importance of carbon substrate availability (Bradley et al. 1992b, Bremner and Argamann 1990, Christensen et al. 1990, Groffman et al. 1996, Knowles 1982, Parkin 1987, Payne 1981, Smith and Duff 1988, Sprent 1987) and nitrate concentration (Bengtsson and Bergwall 1995, Bradley et al. 1992a, Korom 1992, Morris et al. 1988, Slater and Capone 1987, Smith and Duff 1988) to denitrification rates.

Because concentrations of organic matter in groundwater are variable (0.1 to 27 mg C l⁻¹, Pabich et al. 2000a, Ford and Naiman 1989, Fiebig et al. 1990, Fiebig 1995) and concentrations of nitrate in Cape Cod groundwaters may vary over several orders of magnitude (0 to 4,400 μM NO₃⁻, our data, Kroeger et al. 1999, Savoie and LeBlanc 1998, Seely 1997, Valiela et al. 2000), our goal in this paper was to explore the use of a saturating kinetics model, not only with respect to nitrate as in Chapter 3, but also with respect to DOC, since higher concentration of DOC in groundwater appear to result in higher rates of denitrification for any given nitrate concentration.

This approach is consistent with other previous studies. Numerous models of varying complexity have been developed to predict denitrification rates, often for the purposes of wastewater treatment system design (Almeida et al. 1995, Brenner and Argamann 1990, Carucci et al. 1996, Engberg and Schroeder 1975, Glass and Silverstein 1998, Griffiths 1994, Kornaros et al. 1996, Kornaros and Lyberatos 1997, 1998, Wang et

al. 1995), or to predict co-metabolism of organic compounds under denitrifying conditions (Jørgensen et al. 1995). This study draws from information on denitrification kinetics in published laboratory experiments, and from our own field measurements, to develop a field-scale model to assess denitrification in a groundwater setting.

2. Saturating Kinetics

Several lines of evidence suggest that denitrification in the Waquoit Bay aquifer is controlled by saturating kinetics with respect to both DOC and nitrate concentrations. We found that first order rate constants for denitrification with respect to nitrate (Ch. 3) were highest where groundwater DOC concentrations were highest: $k = 2.8 \text{ y}^{-1}$ in the septic plume ($\sim 26 \text{ mg C l}^{-1}$), $k = 1.6 \text{ y}^{-1}$ at South Cape Beach (DOC = 0.8 to 23.4 mg C l^{-1}), and $k = .25 \text{ y}^{-1}$ at Crane Wildlife (0.1 to 1.9 mg C l^{-1}), suggesting that both DOC and nitrate concentrations exert important controls on denitrification rate. In addition, Smith and Duff (1988) found that denitrification, measured using an acetylene blockage assay on slurried aquifer core material obtained near wastewater disposal beds, located approximately 1 km to the east of the Crane Wildlife field site on the Massachusetts Military Reservation, was carbon-limited ([DOC] was estimated to be $\sim 12 \text{ mg C l}^{-1}$). Groundwater nitrate concentrations in this aquifer (0 – 4,400 μM ; Seely 1997, Valiela et al. 2000, Kroeger et al. 1999, Savoie and LeBlanc 1998, Pabich, unpublished data) are of similar magnitude to half-saturation constants (K_m) measured for denitrification with respect to nitrate (5-290 $\mu\text{M NO}_3^-$, Knowles 1982; $\sim 1,300 \mu\text{M}$ Reddy et al. 1982), suggesting that denitrification may become saturated with respect to nitrate.

Given this evidence, we modeled denitrification rates using a Michaelis-Menten-type substrate-utilization expression with double substrate limitation (nitrate as the terminal electron acceptor and organic carbon as the electron donor). In Chapter 3, we derived values for maximum denitrification rate (V_{max}) for both the forested sites and for the septic plume from our field measurements of nitrate losses. One of the goals of this paper was to determine whether the literature provided insight into the mechanistics of bacterial metabolism that would allow us to predict maximum reaction rates based on microbial theory. Toward that end, we modeled denitrification rates using the following expression:

$$d[NO_3^-]/dt = [(\mu_{max} * B_{denit})/Y] * [[NO_3^-]/(K_{NO_3} + [NO_3^-])] * [[DOC]/(K_{DOC} + [DOC])],$$

where μ_{max} is the maximum bacterial growth rate (hr^{-1}), B_{denit} is the population of denitrifying bacteria ($mg\ l^{-1}$), Y is the bacterial yield constant ($mg\ biomass\ mg\ C^{-1}$), $[NO_3^-]$ and $[DOC]$ are the substrate concentrations ($mg\ l^{-1}$), K_{NO_3} and K_{DOC} ($mg\ l^{-1}$) are the half-saturation constants for nitrate and dissolved organic carbon, respectively. Maximum reaction velocity (V_{max}) determined from our field data is essentially a lumped parameter equivalent to the first set of terms in the above model ($[(\mu_{max} * B_{denit})/Y]$). The advantage to utilizing this more explicit description of V_{max} is that the population density and activity of denitrifying bacteria have been shown to increase with increasing nitrate concentration (Bengtsson and Bergwall 1995, King and Nedwell 1987), potentially allowing us to develop a model for which only nitrate and DOC concentrations need be

measured in order to use the model to predict denitrification rates. We compare both approaches to estimating V_{max} .

2.1 Assumption of steady state

We assumed that each of the sampling points in the Waquoit Bay aquifer represented the output of a steady state reaction/flow system, with a population of bacteria acclimated to the existing NO_3^- and DOC concentrations within the aquifer. At both the Crane Wildlife and South Cape Beach sites, temporal variability in groundwater chemistry (dissolved O_2 , DOC, NH_4^+ , and NO_3^- concentrations) was minimal (Ch. 3, Fig. 3.4 and Table 3.6), and groundwater flow rates are believed to be relatively constant ($\sim 0.4 \text{ m day}^{-1}$, Leblanc 1991), supporting this assumption.

We also assumed that at each location, there was a specific maximum denitrifier population density, reflected in a constant growth rate (μ) less than μ_{max} , which is often the case when the substrate concentration is below the half-saturation constant ($S \ll K_s$, Alexander 1999). Given this conceptualization, we took each sampling location within the aquifer to represent a specific position on a Michaelis-Menten-like substrate utilization rate curve, that, taken together, would represent denitrification under saturating conditions across the range of nitrate and DOC concentrations measured.

3. Model Parameterization

The literature suggests that the population density and activity of denitrifying bacteria increase with increasing nitrate concentration. Bengtsson and Bergwall (1995) showed that the population (B), growth rate (μ_{max}), and activity (higher K_m) of denitrifying bacteria in groundwater of three Swedish aquifers increased with increasing groundwater nitrate concentration. Similarly, King and Nedwell (1987) found that denitrifying activity increased with increasing concentrations of nitrate in a nitrate gradient in an estuarine sediment, and suggested that nitrate reducers were adapted to the *in situ* concentrations of nitrate at each site. We estimated the effect of increasing nitrate concentrations on the population and activity of denitrifying bacteria.

3.1 Half-saturation constants for nitrate (K_{NO_3}) and DOC (K_{DOC})

For the forested sites, we estimated K_{NO_3} from groundwater profiles measured in three multi-level sampling wells containing a range of nitrate concentrations (0 - 68 μM) derived from soil and fertilizer (Ch. 4). DOC concentrations in the same samples remained low and nearly constant (<2 mg C Γ^{-1}), independent of the NO_3^- concentration. Using measured NO_3^- concentrations and denitrification rates for these samples, we constructed a Lineweaver-Burk plot ($1/d\text{NO}_3^-/dt$ vs. $1/[\text{NO}_3^-]$; Fig. 5.1) to estimate K_{NO_3} (112 μM NO_3^-). We estimated K_{NO_3} from the septic plume samples in the same manner (Fig. 5.2, 1760 μM NO_3^-). Our estimates fall within the range of K_m values for denitrification reported in the literature (5-290 μM NO_3^- , Knowles 1982; ~1,300 μM NO_3^- , Reddy 1982).

Figure 5.1. Lineweaver-Burke plot for forested sites used to estimate the half-saturation constant for denitrification with respect to nitrate (K_{NO_3}) and the maximum denitrification rate (V_{max}).

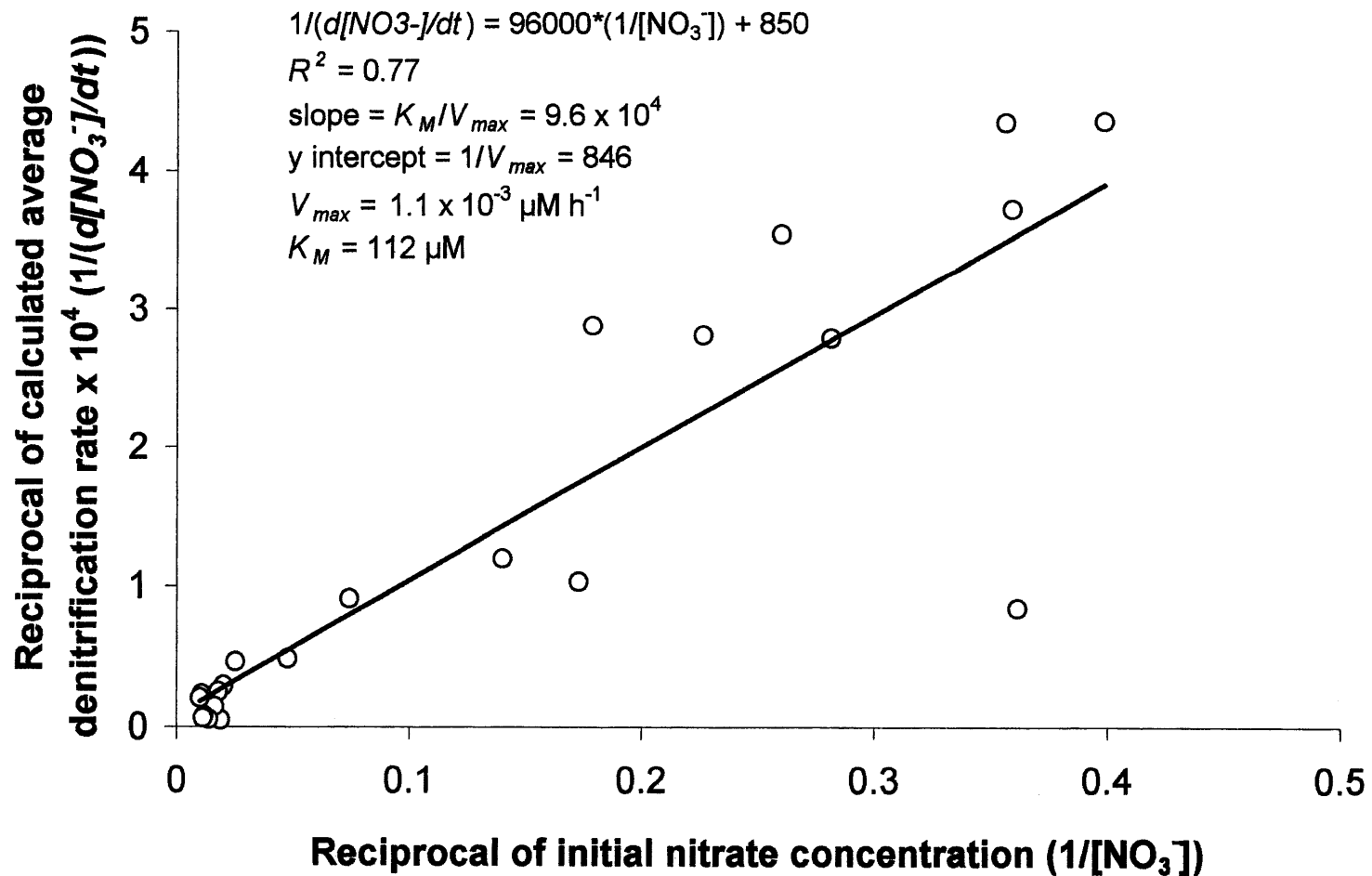
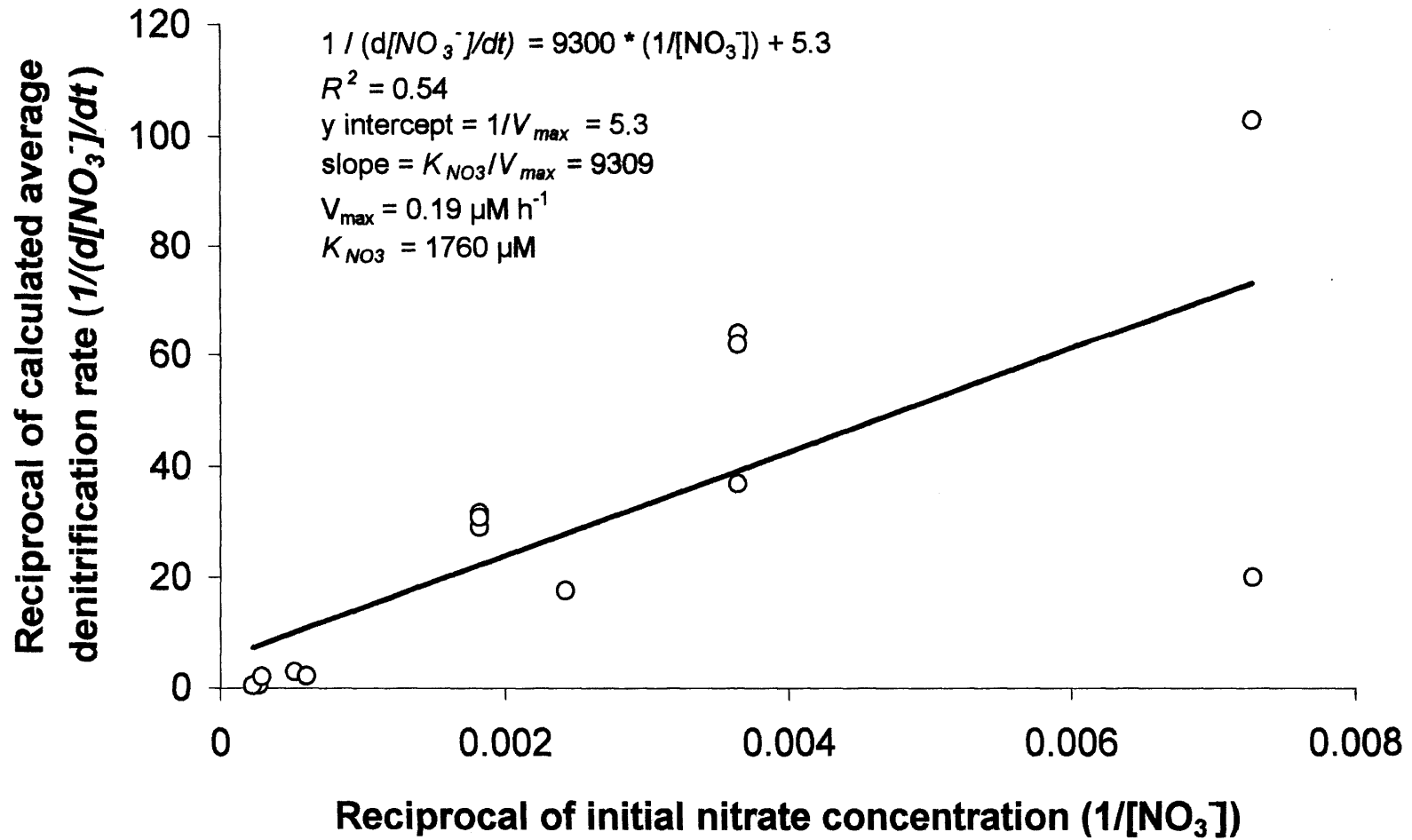


Figure 5.2. Lineweaver-Burke plots for septic system site used to estimate the half-saturation constant for denitrification with respect to nitrate (K_{NO_3}) and the maximum denitrification rate (V_{max}).



While DOC concentrations in the aquifer varied between sites (0.04 to 24 mg C l⁻¹), we were not able to use a Lineweaver-Burke plot to estimate K_{DOC} as we did for nitrate, since nitrate concentrations did not remain constant as DOC varied. Instead, we estimated K_{DOC} from kinetics experiments by Kornaros and Lyberatos (1997), who calculated K_s for growth of *Pseudomonas denitrificans* on glutamic acid (C₄H₉NO₄) at 0.025 mM (or 1.4 mg C l⁻¹, which we assigned as the value for K_{DOC}).

3.2 Denitrifying bacterial population

Deeper regions of the unsaturated zone, and uncontaminated, shallow water-table aquifers contain populations of around 10⁵ to 10⁷ organisms per gram of dry subsurface material or per liter of groundwater (Balkwill and Ghiorse 1985, Fliermans 1989, Ghiorse and Wilson 1988, Webster et al. 1985) with 1-10% of these organisms being metabolically active (Gehlen et al. 1985, Federle et al. 1996, Marxen 1988, Webster et al. 1985). In the same Cape Cod aquifer in which we worked, the USGS estimated the abundance of free-living bacteria in groundwater using fluorescent labeling (Savoie and LeBlanc 1998). Measured bacterial population averaged 6.1 x 10⁷ cells l⁻¹ in clean groundwater (or 0.33 mg l⁻¹, assuming that each cell weighs 5.5 x 10⁻¹⁰ mg, Schwarzenbach et al. 1993). We used this value to represent the total groundwater bacterial population (B_{total}).

Only a small percentage of enumerable groundwater bacteria are metabolically active (~1 – 10 %, Webster et al. 1985). Given the generally low ambient nutrient

concentrations in this aquifer, we assumed that only 1% of the enumerable population was metabolically active. This parameter is essentially a fitting parameter, since in the absence of field measurements to assess bacterial viability, we might reasonably assume that up to 10% of the bacterial population is viable. However, we found that our results were best when we used the lower value for bacterial viability.

Denitrifying bacteria, like viable bacteria, also represent a subset of the total bacterial population. To estimate the fraction of total bacteria that were denitrifiers, we constructed a linear relationship between nitrate concentration and % denitrifiers using data from Bengtsson and Bergwall (1995) from three aquifers in Sweden (Fig. 5.3, % denitrifiers = $.015 \cdot [\text{NO}_3^-] + 15$, $R^2 = 0.95$). For each groundwater sample from the two forested sites, we used measured nitrate concentration and this linear regression to estimate the fraction of denitrifying bacteria. Because nitrate concentrations at our two sites spanned a small range (up to 68 μM) relative to the range measured by Bengtsson and Bergwell (450 to 2500 μM), the calculated percent denitrifiers remained relatively constant at all of our sampling locations ($\sim 15\%$). We multiplied the calculated percent denitrifiers by the total bacterial population (B_{total}), and by the 1% percent metabolically active; the product represented the denitrifying population (B_{denit}). This resulted in a relatively constant estimate of denitrifying population around 9.1×10^5 cells l^{-1} for the two forested sites (Table 5.1).

Figure 5.3. Denitrifying bacteria as a percentage of total bacterial population versus groundwater nitrate concentration measured in 3 Swedish aquifers. Data from Bengtsson and Bergwall (1995).

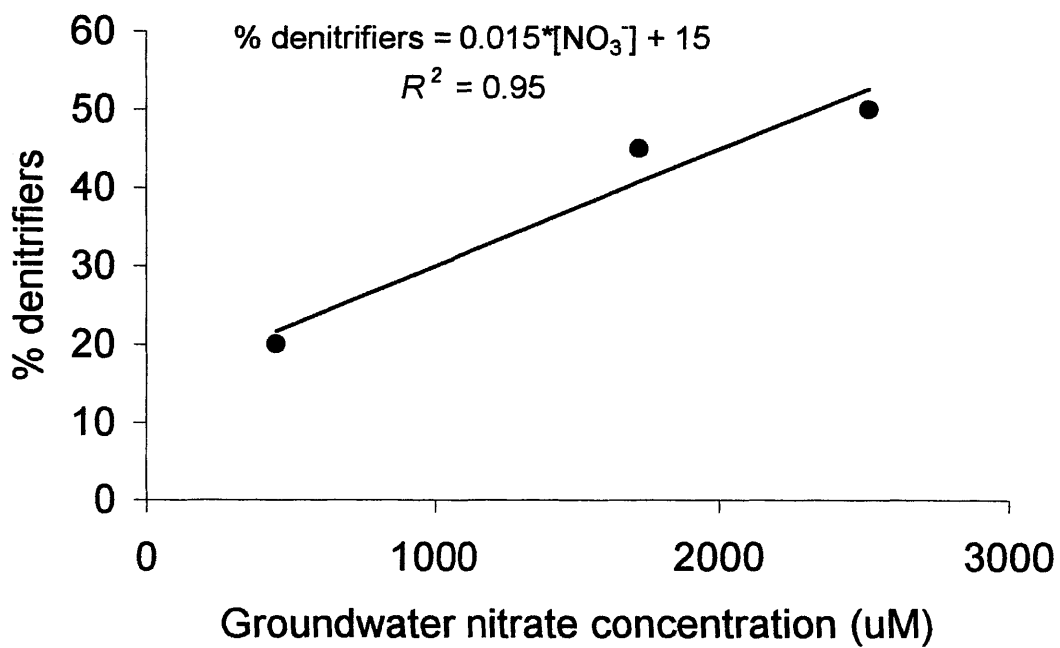


Table 5.1. Parameters and values used in saturating kinetics model for denitrification.

Parameter	Value for Forested Sites	Value for Septic System	Comments	Data Source
Half-saturation constant, NO ₃ (K_{NO_3})	112 μ M	1760 μ M	Lineweaver-Burk plot	this study
Half-saturation constant, DOC (K_{DOC})	1.4 mg C Γ^{-1}	1.4 mg C Γ^{-1}	incubations	Kornaros & Lyberatos (1997)
Total bacterial population ($[B]_{total}$)	6.1×10^8 cell Γ^{-1}		Cape Cod aquifer	Savoie & LeBlanc (1998)
Percent viable	1%	1%	1 - 10 % in groundwater	Webster et al. (1985)
Percent denitrifiers	~15%		linear regression	Bengtsson & Bergwall (1995)
Denitrifying population ($[B]_{denit}$)	~ 9.1×10^5 cells Γ^{-1}	2.1×10^7 cell Γ^{-1}	measured in septic filter	Pell et al. (1990)
Maximum growth rate (μ_{max})	0.23 h ⁻¹	0.23 h ⁻¹	incubations	literature, Table 5.2
Yield constant (Y)	1.11 mg biomass mg C ⁻¹	1.11 mg biomass mg C ⁻¹	incubations	literature, Table 5.2

Pell et al. (1990) measured bacterial populations in a sand-filter system for treating septic-tank effluent. Denitrifying bacterial densities ranged from 1.1×10^9 cells g^{-1} dry weight sediment in the upper several centimeters of the filter to 2.0×10^7 cells g^{-1} dry weight sediment at 20 cm depth into the filter. Using the 10.4% water content figure that these authors reported, we converted these values to 1.0×10^{11} cells l^{-1} in the upper portion of the filter and 2.1×10^9 cells l^{-1} in the lower portion. We assumed that denitrifying bacterial populations (B_{denit}) in the septic plume at our site were similar to those at the base of the sand filter (2.1×10^9 cells l^{-1} or 1.14 mg l^{-1}), and that 1% of that population was metabolically active (2.1×10^7 cells l^{-1} , Table 5.1).

3.3 Maximum bacterial growth rate (μ_{max})

Maximum growth rate has been estimated for various denitrifying species in controlled kinetic experiments (Almeida et al. 1995, Jorgensen et al. 1995, Kornaros and Lyberatos 1997, Wang et al. 1995). Values presented in the literature were surprisingly consistent (Table 5.2). We used the average of μ_{max} values (0.23 h^{-1}) presented for two denitrifying species and wastewater sludge.

3.4 Bacterial yield constant (Y)

Growth yield constants (Y) have been measured in the laboratory for a variety of denitrifying species using various carbon sources. Using the appropriate molecular weights for each of the carbon substrates, we normalized the Y values presented in the literature to $\text{mg biomass mg C}^{-1}$ ($0.15 - 2.74 \text{ mg biomass mg C}^{-1}$, Table 5.2). We also

Table 5.2. Estimated values for maximum growth rate (μ_{max}) and yield constant (Y) from the literature, and from our thermodynamic calculations for Y . Mean values for each parameter were used in the model.

Maximum growth rate (μ_{max} , h ⁻¹)	Culture		Study
0.36	<i>Ps. denitrificans</i>		Kornaros & Lyberatos (1997)
0.10	wastewater sludge		Jørgensen et al. (1995)
0.21	<i>Ps. denitrificans</i>		Wang et al. (1995)
0.26	<i>P. fluorescens</i>		Almeida et al. (1994)
0.23	Mean		

Yield constant (Y , mg biomass mg C ⁻¹)	Culture	Carbon source	Study
0.17	<i>Ps. denitrificans</i>	glutamate	Kornaros & Lyberatos (1998)
0.15	wastewater sludge	toluene	Jørgensen et al. (1995)
0.64	wastewater sludge	wastewater	Slade & Dare (1993)
2.74	<i>Ps. denitrificans</i>	methanol	Wang et al. (1995)
0.82	wastewater sludge	acetate	Rittman & McCarty (1980)
2.14	thermodynamic calc.	acetate	this study
1.11	Mean		

calculated the yield constant for denitrifying organisms growing on acetate (2.14 mg biomass per mg C utilized) using a thermodynamic relationship between free energy of reaction and maximum cell yield (McCarty 1971). The average of these values was 1.11 mg biomass mg C⁻¹, which we used in our model.

4. Results and Discussion

Our estimation of maximum reaction velocity for the bacterial population ($\sim[(\mu_{max} * B_{denit})/Y]$) at the septic system site was 0.17 $\mu\text{M h}^{-1}$, which is surprisingly close to the lumped V_{max} value (0.19 $\mu\text{M h}^{-1}$) estimated using a Lineweaver-Burk plot of our field data (Fig. 5.2). For the forested sites, where we assumed that B_{denit} varied with nitrate concentration, maximum reaction velocity also varied with nitrate concentration. However, because the nitrate concentrations at these two sites (0.2 – 68 μM) were relatively low, our calculations for percent denitrifiers in the system ($\% \text{ denitrifiers} = .015 * [\text{NO}_3^-] + 15$) varied minimally over the range of nitrate concentrations. Thus, maximum reaction velocity across these two forested sites was also nearly constant (7.4×10^{-3} to $8.0 \times 10^{-3} \mu\text{M h}^{-1}$). In comparison, using the Lineweaver-Burke plot and our field measurements (Fig. 5.1), the V_{max} value was lower ($1.1 \times 10^{-3} \mu\text{M h}^{-1}$), but within the same order of magnitude.

The utility of the full expression for V_{max} ($\sim[(\mu_{max} * B_{denit})/Y]$) lies in the fact that both maximum bacterial growth rate (μ_{max}) and yield (Y) are relatively invariable relative

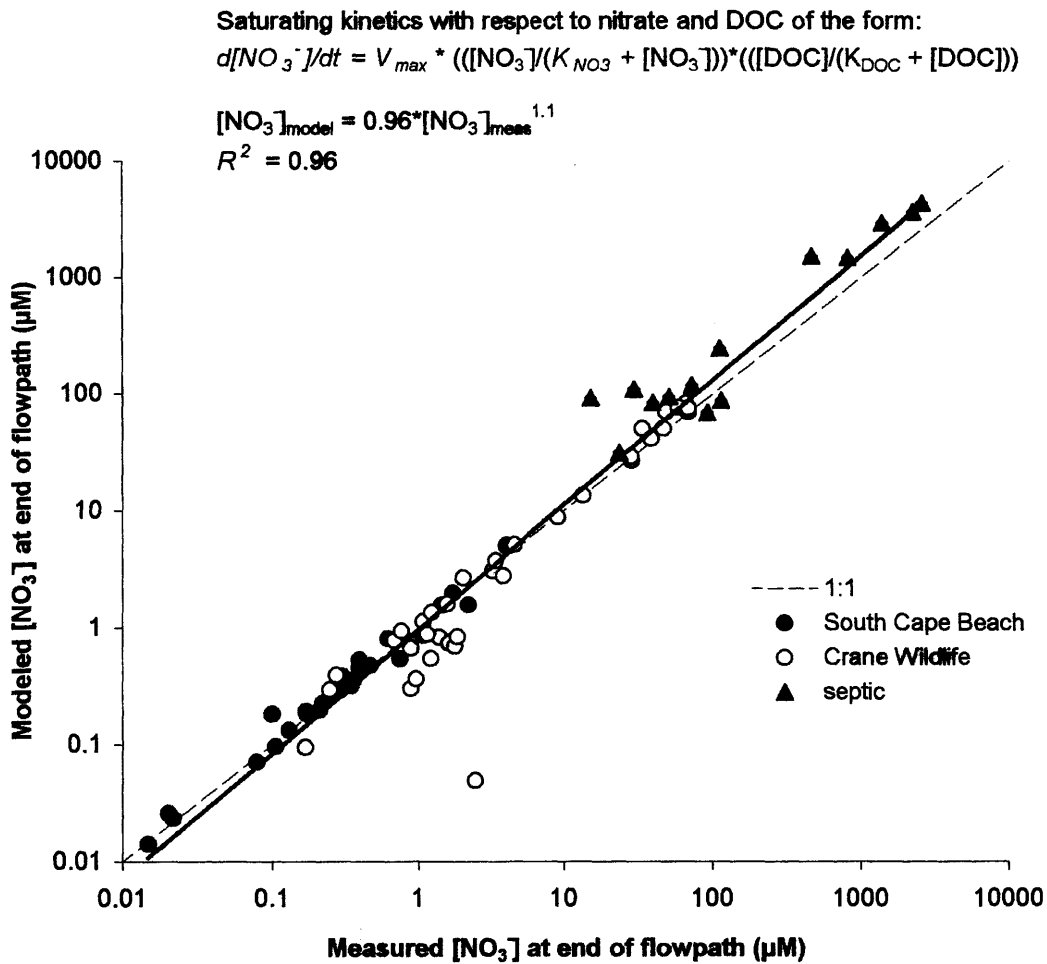
to the large changes that are expected in both total bacterial population (B_{total}) and the percentage of that population that are denitrifiers (B_{denit}) with changing groundwater nitrate and DOC conditions. An expression that accurately characterizes the denitrifying population (and therefore the maximum reaction velocity (V_{max})), would be quite useful in terms of allowing the model to be applied to a wider range of field situations. Had the nitrate concentrations beneath the forested sites varied more widely, we might have been able to test how well our V_{max} expression captures the relationship between nitrate concentration and denitrifying activity, and thus, its utility in predicting losses of N via denitrification from a generalized understanding of bacterial dynamics. Testing our model using nitrate, DOC, and denitrification measurements from another site would be a valuable future exercise.

We tested the model (using the V_{max} values estimated from the full expression $([(\mu_{max} \cdot B_{denit})/Y])$ for maximum reaction velocity) to determine how well we could predict groundwater nitrate loss along the length of groundwater flowpaths across a range of geochemical conditions. We ran a simulation to estimate total N lost in groundwater between recharge and a downgradient sampling location, at two forested sites where nitrate (0-91 μM) and DOC (0-24 mg C l^{-1}) varied considerably, and in groundwater sampled from a septic plume ($[\text{NO}_3^-]_{\text{max}} \sim 4,400 \mu\text{M}$, $[\text{DOC}] \sim 26 \text{ mg C}^{-1}$). We compared predicted downgradient nitrate concentrations $[\text{NO}_3^-]_{\text{model}}$ with those actually measured in the field $[\text{NO}_3^-]_{\text{meas}}$. For each water parcel, we discretized the groundwater flowpath into 4 time steps. For the first time step, we estimated the denitrification rate based on the

initial nitrate concentration ($[\text{NO}_3^-]_{\text{adj}}$), calculated the total mass of N lost to denitrification during that time band ($[\text{NO}_3^-]_{\text{denit}}$), and subtracted the two values ($[\text{NO}_3^-]_{\text{adj}} - [\text{NO}_3^-]_{\text{denit}}$) to estimate the final nitrate concentration at the end of the time band. In each sequential time band we calculated a new denitrification rate, N loss, and final N concentration, based on the mass of nitrate remaining from the previous time band. We did the same for [DOC] concentration, assuming that DOC was utilized in a 5:4 molar ratio relative to nitrate.

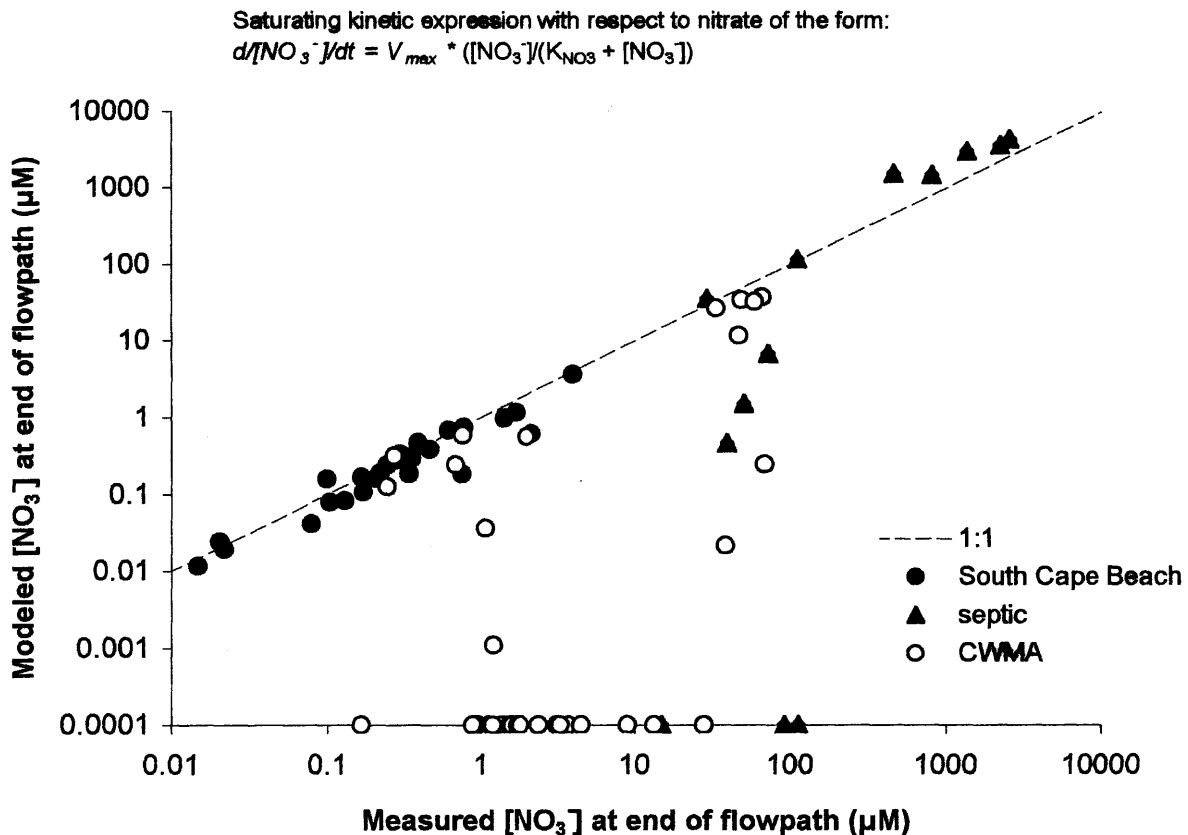
Figure 5.4 shows a plot of expected nitrate concentration determined in the simulation ($[\text{NO}_3^-]_{\text{model}}$) versus nitrate concentration actually measured each well port ($[\text{NO}_3^-]_{\text{meas}}$) for the three sites. Using the same parameter values for both South Cape Beach and Crane Wildlife, and higher values for the bacterial population ($[B]$) and the half-saturation constant (K_{NO_3}) at the septic site, we were able to reasonably predict expected nitrate concentrations at the end of the flowpath ($R^2 = 0.96$, $m = 0.96$ for measured vs. modeled) across the wide range of geochemical conditions represented by these sites: Crane Wildlife (0.2 to $68 \mu\text{M NO}_3^-$ and $< 2.0 \text{ mg C l}^{-1}$), South Cape Beach (0.01 to $4.0 \mu\text{M NO}_3^-$ and 0.8 to 23.4 mg C l^{-1}), and a septic system plume ($[\text{NO}_3^-]_{\text{max}} \sim 4,400 \mu\text{M}$, $[\text{DOC}] \sim 26 \text{ mg C}^{-1}$). The model provided a similar fit to the data when we used the field estimated values for V_{max} specific to each site, suggesting that reasonable approximations of denitrifying bacterial activity in groundwater can be made using data from the literature.

Figure 5.4. Nitrate losses by denitrification simulated over groundwater flowpaths using a saturating kinetics expression with respect to nitrate and dissolved organic carbon (DOC). Modeled nitrate concentration at the end of each flowpath is plotted against the measured nitrate concentration for two forested sites (South Cape Beach and Crane Wildlife) and a septic system plume. Kinetic parameters for the septic system site differ from those used at the two forested sites. Axes are logarithmic.



We also simulated nitrate losses along the groundwater flowpaths using a saturating kinetics expression with respect only to nitrate. We used the V_{max} value estimated from the bacterial parameters, but eliminated the DOC terms ($[\text{DOC}]/(K_{\text{DOC}} + [\text{DOC}])$) from the kinetics expression (i.e., $d[\text{NO}_3^-]/dt = V_{max} * ([\text{NO}_3^-]/(K_{\text{NO}_3} + [\text{NO}_3^-]))$). Figure 5.5 is a plot of expected nitrate concentration determined in the simulation ($[\text{NO}_3^-]_{\text{model}}$) versus nitrate concentration actually measured each well port ($[\text{NO}_3^-]_{\text{meas}}$) for the three sites. We found that, especially where DOC concentrations were low, the model often overpredicted the rate of denitrification, resulting in negative predicted nitrate concentrations. Where predicted nitrate concentrations were negative, we set $[\text{NO}_3^-]_{\text{meas}}$ to 10^{-4} μM in order to include this data on a logarithmic plot. The problem was particularly noticeable for the Crane Wildlife dataset, where low DOC concentrations ($< 2 \text{ mg C l}^{-1}$) clearly limit groundwater denitrification rates. As a typical example, for a groundwater parcel at Crane Wildlife with an initial nitrate concentration of $1.6 \mu\text{M}$, and a DOC concentration of 0.26 mg C l^{-1} , the kinetic expression with respect to nitrate only, predicts loss of $1.9 \mu\text{M}$ nitrate within the first time band (resulting in a $[\text{NO}_3^-]_{\text{model}} < 0$). In comparison, the kinetics expression that uses double substrate limitation by nitrate *and* DOC resulted in a predicted nitrate loss of only $0.09 \mu\text{M}$ during the first time step, reflecting the impact of low DOC concentrations on denitrification rate. The much better fit between $[\text{NO}_3^-]_{\text{model}}$ and $[\text{NO}_3^-]_{\text{meas}}$ using the kinetics expression with respect to both nitrate and DOC (Fig. 5.4), than using the model with respect only to nitrate (Fig. 5.5) illustrates the importance of DOC as a control on groundwater denitrification rates.

Figure 5.5. Nitrate losses by denitrification simulated over groundwater flowpaths using a saturating kinetics expression with respect to nitrate. Modeled nitrate concentration at the end of each flowpath is plotted against measured nitrate concentration for the two forested sites (South Cape Beach and Crane Wildlife) and a septic system plume. Kinetic parameters for the septic system differ from those used for the two forested sites. Where the model overestimated nitrate losses (i.e., $[\text{NO}_3^-]_{\text{model}} < 0$), $[\text{NO}_3^-]_{\text{model}}$ was set to $10^{-4} \mu\text{M}$ in order to present data on logarithmic plot.



These results further confirm our conclusions from Chapter 3, where we show that first order denitrification rates with respect to nitrate are highest where DOC concentrations are highest, suggesting that independent of nitrate concentration, DOC concentrations play a critical role in controlling groundwater denitrification rates. The kinetics model, with double substrate limitation by nitrate and DOC, that we present here, provides a valuable tool for planners and managers interested in designing management strategies to control nitrogen loading to coastal waters. Such a model might be used in the design of setback limits for septic systems, in assessing the value of open spaces for N load reduction, in regulating wastewater disposal, and in watershed-wide land use planning.

5. Acknowledgements

MIT Sea Grant (#65591) and a National Estuarine Research Reserve (NERRS) Graduate Fellowship from the National Oceanic and Atmospheric Administration (NA77OR024) supported this work. The authors would like to thank the many people who assisted us in the field and lab work that provided the data against which we tested this model, including: Denis LeBlanc of the US Geological Survey, Marlborough, MA; Gabrielle Tomasky of the Boston University Marine Program; Vanessa Bhark, Amy Watson, and John McFarland at MIT; Anne Giblin and Kathy Reagan at the Ecosystems Center, Marine Biological Laboratory; and the staff at the Waquoit Bay National Estuarine Research Reserve.

6. References

- Alexander M. 1999. Biodegradation and bioremediation. 2nd edition. Academic Press. San Diego. pp. 453.
- Almeida JS, Julio SM, Reis MAM, & Carrondo MJT (1995) Nitrate inhibition of denitrification by *Pseudomonas fluorescens*. *Biotech. Bioeng.* 46: 194-201.
- Balkwill DL & Ghiorse WC (1985) Characterization of subsurface bacteria associated with two shallow aquifers in Oklahoma. *Appl. Env. Microbiol.* 50: 580-588.
- Bengtsson G & Annadotter H (1989) Nitrate reduction in a groundwater microcosm determined by ¹⁵N gas chromatography-mass spectrometry. *Appl. Environ. Microbiol.* 55:2861-2870.
- Bengtsson G & Bergwall C (1995) Heterotrophic denitrification potential as an adaptive response in groundwater bacteria. *FEMS Microbiol. Ecol.* 16: 307-318.
- Bottcher J, Strebel O, Voerkelius S, & Schmidt HL (1990) Using isotope fractionation of nitrate-nitrogen and nitrate-oxygen for evaluation of microbial denitrification in a sandy aquifer. *J. Hydrol.* 114:413-424.
- Bradley PM, Aelion CM, & Vroblesky DA (1992a) Influence of environmental factors on denitrification in sediment contaminated with JP-4 jet fuel. *Ground Wat.* 30:843-848.
- Bradley PM, Fernandez M, Jr, & Chapelle FH (1992b) Carbon limitation of denitrification rates in an anaerobic groundwater system. *Environ. Sci. Technol.* 26: 2377-2381.
- Bragan RJ, Starr JL, & Parkin TB (1997a) Shallow groundwater denitrification rates measured by acetylene block. *J. Environ. Qual.* 26:1531-1538.
- Bragan RJ, Starr JL, & Parkin TB (1997b) Acetylene transport in shallow groundwater for denitrification rate measurement. *J. Environ. Qual.* 26:1524-1530.
- Bremner A & Argaman Y (1990) Effect of feed composition, aerobic volume fraction and recycle rate on nitrogen in the single-sludge system. *Wat. Res.* 24: 1041-1049.
- Carucci A, Ramadori R, Rossetti S, & Tomei MC (1996) Kinetics of denitrification reactions in single sludge systems. *Wat. Res.* 30:51-56.
- Christensen S, Simkins S, & JM Tiedje (1990) Spatial variability in denitrification: Dependency of activity centers on the soil environment. *Soil Sci. Soc. Am. J.* 54:1608-1613.

Clay DE, Clay SA, Moorman TB, Brix-Davis K, Scholes KA, & Bender AR (1996) Temporal variability of organic C and nitrate in a shallow aquifer. *Water Res.* 30:559-568.

Engberg DJ & Schroeder ED (1975) Kinetics and stoichiometry of bacterial denitrification as a function of cell residence time. *Wat. Res.* 9: 1051-1054.

Federle TW, Dobbins DC, Thorning-Manning JR, & Jones DD (1986) Microbial biomass, activity, and community structure in subsurface soils. *Ground Wat.* 24: 365-374.

Fiebig D, Lock MA, & Neal C (1990) Soil water in the riparian zone as a source of carbon for a headwater stream. *J. Hydrol.* 116: 217-237.

Fiebig D (1995) Groundwater discharge and its contribution of dissolved organic carbon to an upland stream. *Arch. Hydrobiol.* 134: 129-155.

Fliermans CB (1989) Microbial life in the terrestrial subsurface of southeastern coastal plain sediments. *Haz. Water Haz. Materials* 6:155-171.

Ford T & Naiman RJ (1989) Groundwater-surface water relationships in boreal forest watersheds: dissolved organic carbon and inorganic nutrient dynamics. *Can. J. Fish. Aquat. Sci.* 46: 41-49.

Gehlen M, Trampish HJ, & Dott W (1985) Physiological characterization of heterotrophic bacterial communities from selected aquatic environments. *Microb. Ecol.* 11:205-219.

GESAMP (1990) State of the Marine Environment. Rep. Stud. No. 39, Joint Group of Experts on the Scientific Aspects of Marine Pollution. United Nations Environment Programme. 111 p.

Ghiorse WC & Wilson JT (1988) Microbial ecology of the terrestrial subsurface. *Adv. Appl. Microbiol.* 33: 107-172.

Gillham RW (1991) Nitrate contamination of groundwater in Southern Ontario and the evidence for denitrification. NATO ASI SERIES, V G 30 Nitrate Contamination, (edited by Bogardi I, & Kuselka RD) p. 182-198.

Glass C & Silverstein J (1998) Denitrification kinetics of high nitrate concentration water: pH effect on inhibition and nitrate accumulation. *Water Res.* 32: 831-839.

- Gold AJ, Jacinthe PA, Groffman PM, Wright WR, & Puffer PH (1998) Patchiness in groundwater nitrate removal in a riparian forest. *J. Env. Qual.* 27:146-155.
- Griffiths P (1994) Modifications to the IAWPRC Task Group general activated sludge model. *Water Res.* 28: 657-664.
- Groffman PM, Howard G, Gold AJ, & Nelson WM (1996) Microbial nitrate processing in shallow groundwater in a riparian forest. *J. Env. Qual.* 25: 1309-1316.
- Jacinthe PA, Groffman PM, Gold AJ, & Mosier A (1998) Patchiness in microbial nitrogen transformations in groundwater in a riparian forest. *J. Env. Qual.* 27:156-164.
- Jørgensen C, Flyvbjerg J, Arvin E, & Jensen BK (1995) Stoichiometry and kinetics of microbial toluene degradation under denitrifying conditions. *Biodegradation* 6: 147-156.
- King D & Nedwell DB (1987) The adaptation of nitrate-reducing communities in estuarine sediments in response to overlying nitrate load. *FEMS Microbiol. Ecol.* 45:15-20.
- Knowles R. (1982) Denitrification. *Microbiol. Rev.* 46:43-70.
- Koram SF (1992) Natural denitrification in the saturated zone: A review. *Wat. Res. Res.* 28:1657-1668.
- Kornaros M & Lyberatos G (1998) Kinetics modelling of *Pseudomonas denitrificans* under growth and denitrification under aerobic, anoxic and transient operating conditions. *Water Res.* 32: 1912-1922.
- Kornaros M, Zafiri C, & Lyberatos G (1997) Kinetics of aerobic growth of a denitrifying bacterium, *Pseudomonas denitrificans*, in the presence of nitrates and/or nitrites. *Water Res.* 31: 479-488.
- Kroeger KD, Bowen JD, Corcoran D, Moorman J, Michałowski J, Rose C, & Valiela I (1999) Nitrogen loading to Green Pond, Falmouth, MA: Sources and evaluation of management options. *Environ. Cape Cod* 2: 15-26.
- LeBlanc DR, Garabedian SP, Hess KM, Gelhar LW, Quadri RD, Stollenwerk KG, & Wood WW (1991) Large-scale natural gradient tracer test in sand and gravel, Cape Cod, Massachusetts I. Experimental design and observed tracer movement. *Water Res. Res.* 27: 895-910

- Mariotti A, Landreau A, & Simon B (1988) ^{15}N isotope biogeochemistry and natural denitrification process in groundwater: Application to the chalk aquifer of northern France. *Geochim. et Cosmochim. Acta* 52: 1869-1878.
- Marxen J (1988) Investigations into the number of respiring bacteria in groundwater from sandy and gravelly deposits. *Microb. Ecol.* 16:65-72.
- McCarty PL (1971) Energetics and Bacterial Growth; Chap: 21 in *Organic Compounds in Aquatic Environments*, Faust SD & Hunter JV, Eds., Marcel Dekker, Inc., New York, pp. 495-531.
- Morris JT, Whitting GT, & Chapelle FH (1988) Potential denitrification rates in deep sediments from the Southeastern Coastal Plain. *Environ. Sci. Technol.* 22:832-835.
- National Research Council (1994) *Priorities for Coastal Science*, National Academy Press, Washington D.C. 88 p.
- Nixon S, Oviatt CA, Frithsen J, & Sullivan B (1986) Nutrients and the productivity of estuarine and coastal marine ecosystems. *J. Limnol. Soc. S. Africa* 12: 43-71.
- Pabich WJ, Valiela I, & Hemond HF (submitted) The effect of vadose thickness and depth below the water table on DOC concentration in groundwater on Cape Cod, U.S.A. *Biogeochemistry*.
- Pabich WJ, Hemond HF, & Valiela I. Denitrification rates in groundwater, Cape Cod, USA: Control by NO_3^- and DOC concentrations.
- Parkin TB (1987) Soil microsite as a source of denitrification variability. *Soil Sci. Soc. Amer. J.* 51: 1194-1199.
- Payne WJ (1981) Chapter 10: Denitrification as a factor in soil science: general properties. In: *Denitrification*. John Wiley & Sons, New York. pp. 118-133.
- Pell M, Nyberg F, & Lundgren H (1990) Microbial numbers and activity during infiltration of septic-tank effluent in a subsurface sand filter. *Wat. Res.* 24:1347-1354.
- Peterjohn WT, & Correll DL (1984) Nutrient dynamics in an agricultural watershed: Observations on the role of riparian forest. *Ecology* 65: 256-268.
- Rittman BE, & McCarty PL (1980) Evaluation of steady-state-biofilm kinetics. *Biotechnol. Bioeng.* 22: 2358-2373.

- Savoie J, & LeBlanc DR (1998) Water-Quality Data and Methods of Analysis for Samples Collected Near a Plume of Sewage-Contaminated Ground Water, Ashumet Valley, Cape Cod, Massachusetts, 1993-94. U.S. Geological Survey, Marlborough
- Seely BA (1997) Atmospheric deposition and flux dynamics of nitrogen in the coastal forests of the Waquoit Bay watershed, Cape Cod, MA. PhD dissertation, Boston University.
- Slade AH, & Dare PH (1993) Technical note: Measuring maximum specific growth rate and half saturation coefficient for activated sludge systems using a freeze concentration technique. *Wat. Res.* 12:1793-1795.
- Slater JM, & Capone DG (1987) Denitrification in aquifer soil and nearshore marine sediments influenced by groundwater nitrate. *Appl. Environ. Microbiol.* 53:1292-1297.
- Smith RL, & Duff JH (1988) Denitrification in a sand and gravel aquifer. *Appl. Environ. Microbiol.* 53: 1292-1297.
- Sprent JI (1987) Chapter 3: Modified N cycles: effects of environment. In: *The Ecology of the Nitrogen Cycle*. Cambridge University Press, New York. pp. 49-66.
- Valiela I, Collins G, Kremer J, Lajtha K, Geist M, Seely B, Brawley J, & Sham CH (1997) Nitrogen loading from coastal watersheds to receiving estuaries: new method and application. *Ecol. Appl.* 7: 358-380
- Valiela I, Foreman K, LaMontagne M, Hersh D, Costa J, Peckol P, DeMeo-Andreson B, D'Avanzo C, Babione M, Sham CH, Brawley J, & Lajtha K (1992) Couplings of watersheds and coastal waters: sources and consequences of nutrient enrichment in Waquoit Bay, Massachusetts. *Estuaries* 15: 443-457.
- Valiela I, Geist M, McClelland J, & Tomasky G (2000) Nitrogen loading from watersheds to estuaries: Verification of the Waquoit Bay Nitrogen Loading Model. *Biogeochemistry* 49:277-293
- Verchot LV, Franklin EC, & Gilliam JW (1997) Nitrogen cycling in Piedmont vegetated filter zones: II. Subsurface nitrogen removal. *J. Environ. Qual.* 26:337-347.
- Vogel JC (1967) Investigation of groundwater flow with radiocarbon. In: *Isotopes in Hydrology* (pp. 355-369). IAEA-SM-83/24, Vienna
- Wang JH, Baltzis BC, & Lewandowski GA (1995) Fundamental denitrification kinetic studies with *Pseudomonas denitrificans*. *Biotechnol. Bioeng.* 47: 26-41.

Webster JJ, Hampton GJ, Wilson JT, Ghiorse WC, & Leach FR (1985) Determination of microbial cell numbers in subsurface samples. *Ground Wat.* 23:17-25.

CHAPTER 6:
CONCLUSIONS

1. Conclusions

A principal alteration of estuarine and coastal ecosystems worldwide is eutrophication brought about by increasing loads of anthropogenically-derived nitrogen (GESAMP 1990, NRC 1994, Nixon et al. 1996) transported by freshwater to receiving coastal waters (Cole et al. 1993). Nitrogen transport rates are of critical importance because rates of coastal production, as well as many other key processes coupled to production, are set by nitrogen supply (Nixon, in press, Nixon et al. 1986, Howarth et al. 1996). The effects of eutrophication on coastal ecosystems are far-ranging, and can include red tides, fish kills, anoxia and hypoxia as currently observed over wide areas of the Gulf of Mexico, contamination of shellfish beds (NRC 2000), and alteration of valuable habitat including loss of eelgrass beds, such as that documented in Waquoit Bay, MA (Costa 1988).

Understanding how N is transformed and transported within aquifers is necessary to calculating watershed N budgets, understanding basic nitrogen biogeochemistry, and estimating total N delivery to coastal waters. The goal of this study was to estimate groundwater denitrification rates in the Waquoit Bay aquifer on Cape Cod, to examine how they vary as a function of nitrate and DOC concentrations, and to construct a predictive model that might be used to assess groundwater denitrification rates across the range of geochemical conditions present in this aquifer.

2. Controls on Groundwater DOC Concentrations

We show that the thickness of the vadose zone through which recharge occurs and the depth below the water table exert significant control on DOC concentrations in underlying groundwater. We found that the deeper the vadose zone, the lower the concentration of DOC in groundwater near the water table, indicating that considerable attenuation of surface-derived DOC occurred in the vadose zone. Under vadose zones <1.25 m, DOC concentrations at the surface of the water table ranged to >20 mg l⁻¹ C, while for vadose zones >5.0 m, DOC never exceeded 2.0 mg l⁻¹ C. DOC concentrations also decreased with increasing depth below the water table, most notably in the upper two meters, implying continued attenuation in the upper layer of the saturated zone. Ninety-nine percent of the DOC was attenuated by the time the water reached a depth of 19 m below the water table. DOC concentrations in shallow groundwater show considerable spatial variability, but concentration of DOC at any one site is surprisingly stable over time. The largest source of variation in DOC concentration in groundwater therefore is spatial rather than temporal, suggesting that local heterogeneities play an important role in DOC delivery to shallow groundwater. Our results highlight both the importance of shallow vadose areas in DOC delivery to groundwater and the need to distinguish where samples are collected in relation to flow paths before conclusions are made about mean groundwater DOC concentrations. The substantial losses of DOC in the vadose zone and in shallow depths within the aquifer suggest that quite active biogeochemical processing, particularly denitrification, may occur in these boundary environments.

3. Groundwater Denitrification Rates

We used a stable isotopic approach to estimate average denitrification rates occurring along groundwater flowpaths at two forested sites (Crane Wildlife Management Area and South Cape Beach) in and near the Waquoit Bay watershed. These sites provided a large range of groundwater nitrate (<1 to 91 μM) and DOC (0 to 23 mg C l^{-1}) concentrations. We compared these rates to those that we measured using mass balance of N in a septic plume. Denitrification rates increased with increasing nitrate concentration, from 0 to $2.1 \times 10^{-3} \mu\text{M N h}^{-1}$ at the forested sites, and 0.01 to 2.23 $\mu\text{M NO}_3^- \text{ h}^{-1}$ in the septic system plume. First order denitrification rate constants with respect to nitrate were highest where groundwater DOC concentrations were highest: $k = 2.8 \text{ y}^{-1}$ in the septic plume ($\sim 26 \text{ mg C l}^{-1}$), $k = 1.6 \text{ y}^{-1}$ at South Cape Beach (DOC = 0.8 to 23.4 mg C l^{-1}), and $k = .25 \text{ y}^{-1}$ at Crane Wildlife (0.1 to 1.9 mg C l^{-1}), suggesting that, independent of nitrate concentration, DOC concentration exerts a significant control on denitrification rates.

We simulated N losses along groundwater flowpaths for the Crane Wildlife site; the results of this analysis suggested that for the low DOC conditions at this site, a saturating kinetics expression with respect to nitrate best predicts nitrate concentrations measured at the downgradient well-ports ($R^2 = 0.96$ for $[\text{NO}_3^-]_{\text{model}}$ vs. $[\text{NO}_3^-]_{\text{meas}}$).

4. Modeling of Denitrification Using a Saturating Kinetics Expression

We developed an empirically-based saturating kinetics expression to describe groundwater denitrification under carbon and nitrate-limited conditions. Denitrification rates were described using a kinetic expression with double substrate limitation (with nitrate as the terminal electron acceptor and dissolved organic carbon (DOC) as the electron donor). The kinetic parameters were estimated from our field data (half saturation constant for NO_3^- (K_{NO_3})) and USGS field data (bacterial population [B]), and from data available in the literature (maximum bacterial growth rate (μ_{max}), half saturation constant for DOC (K_{DOC}), and bacterial yield constant (Y)). The proposed model was able to reasonably predict N losses along groundwater flow paths, measured at the two forested sites, where DOC ranged from 0 to 23 mg C l^{-1} and nitrate ranged from <1 to 91 μM . Using higher values for the bacterial population (B) and the half-saturation constant (K_{NO_3}), we were also able to predict N losses due to denitrification within the very different biogeochemical conditions of the septic system plume ($[\text{NO}_3^-]_{\text{max}} \sim 4,400 \mu\text{M}$, $[\text{DOC}] \sim 26 \text{ mg C}^{-1}$, and presumably a larger and more active bacterial population). The model performs well over the wide range of geochemical conditions found at the three sites within this watershed ($R^2 = 0.96$, $m = 0.96$ for measured vs. modeled). Eliminating the DOC term from the saturating kinetics expression, so that denitrification is limited only by nitrate concentration, results in an overprediction of nitrate losses along groundwater flowpaths, particularly where DOC concentrations are low. These results further confirm our previous conclusion that DOC concentrations exert a significant control on groundwater denitrification rates.

We conclude that the magnitude of the nitrate source, its travel distance to shore, and the DOC concentration in groundwater are useful predictors of N downgradient. The saturating kinetics model, with double substrate limitation by nitrate and DOC, developed here, provides a valuable tool for planners and managers interested in designing management strategies to control nitrogen loading to coastal waters. Such a model might be used in the design of setback limits for septic systems, in assessing the value of open spaces for N load reduction, in regulating wastewater disposal, and in watershed-wide land use planning.

5. References

Costa JE (1988) Distribution, production, and historical changes in abundance of eelgrass (*Zostera marina*) in southeastern Massachusetts. Ph.D. Thesis. Boston University, 352 p.

Cole JJ, Peierls BL, Caraco NF & Pace ML (1993) Nitrogen loading of rivers as a human-driven process *in* McDonnell MJ & Pickett STA (eds.) *Humans as Components of Ecosystems: The Ecology of Subtle Human Effects and Populated Areas* (pp 138-154). Springer-Verlag, New York, New York, U.S.A.

GESAMP (1990) *State of the Marine Environment. Rep. Stud. No. 39, Joint Group of Experts on the Scientific Aspects of Marine Pollution. United Nations Environment Programme.* 111 p.

Howarth RW, Billen G, Swaney D, Townsend A, Jaworski N, Lajtha K, Downing JA, Elmgren R, Caraco N, Jordan T, Berendse F, Freney J, Kudeyarov V, Murdoch P, & Zhao-Liang Z (1996) Regional nitrogen budgets and riverine nitrogen and phosphorus fluxes for the drainages to the North Atlantic Ocean: natural and human influences. *Biogeochemistry* 35:75-79.

National Research Council (NRC) (2000) *Clean Coastal Waters: Understanding and Reducing the Effects of Nutrient Pollution.* National Academy Press, Washington, D.C. 405 p.

National Research Council (NRC) (1994) *Priorities for Coastal Science,* National Academy Press, Washington D.C. 88 p.

Nixon SW, Ammerman JW, Atkinson LP, Berounsky VM, Billen G, Boicourt WC, Boyton WR, Church TM, DiToro DM, Elmgren R, Garber JH, Giblin AE, Jahnke RA, Owens NJP, Pilson MEQ, & Seitzinger SP (1996) The fate of nitrogen and phosphorus at the land-sea margin of the North Atlantic Ocean. *Biogeochemistry* 35: 141-180.